Alma Mater Studiorum – Università di Bologna

DOTTORATO DI RICERCA IN

Biologia Cellulare e Molecolare

Ciclo XXVII

Settore Concorsuale di afferenza: 05/I1

Settore Scientifico disciplinare: BIO/18

TITOLO TESI

Epigenetic role of N-Myc in Neuroblastoma

Presentata da: Giorgio Milazzo

Coordinatore Dottorato **Relatore**

Prof. Davide Zannoni **Prof.Giovanni Perini**

Esame finale: Bologna, Aprile 2015

Abstract

Childhood neuroblastoma is the most common solid tumour of infancy and highly refractory to therapy. One of the most powerful prognostic indicators for this disease is the N-Myc gene amplification, which occurs in approximately 25% of all neuroblastomas.

N-Myc is a member of transcription factors belonging to a subclass of the larger group of proteins sharing Basic-Region/Helix–Loop–Helix/Leucin-Zipper (BR/HLH/LZ) motif. N-Myc oncoproteins may determine activation or repression of several genes thanks to different protein-protein interactions that may modulate its transcriptional regulatory ability and therefore its potential for oncogenicity. Chromatin modifications, including histone methylation, have a crucial role in transcription de-regulation of many cancer-related genes. Here, it was investigated whether N-Myc can functionally and/or physically interact with two different factors involved in methyl histone modification: WDR5 (core member of the MLL/Set1 methyltransferase complex) and the de-methylase LSD1.

Co-IP assays have demonstrated the presence of both N-Myc-WDR5 and N-Myc-LSD1 complexes in two neuroblastoma cell lines. Human N-Myc amplified cell lines were used as a model system to investigate on transcription activation and/or repression mechanisms carried out by N-Myc-LSD1 and N-Myc-WDR5 protein complexes. qRT-PCR and immunoblot assays underlined the ability of both complexes to positively (N-Myc-WDR5) and negatively (N-Myc-LSD1) influence transcriptional regulation of crititical neuroblastoma N-Myc-related genes, MDM2, p21 and Clusterin.

Ch-IP experiments have revealed the binding of the N-Myc complexes above mentioned to the gene promoters analysed. Finally, pharmacological treatment pointed to abolish N-Myc and LSD1 activity were performed to test cellular alterations, such as cell viability and cell cycle progression.

Overall, the results presented in this work suggest that N-Myc can interact with two distinct histone methyl modifiers to positively and negatively affect gene transcription in neuroblastoma.

Index

Introduction

NEUROBLASTOMA, AN OVERVIEW

Neuroblastoma is one of the most common, enigmatic and heterogeneous tumors it is characterized by different phenotypes ranging from spontaneous regression to metastatic disease (1, 2).

Nerve cells of the sympathetic nervous system normally develop in the neural crest and neuroblastomas are neuro-ectodermal tumors arising from these pluripotent precursor cells (2).

The transient migratory potential of pluripotent Neural Crest Cells (NCCs) is probably the cause behind the complicated and fine-regulated journey across the dynamic landscape of the developing embryo. This migration, finally, determines a remarkable variety of differentiated cell types, including sensory, autonomic, and enteric ganglia in the peripheral nervous system, the adrenal medulla, melanocytes and a range of skeletal, connective, adipose and endocrine cells (3).

Neuroblastomas may arise anywhere along the sympathetic ganglia because of their neural crest origin. Indeed, most primary tumors (65%) occur within the abdomen, with at least half of these arising in the adrenal medulla. Other frequent sites of disease include the neck, chest, and pelvis. The disease is notable for its extensive spectrum of clinical behaviour. Although substantial recovery in outcome of some well-defined subgroup of patients has been registered during the past few decades, the outcome for children with a high-risk clinical phenotype has improved only modestly, with long-term survival still less than 40% (4).

Because of its neuro-ectodermal origin, neuroblastoma can be resolved into three main clinical scenarios:

- Localized tumors
- Metastatic disease
- 4S disease

D'Angio and colleagues (5) first described the striking clinical phenotype of stage 4S (S=special) disease (about 5% of cases). Infants with this disease have small localized primary tumors with metastases in liver, skin, or bone marrow that almost always spontaneously regress. Neuroblastoma is characterized by the highest percentage of spontaneous regression or differentiation (i.e. into a benign ganglioneuroma) observed in human cancers: the current frequency of neuroblastoma tumors that are detected clinically and subsequently regress without pharmacological treatment is 5–10% (6). However, the amount of authentic asymptomatic neuroblastoma patients in which the tumor regress spontaneously is probably much higher, and might be equal to the number detected clinically. These clinical information arouse considerable interest in discerning the mechanisms

underlying spontaneous regression or differentiation, which in turn may advantage to therapeutic approaches to stimulate these phenomena (6).

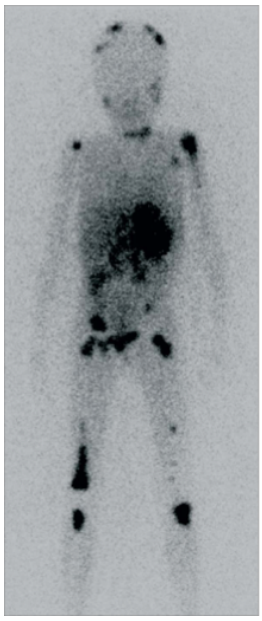

Figure 1: Onset sites of Neuroblastoma (4).

From a histological point of view, neuroblastomas can be classified into:

- immature, consisting of a large population of small neuroblasts, highly undifferentiated, with little cytoplasm (neuroblastoma, malignant).
- partially mature, consisting of ganglion cells (ganglioneuroblastoma, with reduced malignancy but capable of metastasizing)
- fully mature ganglion cells in clusters surrounded by a dense stroma of Schwann cells (ganglioneuroma, benign)

The differentiation state of the tumor has some prognostic significance, but a more sophisticated histopathological classification has been developed to help predict outcome and select therapy. The generally accepted method is the International Neuroblastoma Staging System (INSS) (7) which subdivide Neuroblastoma into 5 different stages as follows:

Stage 1 Localized tumor with grossly complete resection with or without microscopic residual disease; negative ipsilateral lymph nodes.

Stage 2A Localized tumor with grossly incomplete resection; negative ipsilateral non adherent lymph nodes.

Stage 2B Localized tumor with or without grossly complete resection with positive ipsilateral nonadherent lymph nodes; negative contralateral lymph nodes.

Stage 3 Unresectable unilateral tumor infiltrating across the midline with or without regional lymph node involvement, or localized unilateral tumor with contralateral regional lymph node involvement, or Midline tumor with bilateral extension by infiltration (unresectable) or by lymph node involvement.

Stage 4 Any primary tumor with dissemination to distant lymph nodes, bone, bone marrow, liver, skin or other organs (except as defined for stage 4S).

Stage 4S Localized primary tumor (as defined for stages 1, 2A or 2B) with dissemination limited to skin, liver and bone marrow (limited to infants <1 year age).

In a recent study, diagnostic biopsies from 240 neuroblastomas were analysed for genome sequencing revealing a low mutation rate in a small number of individual genes. The median frequency of mutation rate was 0.60 mutations per Mb, which is markedly lower than that found in adult solid tumors (8, 9).

Constitutional chromosome abnormalities have already been reported in some neuroblastoma patients, but no consistent pattern has emerged as yet. Because of the majority of neuroblastomas occurs spontaneously, many genetic changes are already associated with these sporadic tumors. Among all, de-regulation of oncogenes expression, gain and/or loss of alleles and changes in cell ploidy have been shown to be critical in the development of sporadic neuroblastomas (7).

Taken together, the multiplicity of several and heterogeneous initiating events proposes that neuroblastoma is a complicated genetic disease in which interconnection between different effects from multiple genetic alterations might be needed for tumourigenesis.

GENETIC ABNORMALITIES IN NEUROBLASTOMA

Subsets of patients show a genetic predisposition to develop neuroblastoma following an autosomal-dominant pattern of inheritance.

The literature data suggest that almost 22% of all neuroblastomas could be the result of a germinal mutation (10). This hypothesis is fortified by several clinical observations showing that the median age at diagnosis of patients with familial neuroblastoma is reduced from 18 months to 9 months (7). Although some patients have a predisposition to develop the disease, most neuroblastomas occur sporadically (2).

In spite of the fact that most tumors have a diploid karyotypes, low stages tumors are often hyperploid. Unfortunately, this aspect is not easy to assess since cells karyotyping assays are mostly unsuccessful (11).

Another important and significant abnormality is amplification of DNA loci, which in neuroblastoma involves at 2p24 (N-Myc gene's locus) and also at 2p22, 12q13 (MDM2 gene), 2p13, and 1p32 (MYCL gene) (12-15).

Trisomy of 17q is one of the most recurrent genetic abnormalities in neuroblastoma (16). How genes mapping in this region are responsible for selective advantage is still largely unknown, though they have convincingly been proposed to have an anti-apoptotic role, with consequences for the survival rate (17).

Activating mutations of RAS proto-oncogene are rare in neuroblastoma, however some studies have shown a possible correlation between high expression of HRAS with a lower stage disease and good prognosis. Activation of RAS proteins may result from activation of tyrosine kinase receptor, such as TRKA (18-20). Deletions of some chromosomes are common in neuroblastoma and generally correlate with different clinical stages (4). Loss of Heterozygosity 1p (LOH 1p, 30-35% of neuroblastomas) is strictly associated with N-Myc amplification and aggressive stage of tumor. Normally, and in case of N-Myc amplification, LOH 1p cause chromosomic deletions in DNA regions encoding for several important oncosoppresor genes like: CDH5, miR34a and KIF1β (21, 22).

On the other hand, deletions in 11q and 14q have not ever been found together with 1p and N-Myc genetic status (23). Notably, Loss of heterozygosity in 11q has been linked with event-free survival but only in patients that lack N-Myc amplification. Apparently the cause is that only few of these tumors have 11q loss and N-Myc amplification and the prognostic N-Myc value is dominant (6).

Among all genetic abnormalities, N-Myc amplification (20% of all neuroblastomas) is the most important biological feature of aggressive neuroblastomas. The average number of N-Myc genomic amplification is between 50 and 500 and because of the length of genomic region amplified (from 100kb to 1Mb) other important genes and/or genomic elements are co-amplified together with N-Myc gene (6).

MYC FAMILY

In 1980s a viral oncogene directly responsible in transformation induced by Rous Sarcoma Virus (RSV) and the human homologue c-Myc were discovered (24). This new human oncogene was thoroughly investigated and two other homologous genes were discovered: N-Myc and L-Myc (25, 26). These three genes are characterized by a good degree of homology and are members of the Myc family.

It is known that all the Myc family members are differentially expressed in distinct temporal patterns during embryonic development (27). c-Myc is highly expressed in most proliferating cells and is generally low or absent during quiescence. N-Myc, although present at low levels in many neonatal tissues, is highly expressed in pre-B cells, the kidney, the hindbrain and the intestine. In other tissues such as the telencephalon, retina, and intestine, N-Myc expression has been detected throughout differentiation stages whereas c-Myc is downregulated (28-30).

During gastrulation, c-Myc is expressed at high level in extra embryonic tissues, whereas N-Myc expression is mostly detected in the expanding primitive streak and in other regions of the embryonic mesoderm; during the differentiation to epithelium N-Myc expression has been shown to be down-regulated (29).

The L-Myc genic expression is detected in the developing kidney, lung and in both proliferative and differentiative areas of the brain and neural tube (31).

The three Myc family members are transcription factors belonging to a subclass of the larger group of proteins sharing Basic-Region/Helix–Loop–Helix/Leucin-Zipper (BR/HLH/LZ) motif. Molecular phylogenetic studies on MYC family members have revealed large segments of moderate conservation that are marked by six regions of straight homology: five MYC-boxes and one BR/HLH/LZ (32, 33).

The general structural organization of proteins belonging to the MYC family (Figure 2) is similar for all members and consist of:

- A large N-terminal portion including MYC-box I and II, involved in positive transcription regulation (TAD domain).
- An internal segment including proline rich residues (PEST) as well as two conserved regions MYC-box III and IV.
- A C-terminal portion comprising the basic-Helix-Loop-Helix leucine zipper domain (BR/HLH/LZ).

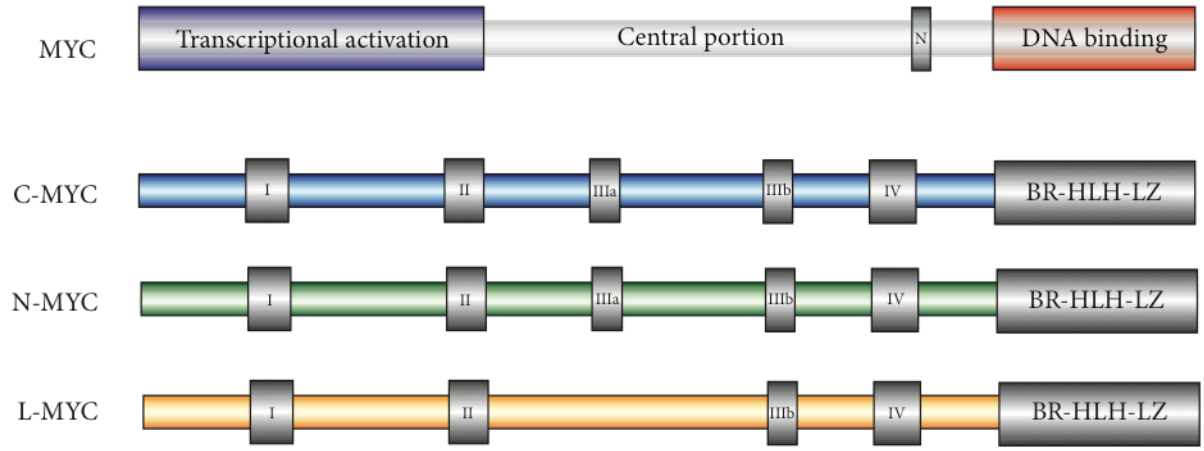

Figure 2: Structure of MYC family members (34).

The N-terminal MYC TAD domain, comprising MYC-box I and II, fused to heterologous DNA Binding Domain (DBD), is sufficient for transcriptional activation and is also chiefly responsible for MYC Ubiquitin-mediated degradation (23).

Several studies have demonstrated that MYC-box II is essential to promote, both *in-vitro* and *in-vivo,* cellular transformation and to positive and/or negative regulating transcriptional events. The main importance of MYC-box II in transcriptional regulation of several targets genes is surely attributable to its role in binding of co-activators like: TRRAP, GCN5, BAF53, SL1, BIN1 and PML(35-37).

In 2005 Herbst A. and collegues focused their attention on the "little studied" MYC-box III. Thanks to conditional expression of delta ER_c-MYC mutants in Rat1a mouse cell line, the critical role of MYC-box III in transcriptional repression activity of tumor related genes like P21, P15 and GADD45 was underlined (36).

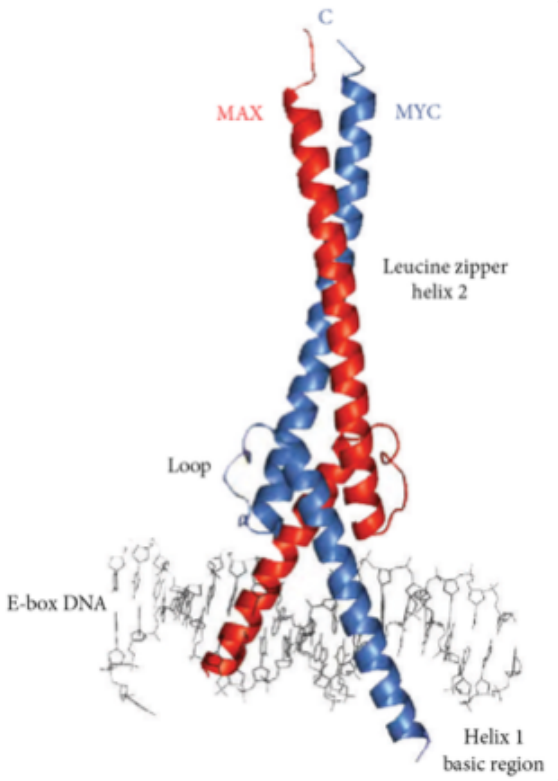

Figure 3: Heterodimer Myc-Max bound to consensus E-box DNA sequence (34).

C-terminal segment of MYC factors is essential for heterodimerization with another small bHLH-LZ protein named MAX. MYC-MAX heterodimer acts as a "core DNA-binding module" (Figure 3) recognizing consensus DNA sequence "CACGTG" also called "Enhancer-BOX" (E-box) (32, 34).

THE MYC/MXD/MNT/MAX NETWORK AND THE TRANSCRIPTIONAL CONTROL OF CELL BEHAVIOR

MYC members are incapables of forming homodimers and binds to specific DNA sequences. The primary partner for MYC transcriptional regulation activity is the small bHLH-LZ protein MAX (38).

Unlike that of Myc genes, Max expression is ubiquitous and constitutive, and this 160 aminoacid protein is stable, resulting in Max levels that far exceed those of Myc (39).

MAX is a bHLH-LZ transcription factor that lack all conserved MYC box domains and can both form homodimers and heterodimers capable of directly bind to E-box DNA consensus sequences. As well as with MYC factors, MAX can heterodimerize with other bHLH-LZ proteins of the MXD family (MXD1-4), MNT and MGA (37, 38).

MXD1 and MXD4 are generally expressed in differentiated cells, whereas Mxi1 (MXD2), Mad3 (MXD3) and Mnt, like all Myc genes, are also expressed in proliferating cells. These findings give rise to the hypothesis by which the MYC/MXD/MNT/ MAX constitute a fine tuned homo and hetero dimerization network surrounding the small ubiquitously expressed bHLHLZ protein MAX.

Overexpression experiments have suggested that MAX interacting proteins can antagonize the transcription regulatory activity of MYC family members. MAX homo- and/or hetero-dimerization with MXD and MNT result in repression of MYC-MAX activated gene targets. Transcriptional repression is establish by both MXDs and MNT by recruiting co-repressor complexes like N-CoR, Sin3a/Sin3b and the histone deacetylases 1 and 2 (Figure 4). The ability of MXD and MNT to physically interacts with Sin3a/Sin3b is allowed by an internal Sin3 Interaction Domain (SID) (18, 19, 39, 40).

Recent studies carried out using a negative Myc mutant called "MadMyc", in which DNA binding and dimerization domain of Myc were fused with SID of MAD, have shown inhibition of cell proliferation and cell cycle arrest (41).

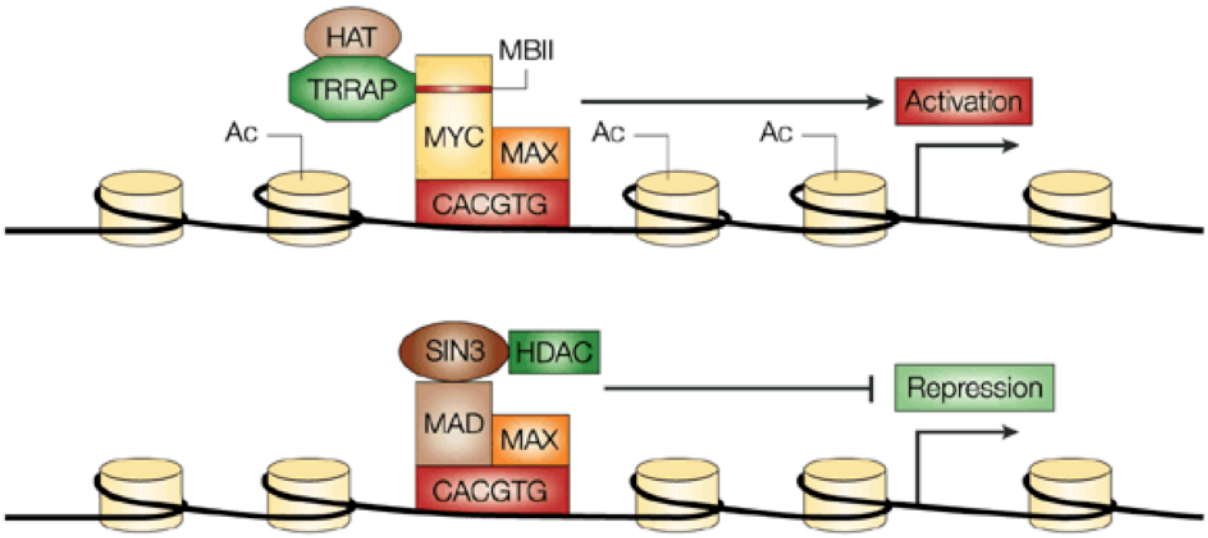

Figure 4: Differences between transcriptional regulation by MYC-MAX heterodimer and MAD-MAX heterodimer at level of E-box DNA elements (19).

Our understanding of the MYC/MXD/MNT/MAX network grew out of research on the MYC oncogene family. The first compelling idea about MYC was that its function drive cell growth and proliferation in response to a wide range of signals. Indeed, MYC genes are widely expressed during embryogenesis, and targeted deletions of c-MYC or N-Myc genes in mice lead to lethality in mid-gestation embryos (37, 38). Moreover, there is a strong correlation between MYC expression and

proliferation (9, 18, 19, 39-41). In cells with activated MYC, G1 phase is often shortened as cells enter the cell cycle, and MYC is essential for G0/G1 to S phase progression (23, 42, 43).

BIOLOGICAL FUNCTIONS OF MYC

It is now clear that a wide range of growth factors, cytokines, and mitogens induce MYC expression in many cellular backgrounds (11, 33). Both transcriptional and/or post-transcriptional regulation can determine an increase in endogenous MYC and appears to occur as an immediate early response (about 2 hours) to most mitogenic factors (44).

On the other hand, anti-proliferative signals must down regulate MYC expression, constituting a signal for cells to exit the cell cycle and undergo differentiation. Moreover, the induction of MXD family members, in response to different cues, is another important point of regulation to allow cell differentiation (20, 39, 42).

In the case of specific lineage commitment, an increase of MYC, determining boost of proliferation, also constitutes physiological event that is essential cell differentiation. Clearly, these data strongly suggest that MYC is a nexus for multiple growth signal response pathways. Therefore both MYC expression and activity are tightly regulated in non-transformed cells and finely tuned to quickly respond to proliferative cues from the extracellular milieu (14, 45).

The ability of MYC overexpressing cells to facilitate proliferation and inhibit terminal differentiation perfectly fits with different genetic rearrangements involving MYC family genes in several types of cancer, such as genomic amplification of N-Myc in almost 25% of neuroblastoma tumors (6).

Indeed, many of the genomic alterations in the MYC gene result in increased MYC mRNA levels through increased transcription initiation, decreased transcription attenuation, and augmented stability of the MYC mRNA (20, 41). Moreover, many tumor-related mutations in Myc result in significant protein stabilization (23, 43).

One of the most striking findings of the past years was the discovery of the important role of enhanced expression of Myc proteins in almost every aspect of tumor cell biology (33). Whereas the ability of Myc to drive unrestricted cell proliferation and to inhibit cell differentiation has long been recognized, many studies have already underlined that deregulated Myc expression can drive cell growth and vasculogenesis, reduce cell adhesion and promote metastasis and genomic instability. Conversely, the loss of Myc proteins inhibits cell proliferation and cell growth and also accelerate differentiation, increases cell adhesion and leads to an excessive DNA damage response (33).

In the last 15 years, in several neuroblastoma cell lines, there were analysed possible interconnections between N-Myc level and miRNA expression profile, stressing that N-Myc can both activate and repress many of non coding RNAs like mir 17-92 cluster, Mir 9 and Mir-421 (46).
This findings reflects the surprisingly high number of target genes regulated by Myc, as emerged in large-scale analyses of MYC-regulated genes. Indeed, in normal cells, Myc protein appear to integrate environmental signals in order to modulate a wide, and sometimes opposite, group of biological functions including proliferation, growth, apoptosis, energy metabolism and differentiation (45).

MYC AS AN ACTIVATOR

MYC factors, as already indicated, must heterodimerize with the small b-HLH-BZ protein MAX to directly bind DNA. MYC-MAX complex have relatively weak transactivation activity both at endogenous level and in transient assays (47). Recently published transcriptomic analysis have underlined the weak ability of Myc proteins to activate the majority of target genes (generally ranging from 3- to 10-fold transactivation) (48).
In general, the transactivation domain of Myc (TAD) recruits the basal transcription machinery either directly or indirectly, thanks to different protein complexes formed with several accessory factors. The most relevant model of MYC-mediated transcription activation postulates that MYC increases local histone acetylation in the promoter regions (33). In this connection, MYC binds to histone acetyltransferase complexes including TRRAP (transformation/transcription-domain-associated protein) and either general control of amino-acid-synthesis protein-5 (GCN5) or TIP60, which preferentially acetylate histones H3 or H4, respectively (49, 50). Myc can also binds to the p300/CBP (CREB-binding protein) acetyltransferase (51, 52).

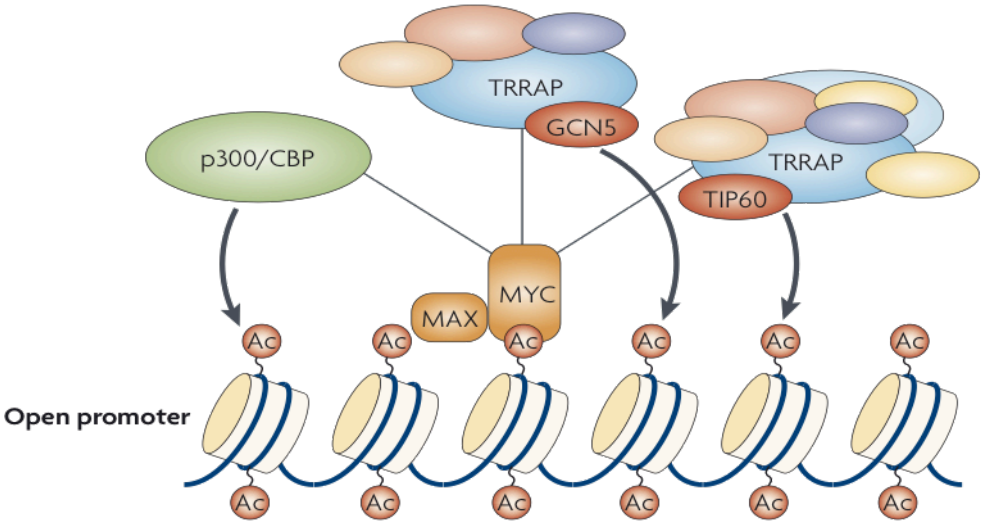

Figure 5: Mechanisms of MYC-induced transcription. Myc recruits histone acetyltransferases, which promote localized modification of chromatin through nucleosomes acetylation (52).

The action of acetyltransferase complexes, recruited by MYC factors, determine positive signal for transcription activation. The acetylated and more relaxed chromatin status provides docking sites for acetyl-histone-binding proteins, including GCN5 and the SWI/SNF chromatin-remodelling complex, both correlating with increased transcription levels (Figure 5). Moreover, acetylated euchromatic DNA regions would permit subsequent binding of constitutive and general transcription factors that allow RNA polymerase II promoter docking (52, 53).

The recruitment of histone modifiers by transcription regulators is accepted to be a major mechanism of transactivation, shared by many other transcription factors, like: TCF (T-cell factor), E2F, the tumor suppressor TP53 and Gal4 (54).

In the last decade genome-wide expression analysis, performed by many groups and in many cellular backgrounds, has revealed a staggering number of MYC target genes, around 10-22% of all genes in most models. Chip-seq analysis have shown higher Myc affinity for cell cycle related promoters than through all Myc-related promoters (41).

Among others, target genes include the Cyclin-Dependent Kinase-4 (CDK4), the Cdc25A phosphatase which activates CDKs, cyclin D2, CKN1A(p21), p27 and the E2F family. E2F gene family encodes for transcription factors critical for G1-S progression and in quiescent cells $E2F^{-/-}$ Myc fails to induce G1-S progression (41, 55). Recently, Myc has been shown to promote oxidative phosphorylation as well as glycolysis through coordinate transcriptional control of the mitochondrial metabolic network (56).

In addition to cell cycle control and metabolic target genes, Myc has been found to activate several essential genes involved in many biological functions like control of cell size and growth, including those encoding ribosomal proteins, translation factors, and metabolic enzymes (57-60). These findings stress the role of MYC factors in recruitment of co-activator complexes into regulatory regions contacted by RNA polymerase I and III (61-64).

MYC regulation can also occurs at the level of transcriptional elongation and not just at transcriptional initiation. The C-terminal domain (CTD) of RNA pol II undergoes to cycling phosphorylation and de-phosphorylation during transcription. Hypo-phosphorylated form of CTD determines RNA pol II recruitment to promoters, while high level of phosphorylation occurs during initiation and elongation steps. Sub-sequent de-phosphorylation allow RNA pol II recycling for another round of transcription (65). RNA pol II has been found to pause on most promoters after transcribing approximately 20–40 bases. This model fits well with the finding that Myc stimulates the release of paused RNA pol II from the promoter and stimulates subsequent transcriptional elongation (66). Myc transactivation domain (TAD) binds directly to CTD kinases determining an increase in RNA pol II phosphorylation and elongation. Myc induction occurs globally throughout the nucleus and it can be detected in the total cellular pool of RNA pol II rather than simply at MYC target-gene promoters (66, 67).

Moreover, Myc factors are also involved in control of mRNA stability, by promoting 5' methylation of guanine or 'cap', which is an essential step for protein-coding gene expression. This transcription-independent activity underlines the critical role of MYC in transcription and post-transcription regulation in both normal and tumor cells (68, 69).

Along with transcription, the most important nuclear process is DNA replication. The genome must be faithfully replicated each cell cycle and the chromosomes must be segregated to the daughter cells. Disruption of any step in this process, such as a stalled replication fork or DNA damage occurring during S phase, activates checkpoints that halting the cell cycle until the lesion can be repaired. Failure to correct this damage leads to a mutation and/or genomic instability. In fact, it has been hypothesized that high MYC expression correlate with genomic instability because of the indirect consequence of MYC mediated de-regulation in normal transcriptional activity (70, 71).

A recent study have described a direct, non-transcriptional, role for MYC in the initiation of DNA replication. Myc has been found to bind numerous components of the pre-replicative complex, and localize to early sites of DNA replication. These observations have suggested that MYC might directly control the initiation of S phase and this effect on genomic instability might not depend on the transcriptional induction of S-phase-promoting genes. Furthermore much excitement has been

generated in the past few years about the role of noncoding regulatory RNAs. The first oncogenic polycistronic microRNA is shown to be regulated by MYC (42).

Taken together, these findings raise the question: are MYC factors just like traditional transcription factors or are they guardians of cell metabolism?

Surely the transcription activity is the main known function of the oncogenic MYC protein. Apparently, a disconnection seems to exist between MYC's dramatic effects on multiple cellular functions and its biological and molecular characterization as a relatively weak transcriptional activator. Indeed, the notion that Myc is a general chromatin regulator is nonetheless consistent with several recent observations concerning MYC function. First, independent expression microarray analysis have collectively identified a large group of genes regulated by Myc. Second, chromatin-IP experiments directly assessing Myc binding to thousands of sites throughout the genome encompassing approximately 15% of genes as well as intergenic regions (48, 66, 72, 73). Potentially, therefore, Myc can regulates a significant percentage of all genes in an organism.

The number of *in-vivo* binding sites exceeds the number of Myc molecules in proliferating cells, indicating that each site is bound by Myc only temporarily. Most probably, therefore, transcriptional regulation by Myc occurs by a 'hit-and-run' mechanism whereby the relatively brief binding of Myc triggers longer-lasting changes in the chromatin organization at the bound loci (45).

Many recent evidences underline the role of N-Myc in the global regulation of human genome euchromatin, including that of intergenic regions. Strikingly, N-Myc maintains 90% to 95% of total H3K9 acetylated and H3K4Me marks, with enhancer-like function, in human several neuroblastoma cell lines (74). Furthermore Myc may regulate chromatin at a distance so that Myc binding at one location can influence chromatin at another site through an high order chromatin structure (75).

Intriguingly intergenic binding sites for MYC are not enriched for E-boxes. Although E-box independent binding has been reported and may be fairly widespread, such binding may be of particular importance for Myc intergenic function (70).

Furthermore, Myc has been shown to possess another feature outside the context of E-boxes: surprisingly Myc can also act as well as a transcriptional repressor at certain target promoters consistent with the wide distribution of MYC along the genome(see below) (76-78).

MYC AS A REPRESSOR

One of the first finding highlighting the idea that MYC can also act as a transcriptional repressor derived from studies published in the 1980s, suggesting that MYC participates in a negative feedback loop (79, 80). Genome-wide analyses demonstrate that MYC represses at least as many targets as it activates, further emphasizing the role of repression in MYC function, including transformation (45, 81).

No simple consensus sequences for transcriptional repression by Myc has emerged, this finding opens up the possibility that transcriptional repression is a simply indirect consequence of the altered physiological (e.g., transformed) state of a cell induced by Myc (82, 83).

In the last 10 years a lot of studies have been carried out to fully understand the mechanism of MYC repression. Many investigators have exploited a chimeric MYC-MAD protein to better define MYC transcriptional activity, but this chimera cannot fully recover the transformation potential of wild-type MYC factors *in-vivo*; for example, they are unable to immortalize primary mouse embryo fibroblasts and to induce apoptosis in immortalized cells and are impaired in rescuing the proliferation defect of c-myc $^{-/-}$ fibroblasts (84).

These important findings, together with several other illuminating researches, support the hypothesis that the oncogenic potential of MYC factors is fulfilled by both activation and repression activity.

The actual model of MYC repression is based on the indirect DNA binding on *cis*-genomic elements, interacting directly with other transcription regulators bound to DNA. The repressed genes, like induced genes, fall into multiple functional classes. Among all, genes encoding for factors selectively expressed in quiescent cells or involved in inhibit cell proliferation. This group encompasses the cell cycle inhibitors p21 (85-88), p27kipl (89, 90), pl5ink4b (91, 92), pl8ink4c (93), and p57kip2 (94), as well as the differentiation-inducing proteins C/EBP-a (95), the growth-arrest proteins gas1 and gas2 (96), the growth arrest and DNA damage proteins gadd34, gadd45, gadd153 (70, 97, 98), and the Myc-antagonist Mad4 (99). Myc can also down regulate genes encoding for proteins deeply involved in cell adhesion, including a large number of integrins: these genes include those encoding cell surface proteins such as the class I HLA molecules in melanoma cells, the α3 β1 integrin in neuroblastomas, and the LFA-1 (αL β2 integrin) cell adhesion protein in transformed B cells as well (100). Altered cell adhesion is a hallmark of many Myc-transformed cells and has been observed in different cell types (101). Metabolic pathways such as thrombospondin and H-ferritin are also affected by Myc mediated repression (102, 103). Suppression of thrombospondin plays a causative role in the induction of angiogenesis by Myc. In the last 10 years

ABCC3 has been identified as MYC repressed gene, it encode for an important multi-drug resistance protein involved in chemo-resistance and also in cell migration (104). Therefore, Myc-mediated gene repression in the control of cellular differentiation and in the response to growth arrest signals makes a significant contribute to the phenotype of MYC-transformed cells. The basic mechanism underlying MYC's activation of transcription is well understood, but the way in which MYC negatively regulates or represses transcription is far less understood (81).
A number of Myc-repressed targets contain a subclass of initiator elements (INRs; consensus, YYCAYYYYY, where Y is a pyrimidine base), which are usually, but not invariably, present at TATA-less promoters. Inr elements are recognized by TFIID as well as by a number of regulatory proteins, such as the transcription initiation factor TFII-I, YY-1, and the Myc interacting zinc-finger protein 1 (Miz-1). Interestingly, the last three proteins have been reported to associate with the C-terminal BR/HLH/LZ region of Myc (101).

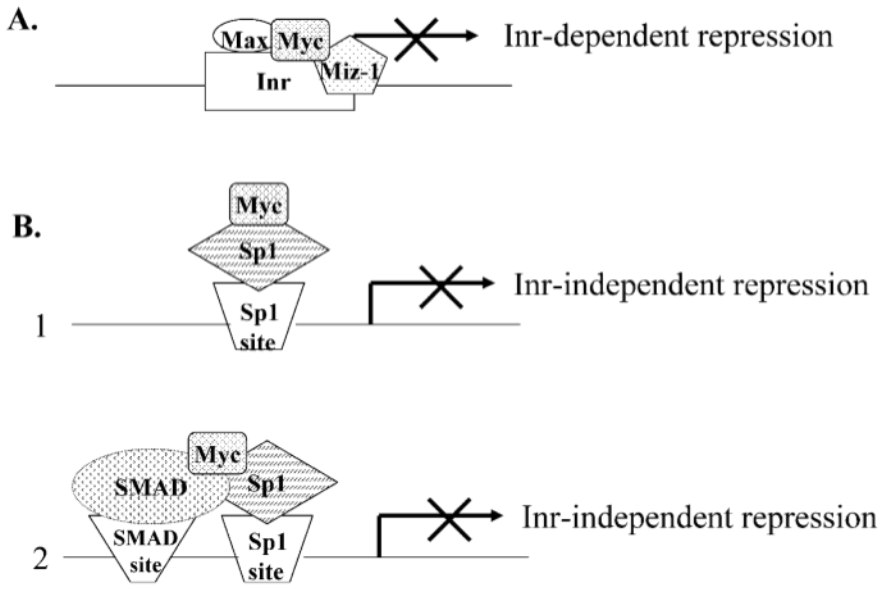

Figure 6: Mechanisms of transcriptional repression by c-Myc. (A) Inr-dependent mechanism of MYC repression. Myc–Max heterodimers bind to the Inr element and associate with Miz-1 or other TFs, thus interfering with their activities. (B) c-Myc represses target genes transcription by Sp1-dependent mechanism. c-Myc interacts with the Sp1 transcription factor (1) or with the Smad–Sp1 complex (2) via the c-Myc central region and inhibits Sp1 transcriptional activity. This mechanism does not require DNA binding or interaction with the c-Myc partner Max (105).

MYC mediated repression of p15 and CKN1A(p21) promoters has been thoroughly described and could be perceived as prototypical for MYC dependent transcriptional repression of growth arrest genes.

There are two main independent mechanisms of MYC mediates repression. The first is based on the ability of MYC-MAX heterodimer to bind the zinc-finger protein Miz-1 and this complex is now capable of binding to transcriptional initiator elements (Inr) (figure 6, A) (101). Miz1 contains 13 zinc fingers and, at its amino-terminus, carries a BTB/POZ-domain, which is a protein-protein interaction domain found in multiple zinc-finger proteins. Miz1 binds to the 'outside' of the helix–loop–helix domain of Myc, but does not interact with Max, Mad or Mnt proteins (106, 107). The second mechanism by which MYC-MAX represses transcription implies interaction with SMAD 2/3 proteins and consequent complex formation with another TF called Sp1 (figure 6, B2) (108).

In case of p15 transcriptional regulation, Miz-1 acts as positive factor but the interaction with MYC-MAX inhibit the Miz-1 mediated p300 recruitment at Inr element. Conversely, MYC-MAX can carry out p15 repression in Inr independent manner. In fact, p15 gene activation can be establish by positive transcription complex formed by several combination of SMAD2, SMAD3 and SMAD4 with Sp1. MYC-MAX can interact with SMAD2/3 to form a larger, inactive but more stable complex formed by MYC-MAX/SMAD2/3/Sp1 (101).

Several published data have revealed both c-Myc and N-Myc repression activity on CKN1A(p21) gene transcription. MYC factors do not directly bind to DNA but they form complexes with Sp1 factors determining, as already mentioned for p15 repression, the absence of transcriptional activation (86).

On the other hand, there are some genes repressed by MYC through a mechanism that does not involve the Max protein (109, 110).

In 2005 Brenner and colleagues demonstrated recruitment of DNA methyltransferase, DNMT3a, by c-Myc to CKN1A(p21) promoter in a MAX independent complex composed by c-Myc and Miz-1. This finding disclosed the important interconnection between c-Myc repression activity and DNA methylation (106, 107). Since DNMT3a is complexed with histone deacetylases enzymes, its recruitment by Myc might lead to local histone deacetylation and inhibition of transcription (107). Recruitment of DNMT3a by Myc is an attractive mechanism for repression, since it might provide an explanation of the aberrant DNA methylation of some tumor suppressor genes that is observed in some human tumors.

Recent studies have shown that not all genes repressed by Myc are silenced by the same mechanism.

Another finding that reinforce the idea that there exist multiple and variegates MYC repressive pathways is the discovery of N-Myc-PRC2 (via N-Myc and EZH2 physically interaction) repressive complex on the promoter of the tumor suppressor gene CLU in neuroblastoma cellular background (111).

All these data clearly support the notion that several pathways of repression exist. Finally, the present model is that Myc interacts with transcriptional activators that are bound directly to DNA through enhancer or initiator elements either cooperating with MAX or not. These multi-protein complexes are thought to inhibit recruitment of co-activators, facilitating the negative and oncogenic activity of co-repressors like DNA methyltransferases, histone methyltransferases and deacetylases (105, 112).

The definition of epigenetic, coined by Conrad Waddington, is: "An epigenetic trait is a stably heritable phenotype resulting from changes in a chromosome without alterations in the DNA sequence" (113).

Shelley L. Berger and colleagues, proposed three categories of signals that trigger different establishment of stably heritable epigenetic states (Figure 7):

- "Epigenator,'' which emanates from the environment and triggers an intracellular pathway;
- ''Epigenetic Initiator'' signal, which responds to the Epigenator and is necessary to define the precise location of the epigenetic chromatin environment;
- ''Epigenetic Maintainer'' signal, which sustains the chromatin environment in the first and subsequent generations (114).

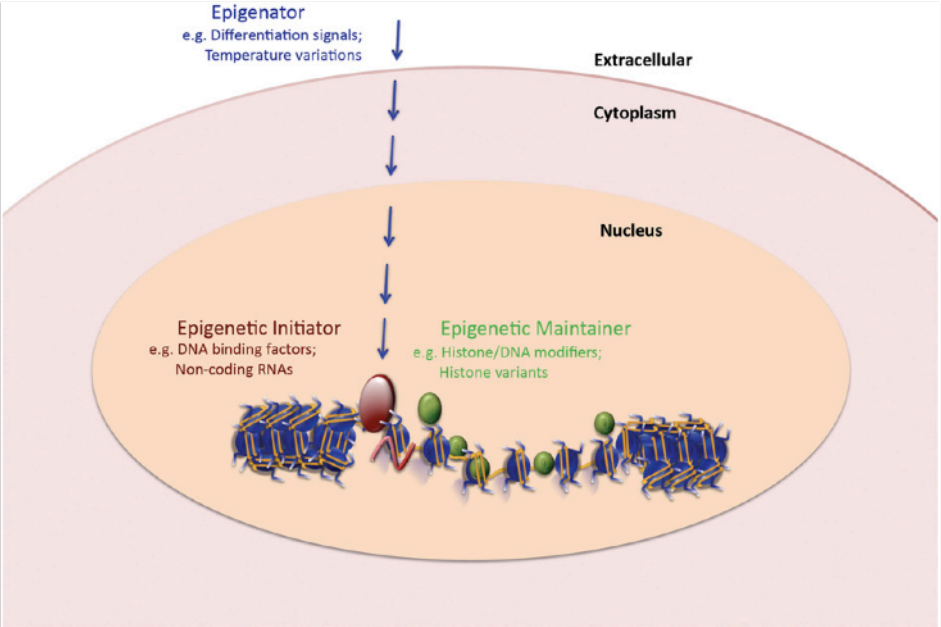

Figure 7: The epigenetic pathway.

The fine tuned DNA organization inside the nucleus is an essential aspect of eukaryotic cell life. Chromatin is the macromolecular complex composed by DNA, RNA and proteins, determining genomic DNA condensation inside the nucleus. Mainly, there are four chromatin packaging degrees ranging from 11nm DNA fibers to 700nm interphasic DNA domains (Figure 8) (114, 115).

The plastic, finely tuned and rapid exchange of different levels of genomic DNA condensation is a critical step for almost all the biological issues linked to DNA.

Every 147bp, DNA is wrapped around an octameric protein complex, the nucleosome. Five different proteins (Histones) compose this functional unit: H2A, H2B, H3, H4 and H1. The nucleosome structure is globular except for the histone n-terminal "tails", which are unstructured. As mentioned above, chromatin condensation is an essential regulating "tool" of many important biological aspects like DNA transcription (114, 115).

The nucleosome is also target of several dynamic post-translational modifications of histone n-tails which determine the "fate" of transcriptional activity of all the genes encoded by genomic DNA (116). Indeed, histone modifications are crucial to dictate different genomic packaging levels inside the nucleus (Figure 8). These changes in DNA condensation ranging from heterochromatin, highly condensed and transcriptionally repressed or silenced to a more accessible status of DNA defined as euchromatin in which genomic regions are tightly packaged and are transcriptionally active (114-117).

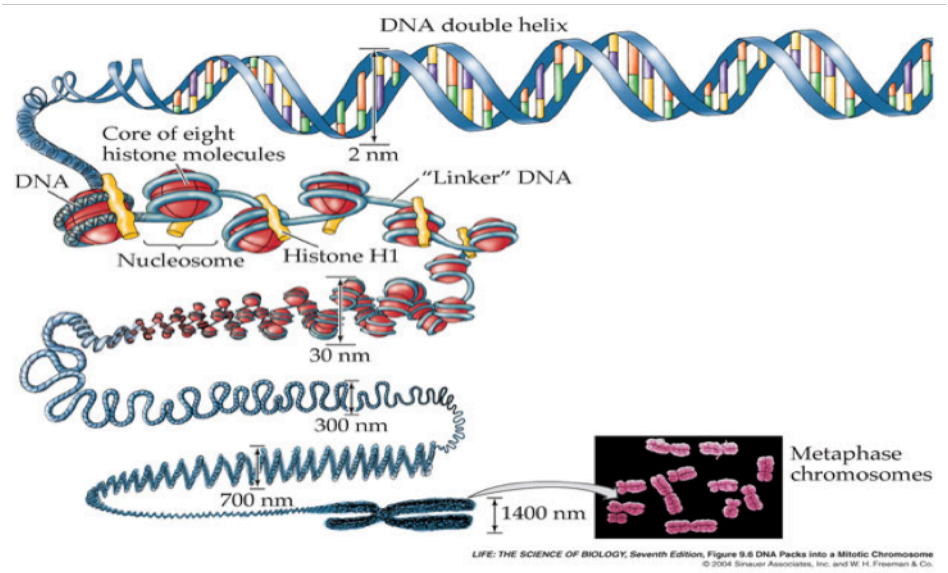

Figure 8: Graphical representation of different chromatin condensation degrees (36).

DNA METHYLATION AND HISTONE MODIFICATIONS

Among all the chromatin modifications, we can distinguish direct DNA modification, including 5-methylcytosine (5mC), 5-hydroxymethylcytosine (5hmC), 5-formylcytosine (5fC) and 5-carboxycytosine (5caC) and n-tail covalent nucleosome modifications such as: acetylation, methylation, sumoylation, ubiquitination and phosphorylation (116-118).

DNA methylation is the covalent addition of a methyl group (CH_3) to the C5 position of cytosine in CpG dinucleotides. Genomic regions containing multiple stretches of CpG dinucleotides termed as "CpG islands" and they are often associated with promoters elements (119).

In mammals somatic cells, methylated cytosines account for 1% of total DNA bases, but only 10% of these are located in CpG islands (120). Unlike the dispersed CpG elements, those in CpG islands are more resistant to methylation events (119, 121).

Cytosines are methylated by the DNA methyltransferase machinery composed of two subunits: the DNA methyltransferase (DNMTs) and the methyl CpG binding protein (MBDs). Until now there no evidences have been found about activity responsible for DNA de-methylation (119).

In 1983 the clear correlation was first demonstrated between hypomethylation and genomic instability of cancer cells. In the last 20 years many studies have corroborated the hypothesis that loss of genomic methylation is an early event in many type of cancer (122).

Many genes involved in cell-cycle regulation, tumour cell invasion, DNA repair, chromatin remodelling, cell signalling, transcription and apoptosis are known to become aberrantly hypermethylated and silenced in many tumour type. Probably the hypermethylation status increases genetic instability, allowing cancer cells to acquire advantageous genetic changes and to proliferate and to metastasize (122, 123).

Ever since Allfrey's studies in the early 1960s, we have known that histones can be post-translationally modified by a large number of different histone post-translational modifications (PTMs) (124). There are at least eight distinct types of modifications found on histones (Table 1).

The dynamic and heterogeneous network of histone modifications determine the transcriptional "fate" of all the genes encoded by genomic DNA (125).

Extra complexity comes partly from the fact that methylation at lysines or arginines may be one of three different forms: mono-, di-, or trimethyl for lysines and mono- or di- (asymmetric or symmetric) for arginines (116).

Chromatin Modifications	Residues Modified	Functions Regulated
Acetylation	**K**-ac	Transcription, Repair, Replication, Condensation
Methylation (lysines)	**K**-me1 **K**-me2 **K**-me3	Transcription, Repair
Methylation (arginines)	**R**-me1 **R**-me2a **R**-me2s	Transcription
Phosphorylation	**S**-ph **T**-ph	Transcription, Repair, Condensation
Ubiquitylation	**K**-ub	Transcription, Repair
Sumoylation	**K**-su	Transcription
ADP ribosylation	**E**-ar	Transcription
Deimination	**R > Cit**	Transcription
Proline Isomerization	**P-cis > P-trans**	Transcription

Table 1: Overview of different classes of modification identified on histones (114).

The combinatorial complexity of all the different histone modifications that can occur at the same time in the same nucleosome had always lead to several hypotheses attempting to define "the histone code" which actually is not fully understood (126). The histone code is read and construe by the non-histone proteins and multiprotein complexes that form the transcription-activating and/or -repressing molecular machinery. Moreover, different chromatin binding proteins can be recruited by specific n-tail histone markers, but the simultaneous existence of two or more marks in the same nucleosome can lead to a different scenario (126-128).

Chromatin-regulating proteins can be divided into three main groups (Figure 9):

- "Epigenetic writers" that directly modify specific N-tail residues;
- "Epigenetic readers" that bind specifically to a type of covalently modified amino acid;
- "Epigenetic erasers" that remove and/or convert distinct N-tail covalent modifications.

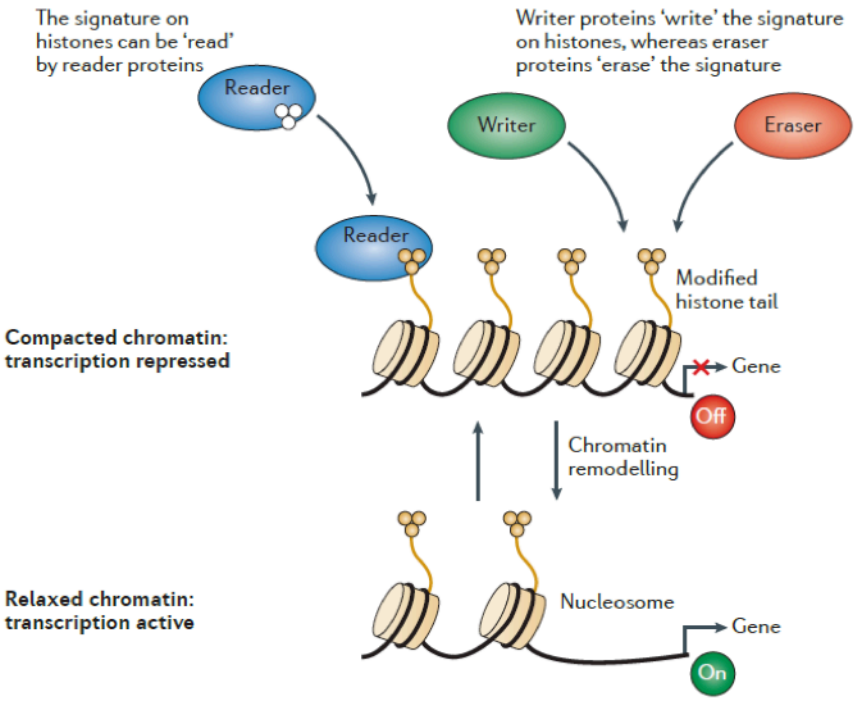

Figure 9: Graphical representation of Chromatin binding proteins: Writers, readers and erasers (129).

In the last decade the already quirky network of histone writers and erasers has been complicated by the discovery of many modifiers able to methylate and demethylate specific residues of protein factors involved in transcription regulation. These modification also significantly affect the ability of transcription factors to form the protein complexes required to activate and/or to repress transcription of specific genes (128, 130).

N-tail histone acetylation is the most common histone marker of opened chromatin and it occurs exclusively on lysine residues of histone H3 and H4. N-Acetylation of positively charged lysines determines an electrostatic neutralization, because of its negative charge. The effect of this change in net positive charged of histone determines an important loss of electrostatic interaction between nucleosome and DNA leading to a more relaxed and accessible chromatin status (124, 125).

In 1964 Allfrey et al. first demonstrated the highly dynamic and finely regulated balance between histone acetylation and de-acetylation of chromatin. The plastic balance between histone acetylation and de-acetylation is respectively controlled by histone acetyltransferases (HATs) and histone deacetylases (HDACs). HATs, also known as K-acetyltransferases, catalyze the addition of acetyl groups to histone lysines using acetyl coenzyme A as cofactor. GCN5, p300/CBP, and MYST families composed the three main groups of HATs (51, 53). Just as HATs are a diverse set of enzymes, the multi-protein complexes in which they reside also vary in subunits composition. The considerable combinations of these accessory subunits lead to several unique features of each HAT complex. For example, some subunits have conserved domains that cooperate to recruit the HAT to the appropriate location in the genome; these include bromodomains, chromodomains, WD40 repeats, Tudor domains and PHD finger (54, 131).

Unlike positive transcriptional HATs activity, Histone DeACetylases (HDACs) led to repressed chromatin because of the increase in electrostatic interaction between nucleosomes and wrapped DNA. Until now, eighteen distinct human HDACs have discovered and grouped into four classes.

Class I HDACs (HDAC1, -2, -3, and -8) are predominantly nuclear proteins and ubiquitously expressed in most tissues and cell lines. Class II HDACs can be subdivided into two subclasses, IIa (HDAC4, -5, -7 and -9 and its splice variant MITR) and IIb (HDAC6 and HDAC10), based on the protein sequence homology and domain organization. Class IIa HDACs have one catalytic domain and a long amino-terminal adaptor domain, while class IIb HDACs contain two catalytic domains. Class III HDACs, known as sirtuins, do not contain zinc and their activity requires nicotinamide adenine dinucleotide (NAD+). Class IV HDACs include only HDAC 11, a relatively newly discovered protein, which resembles class I HDACs (128, 132).

HATs and HDACs complexes have been shown to play a critical role in carcinogenesis, trough either inappropriate activation or repression of target gene activity (53, 125, 133).

As already discussed, HATs complexes are co-activators of many TFs like MYC family oncoproteins. The role of HATs complexes in cancer, especially for p300 is not well understood, probably because its activity depends on different tumor backgrounds (134). p300 has been recognized as a potential anti-cancer drug target because its gene was found altered in most colon cancer cell lines and in some primary tumors (135, 136).

p300 is also a target of viral oncoproteins, it can be fused to MLL in leukaemia and two missense mutations were found in epithelial malignancies (137). Conversely to its supposed oncosoppressor function, in prostate cancer p300 was found to have to a clearly oncogenic potential (134).

HDACs have been intensely studied for their involvement in mediating the function of oncogenic translocation products in specific forms of leukaemia and lymphoma. For example, in acute promyelocytic leukaemia (APL), PML–RARα, represses transcription by associating with a corepressor complex that contains HDAC activity. In non-Hodgkin's lymphoma, the transcriptional repressor LAZ3/BCL6 (lymphoma-associated zinc finger-3/B cell lymphoma 6) is strongly overexpressed and associated with aberrant transcriptional repression through recruitment of HDACs, leading to lymphoid oncogenic transformation (128).

Another histone modification that leads to a change in the electrostatic balance between nucleosomes and DNA is the phosphorylation of serine, threonine and tyrosine residues on histone N-tails (138).

The exact mechanism by which histone phosphorylation affects gene expression is not well understood; it is thought that, similarly to N-acetylation, the addition of phosphate group (negatively charged) to histone N-tails may interfere in the electrostatic interaction between nucleosomes and DNA. Like N-acetylation of histone N-tails, phosphorylation probably increases the accessibility of DNA to nuclear factors (138).

Less is known regarding the roles of histone phosphatases. Certainly, given the extremely rapid turnover of specific histone phosphorylations, there must be high phosphatase activity within the nucleus. We know, e.g., that the PP1 phosphatase works antagonistically to Aurora B, the kinase that lays down genome-wide H3S10ph and H3S28ph at mitosis (124, 139).

For the majority of kinases it is not yet clear how they are accurately recruited to their sites of action on chromatin. The mammalian MAPK1 enzyme possesses an intrinsic DNA-binding domain with which it is tethered to the DNA. Alternatively, histone kinases recruitment may require association with a chromatin bound factor before it directly contacts DNA to stabilize the overall interaction.

Even though the majority of histone phosphorylation sites lie within the N-terminal tails, there are examples of phosphorilation sites within the core histone region. For example, it was determined that the non-receptor tyrosine kinase JAK2 is responsible of H3Y41 phosphorylation (124, 140). Histones H1, H2A, H2B, H3, and H4 are all phosphorylated at multiple residues, but the most studied are so far the phosphorylations of histone H3. Phosphorylation reaction is catalysed by many distinct kinases that are mostly specific for individual histone residues (139).

A huge number of studies have underlined the important role of H3S10 phosphorylation in positive gene regulation. This histone modification can be deposited by various kinases in relation to the biological context. Phosphorylation of H3S10 by mitogen and stress-activated protein kinases 1 and 2 (MSK1 and MSK2) as well as RSK2 kinase has been shown to play a role in the activation of mitogen-stimulated immediate-early response genes, such as c-fos and c-jun (139, 141, 142).

Furthermore, Pim1 kinase catalyses H3S10 phosphorylation at the E-boxes in Myc target genes, contributing to their transcriptional activation after growth factor stimulation (139). While histone acetylation and phosphorylation balance can deeply change the net charge of nucleosomes, methylation is a chemical modification that does not alter electrostatic interaction between nucleosomes and DNA. As already mentioned above, mono-, di- or tri-methylation of histone N-tails can occur on lysine, arginine and histidine residues (143). Methyltransferase activity lies with the catalytic ability to add methylic groups from S-Adenosyl methionine to specific aminoacid residues K, R and H. There are three main families of methyltransferases based on protein domains homology: Set1, DOT-1 like and PRMT (144).

Methylation of H3K4, H3K36 and H3K79 are strongly associated with euchromatic regions, while methylation on H3K9, H3K27 and H4K20 is often found on repressed heterochromatin regions. Specifically, di- or tri- methylation of H3K4 are strictly associated with Trascriptional Start Site (TSS) DNA regions, whereas H3K4Me is closed linked with enhancer elements of active genes. While mono-methylation of H3K9 is often associated with active transcription, H3K9Me3 is a marker of transcription repression (114).

Several scientific reports have already discussed the important interconnection between nucleosome methylation pattern and carcinogenesis in many tumor backgrounds.

EZH2, together with SUZ12 and EED, forms the polycomb repressive complex 2 (PRC2), which is responsible for tri-methylation of H3K27. In cancer, EZH2 is one of the widely studied methyltransferase because of its clear relationship with many type of tumors like breast, prostate and lymphoma (130). As already highlighted for some HAT proteins several mehtyltransferases and

HDACs to cannot be absolutely classified as oncosoppresor or oncogene: it depends on the cellular background in which they act (144).

MYC FACTORS AND HISTONE MODIFIERS IN CO-ACTIVATOR AND CO-REPRESSIVE COMPLEXES

In 2014 Susanne Walz et al. performed RNA and ChIP seq analyses on U2OS and Hela cell lines respectively in a condition of doxycycline c-Myc induction and c-Myc silencing by Sh-RNA techniques. Both c-Myc activation and silencing revealed almost 30,000 MYC binding sites, and more than 200 up- and 100 down-regulated genes. Consistently, a linear support vector machine algorithm based on the set of MYC-regulated genes correctly classified 37 of 38 neuroblastomas as harbouring a single copy or amplified N-Myc gene. The most important finding that was suggested by Susanne Walz and colleagues is the correlation between high c-myc level and the occupancy of low affinity non-consensus E-box (CANNTG) sites. Conversely, change in c-myc levels did not affect occupancy in high affinity consensus E-box sequences (CACGTG) (81).

These findings strongly suggest that the dynamic role of both c-Myc and N-Myc determines a profound change in the transcription profile of different tumors. Accordingly, MYC factors are widely studied in relation with different *cis*-elements in the whole cell genome and with heterogeneous multiprotein complexes composed by different histone modifiers.

As already underlined before, protein-protein interactions may modulate MYC's transcriptional regulatory ability and therefore its potential for oncogenicity. A variety of proteins that interact with both c-Myc and N-Myc have been identified. Few of these have been shown to be directly recruited by MYC factors and to mediate the transactivating functions of MYC (78).

One of the most widely studied MYC co-activator "partner" is the transactivation/transformation-associated protein (TRRAP), which, together with several histone acetyltransferases (HATs), stably associated with TRRAP and the positive transcription elongation factor b (PTEFb), form large multiprotein complexes (145). Accordingly, it was reported that dominant-negative TRRAP genes or antisense TRRAP RNA can blocks MYC transformation activity (146). In 2002, Elizabeth M. Flinn et al., definitively define Myc box II as domain responsible for c-Myc interaction with GCN5 or its associated protein, TRRAP (146).

The basal transcription factor 1 (SP1), a critical zinc-finger GC binding protein, is clearly involved in N-Myc-mediated repression mechanism (147-150). The N-Myc and SP1 interaction was fully investigated (151) through both *ex-vivo* and *in-vitro* techniques, resulting in demonstrating the importance of Myc Box 2 as the domain responsible for the interaction with SP1. As already

mentioned, N-Myc-SP1 complex exerts repressive function via recruitments of chromatin modifiers such as histone deacetylases. In 2007, Marshall et al. demonstrated the role of N-Myc-SP1 complex in repression activity of the transglutaminase 2 (TG2) gene expression through recruitment of histone deacetylase 1 (HDAC1)(147). Importantly, ChIP assays have determined that MAX is not present at DNA level and is not necessary for HDAC1 recruitment. Hence, N-Myc-SP1 repressive activity can be established in absence of N-Myc "partner" and can be disrupted by the use of an HDAC1 inhibitor (trichostatin A) (148).

In 2010 Marshall et al. have also demonstrated the N-Myc-SP1 mediated inhibition of CyclinG2 gene transcription through the interaction with HDAC2. Accordingly, in 2012 Zhang et al. have revealed that both c-Myc and N-Myc can interact with paralogs of HDAC1 such as HDAC2 and HDAC3 (152).

In-vitro analyses of the N-Myc regions required for its interaction with both SP1 and MIZ-1 show that N-Myc Myc Box 2 domain can directly interact with SP1, while the basic helix-loop-helix leucine-zipper (BR/HLH/LZ) domain is required for interaction with MIZ-1. The "ternary complex" can also drives the transcriptional repression of genes such as TRKA (tyrosine kinase receptor A), P75NTR (p75 neurotrophin receptor), and CKN1A(p21) in neuroblastoma by recruitment of HDAC1 on the respective promoters (151).

Collectively, these findings highlight the complexity of N-Myc activity and suggest that many more nuclear components may be critical for N-Myc-mediated transcriptional activation/repression.

The main goal of the present study is to shade light on new possible functional and physical interactions between N-Myc and the two protein factors strictly associated with histone methylation: WDR5 and LSD1.

WDR5 METHYLTRANSFERASE

After the discovery of the COMPASS methyltransferase complex (complex of proteins associated with Set1) in *yeast*, in mammals too more than six COMPASS-like complexes were revealed. Although in *yeast* Set1 is the sole catalytic subunit of COMPASS complex, in mammals the situation is more complicated because of 2 orthologs (Set1a and Set1b) and 2 paralogs (MLLs and Ash1) (Table.2).

COMPASSes are multi subunits complexes with mono-, di- or tri-methylating activity on lysine 4 of histone H3 N-tail. Affinity pull-down experiments in mammals samples revealed the presence of WDR5 protein as one of the COMPASS subunits directly interacting with H3K4 (153, 154).

In this connection, recent studies have underlined the central role of Cps30 in *yeast*, and its mammals homolog WDR5, in the catalytic activity of COMPASS complexes for H3K4Me1-Me2 recognition and tri- or di-methylation (155).

Function	Yeast COMPASS	Mammalian COMPASS/ COMPASS-like complexes
The catalytic subunit	Set1	SET1A/B; MLL1; MLL2; MLL3; MLL4
Required for H3K4me3	Cps60 (Bre2)	Ash2
Required for assembly	Cps50 (Swd1)	RBbp5
Components of the Set1 complexes	Cps40 (Spp1)	CxxC1
	Cps35 (Swd2)	Wdr82
Required for assembly	Cps30 (Swd3)	Wdr5
	Cps25 (Sdc1)	hDPY30
Components of the Set1 complexes		HCF1
Components of the MLL1/2 complexes		HCF1; Menin
Components of the MLL3/4 complexes		PTIP; PA1; NCOA6; UTX

Table.2: Yeast and mammalian COMPASS subunits and their functions (153).

The physical interaction between WDR5 and the conserved "Win" motifs of all the SET1 family members has also already been fully been demonstrated. Moreover, peptides that mimic both "Win" motif and H3K4 can distrupt the interaction between WDR5 and its partners. The actual mechanism hypothesized is the mutually exclusive binding to mono or di-methylated lysine 4 of H3 and the Win motif of Set1 proteins (155-157).

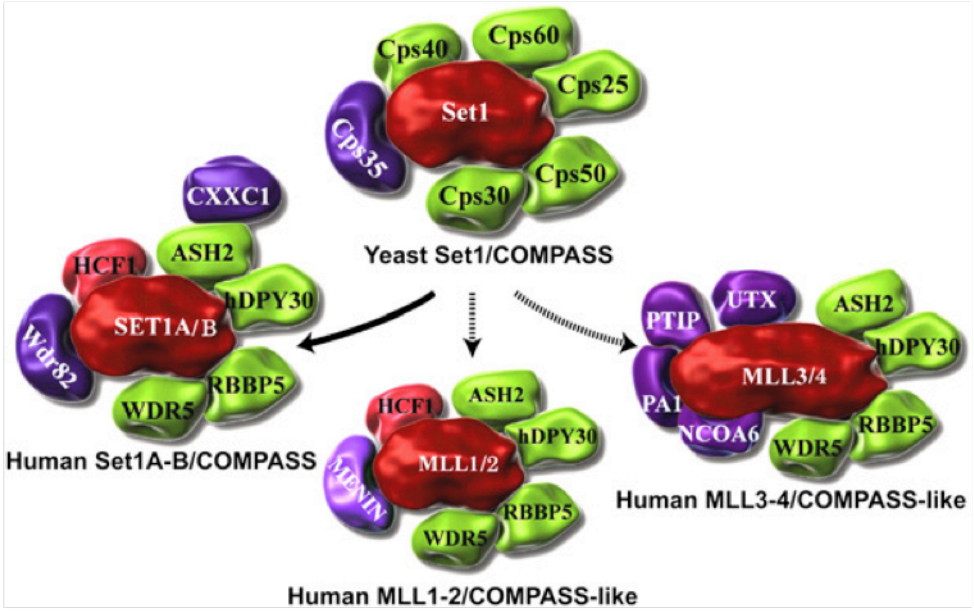

Figure 10: COMPASS and COMPASS-like complexes from yeast to human. COMPASS was identified in yeast as a complex of proteins associated with Set1 that can methylate H3 on Lys 4. Subsequently, six COMPASS-like complexes were identified in humans. All complexes share the core components Cps30 (WDR5), Cps50 (RBBP5), Cps25 (DPY30), and Cps60 (ASH2). COMPASS in humans also has CXXC and WDR82, which are homologous to Cps40 and Cps35 in yeast and regulate H3K4 trimethylation by COMPASS in vivoThe MLL3/4 complexes also contain the H3K27 demethylase UTX. The MLL1–4 COMPASS-like complexes function as coactivators of gene transcription in contrast to the canonical COMPASS complexes in yeast and humans. Set1s/MLLs are colored red, core components are colored green, and subunits with complex- specific functions are colored purple (157).

To better understand the mutual binding of WDR5 with MLL or Set1, *in-vitro* competition assays have shown that only H3K4Me1-Me2 peptides can disrupt the interaction, whereas H3K4 and H3K4Me3 cannot (156, 157). WDR5 interaction with catalytic subunits, MLL or Set1, is an essential step not only for COMPASS complex assembly but also for its core-catalytic methyltransferase activity (Figure 10)(158).

Although, most WDR5 related studies have been confined to its role in methyltransferase complexes, some recent data collected both in *drosophila* and in human cell lines, have revealed its possible role in structural nucleation of other protein complexes in which neither MLL or Set1 were detected (159).

There are very few data about WDR5 implication in carcinogenesis events. Some recent studies have revealed an important pattern of WDR5 over-expression in many human prostate cancer samples; *ex-vivo* experiments carried out on LNcaP cell line have underlined the involvement of WDR5, cooperating with H3T11P, in globally alteration of the methylation status of several AR target genes resulting in a boost of proliferation rate (154).

DE-METHYLASES AND LSD1

In general, histone methylation turn over is slower than of other histone markers, and until the discovery of enzymes capable to de-methylate this marker was believed to be "irreversible" (144).
There are at least two main models that try to explain the turnover of methyl groups on histones. One suggests direct histone tail removal (Allis et al., 1980) or replacing with the methylated histone variant (160). However, this mechanism would not allow for dynamic regulation of histone methylation and the plasticity that may be essential for gene transcription regulation in some biological processes. The second hypothesis is based on the potential activity of de-methylase enzymes that remove methyl groups from lysine and arginine, which would make dynamic regulation possible (144).
In 2004 was discovered the antagonizing activity of the human Peptidyl Arginine DeIminase 4 (PADI4/PAD4) with respect to the methylation of arginine residues (161, 162). Thus far, no specific arginine de-methylases were discovered (144). These findings suggested that histone methylation can be "contrasted" by dynamical regulation and activity of deiminase enzymes (144).
There are two main classes of histone demethylase: FAD dependent LSD de-methylases and JmjC which use Fe^{2+} and α- ketoglutarate as co-factors (144).
In 1973 Paik et colleagues first partially purified histone de-methylating catalytic activity and opened up the possibility of fully understanding the histone de-methylation pathway (163). In 2002 Bannister et al. proposed the role of some amineoxidase enzymes in histone de-methylation via an oxidation reaction that removes methyl groups from lysine or arginine residues (164). In 2004 Shi et el. discovered a protein (encoded by KIAA0601 gene) that shares significant sequence homology with FAD-dependent amine oxidases and because of its ability to specific demethylate lysine 4 of histone H3 was named as LSD1 (Lysine DeMethylase 1A) (163).
Human lysine (K)-specific histone demethylase (LSD1) is a flavin-containing amino oxidase that specifically catalyzes the demethylation of mono- and di-methylated histone H3 lysine residues through a FAD-dependent oxidative reaction. Indeed, about 70% of the C-terminal region of LSD1 displays significant sequence homology with FAD-dependent amine oxidases (163, 165).

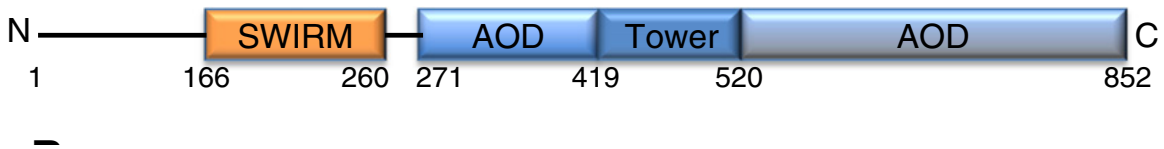

Figure 11: Schematic representation of the LSD1 protein domains organization (166).

As schematized in figure 11, LSD1 protein is composed by three domain: SWIRM (Swi3p/Rsc8p/Moira), TOWER and the Amino Oxidase domains, AOs. The N-terminal SWIRM domain interact with AO domains to form the catalytic site of non covalent FAD binding (166). LSD1 protein has been isolated as a stable component in a number of corepressor complexes(Figure 12) including CoREST, CtBP, and histone deacetylase I and II (HDAC) (167, 168).

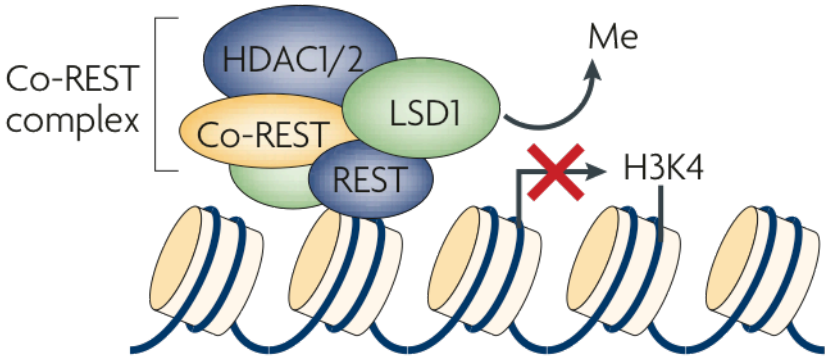

Figure 12: LSD1 as part of the Co-REST complexes contributes to repression of transcription by removing H3K4 methylation (165).

Biochemical characterization of the demethylation activity of LSD1 has shown that FAD is required during the removal of a methyl group in a reaction that produced H_2O_2 and formaldehyde as products (Figure 13) (163). Recombinant LSD1 alone can demethylates H3K4 di-methylated in histone substrates that have been stripped of associated DNA. In vitro studies have revealed that Co-REST, part of LSD1/Co-REST complexes, is required for LSD1 ability to be able to demethylate nucleosomal substrates. Indeed, reconstitution experiments using purified recombinant factors have demonstrated that an LSD1–Co-REST complex is sufficient for demethylation reaction (163, 168).

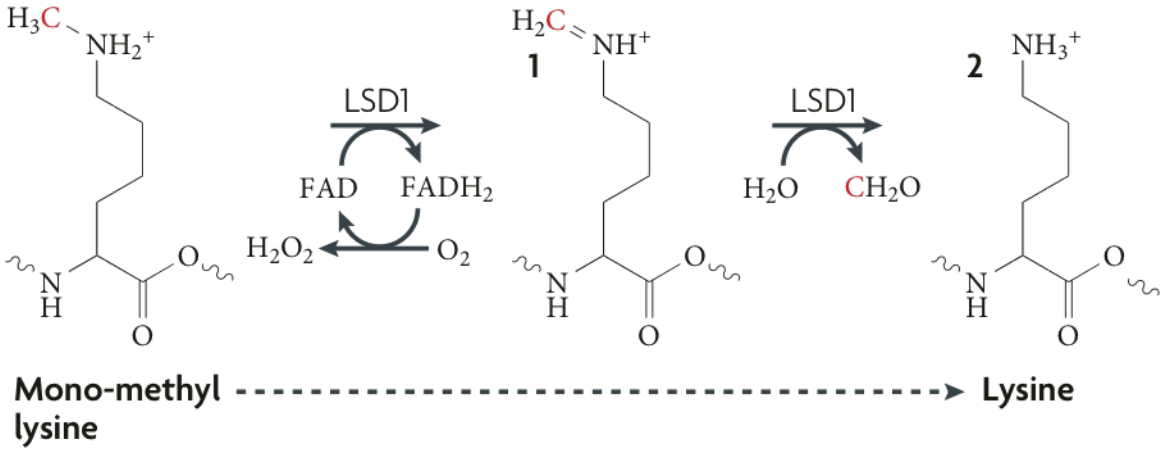

Figure 13: The LSD1 reaction mechanism detailing the removal of a mono- methyl group. LSD1 is proposed to mediate demethylation of mono- and di-methylated lysine residues through an amine oxidation reaction using FAD as a cofactor. Loss of the methyl group from mono-methyl lysine occurs through an imine intermediate (1), which is hydrolysed to form formaldehyde by a non-enzymatic process (165).

The association of LSD1 with Co-REST repression complex unquestionably suggest its role in negative transcription regulation. In 2001 Ballas et al. using mouse inducible cell lines, have reported that REST gain of function represses neural-specific gene expression and blocks the terminal differentiation process (169).

LSD1 being a component of several repressive complexes including deacetylase activity and recognizing an extended portion of the histone H3 tail, it has been hypothesized that specific recognition of lysine 4 of histone H3 might be guided by deacetylation events at other residues on the same histone tail. In support of this hypothesis, less efficiently activity of the LSD1–Co-REST complex on hyperacetylated nucleosomes has been reported (170). Further, LSD1 mediated demethylation of H3K4 peptides is completely abolished when the latter also contain acetyl groups on K9, K14 and K18. Furthermore, *in-vitro* experiments using purified factors show that demethylation of histone N-tails is favoured by the presence of HDAC1 in the LSD1–Co-REST complex (171).

Therefore, H3K4 demethylation and histone deacetylation by LSD1-containing complexes seems to be tightly coupled with both activities, contributing to the overall repressive functions of these complexes. As mentioned above, the heterogeneous methylation pattern in different N-tail residues may determine a different pattern of regulatory proteins that can both determine active transcription or repression.

In addition to its role as a repressor, LSD1, has been reported to form a complex with the androgen receptor (AR) producing a demethylase activity on H3K9, allowing it to function as a transcriptional

activator. During hormone-induced transcriptional activation, LSD1 is partially required for H3K9 demethylation and AR transactivation. The specific mechanism by which the AR alters LSD1 specificity remains unknown (172).

In 2010 Amente et al. have reported the association of LSD1 with c-Myc in Rat-1 cell line and also demonstrated the functional activity of H3K4Me2 de-methylation in c-Myc-mediated gene activation (173).

Results

NEUROBLASTOMA AND WDR5

Chromatin modifications, including histone methylation, have a crucial role in transcription mis-regulation of many cancer-related genes. Mono-, di-, and tri-methylation of H3K4 mark the promoter and enhancer regions of active genes (174, 175). These three methylation variants are deposited by the SET1/MLL histone methyltransferase (HMTase) complex (COMPASS), which, at its core, is composed of either KMT2A/MLL1, KMT2B/MLL2, KMT2C/ MLL3, KMT2D/MLL4, SETD1A, or SETD1B associated with WRAD module (WDR5, RBBP5, ASH2L, and DPY30) and other variable partners (157, 176). Interestingly, WDR5 subunit directly binds both unmodified and methylated H3K4 *in-vitro* and is required for the tri-methylation of this residue by the SET1/MLL complex (154, 156).

To this day, there are not studies focusing on the role of WDR5 in neuroblastoma cancer development and/or progression.

In collaboration with Prof. Tao Liu (CCIA-Sydney), protein expression analysis from 69 neuroblastoma tumor tissues samples (data not shown) have revealed that high levels of WDR5 protein are significantly associated with reduced overall survival.

Accordingly, meta-analyses of the publically available (*http://r2.amc.nl*) Versteeg (177) microarray gene expression datasets showed that high levels of WDR5 mRNA expression in neuroblastoma tissues are directly correlated with N-Myc mRNA expression (Versteeg dataset: R = 0.269, 95% CI = 0.06 to 0.45; P = .012)(Figure 14, upper graph) and poor overall survival rates (Figure 14, lower graph) (Versteeg dataset: HR = 4.17, 95% CI = 1.27 to 5.65; P = .0096)

Additionally, high levels of WDR5 expression in 72 N-Myc-amplified (data not shown) neuroblastoma tissues were positively associated with poor overall patient survival in the large Kocak dataset.

Based on these finding it has been decided to investigate the role of N-Myc in direct regulation of WDR5 expression and also to better define the mechanisms by which N-Myc and WDR5 can directly or indirectly interact to alter the expected neuroblastoma prognosis. Specifically, qRT-PCR expression analyses and immunoblot assays were carried out on N-Myc amplified Neuroblastoma cell lines SK-N-BE (2C) and CHP-134 to assess the role of both N-Myc and WDR5 in the alteration of WDR5, CCNE1 and MDM2 gene signature. Moreover, Ch-IP experiments were performed in order to assess the role of both N-Myc and WDR5 factors in transcription factors occupancy and H3K4Me3 signature.

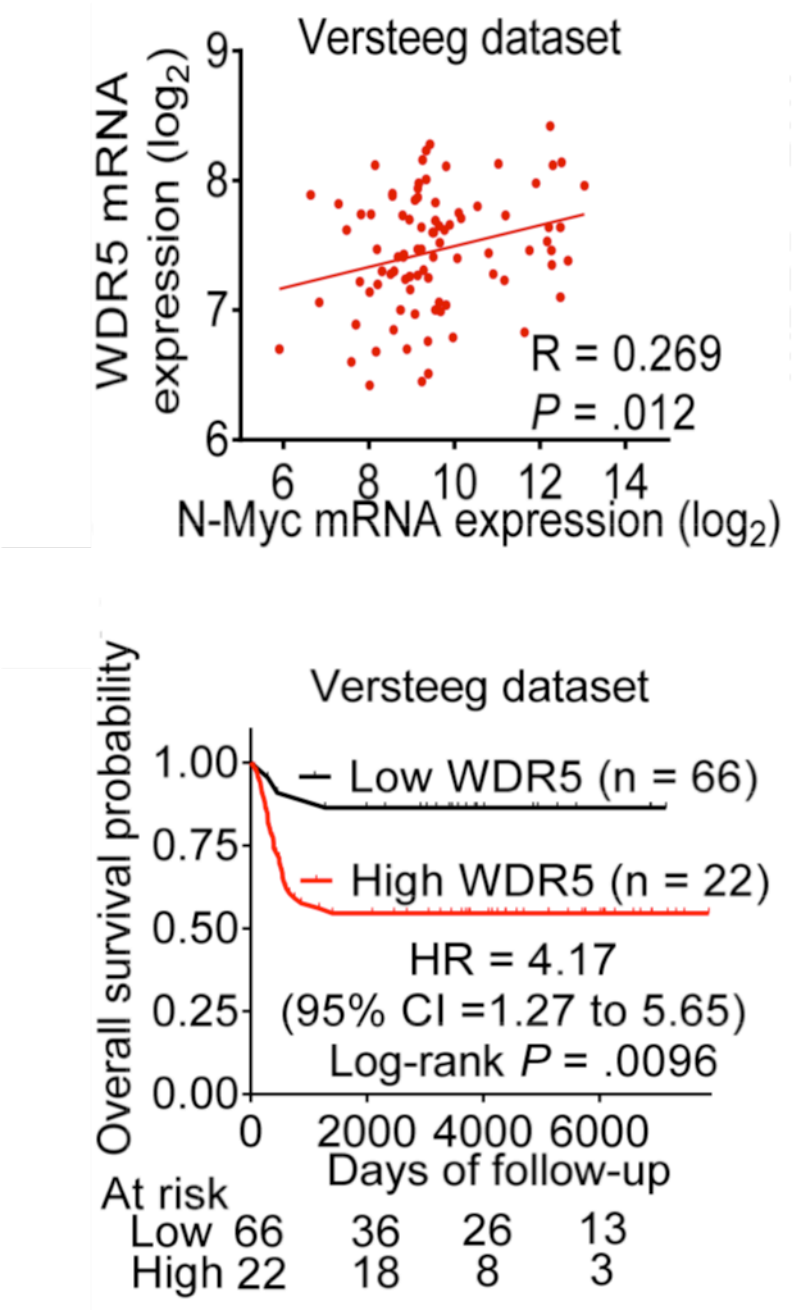

Figure 14: Prognostic significance of WDR5 expression in neuroblastoma. Upper graph, two-sided Pearson's correlation was employed to analyze correlation between WDR5 and N-Myc mRNA expression in 88 human neuroblastoma samples in the publically available microarray gene expression Versteeg dataset downloaded from R2 microarray analysis and visualization platform (*http://r2.amc.nl*). Lower graph) Kaplan–Meier curves showed the probability of overall survival of patients according to the levels of WDR5 mRNA expression in the 88 neuroblastoma patients in the Versteeg datasets.

N-MYC POSITIVELY REGULATES WDR5 EXPRESSION BY DIRECLY BINDING E-BOXES

N-Myc activates gene transcription by binding to E-Box sequences at target gene promoters (33).
In silico analysis of WDR5 gene promoter have revealed two non-canonical (CACGCG) (-13 to -18 bp) and two canonical (CACGTG) (+85 to +90 bp) E-box sequences (Figure 15, left). Based on this, it was decided to examinee whether N-Myc modulates WDR5 expression. To address this point qRT-PCR analysis and immunoblot assays were performed in the N-Myc-amplified human neuroblastoma cell lines, SK-N-BE(2)-C and CHP134. Specifically, siRNA silencing of N-Myc (20pmol 72h) was performed in both cell lines to seek differences in WDR5 RNA and protein level. All the qRT-PCR experiments were carried out in triplicate and the reference genes used for 2^(-DDCT) normalization are GUSB (GlUcuronidaSeBeta) and B2M (Beta 2 Microglobulin).
As shown in Figure 15 A and B, qRT-PCR analysis carried out on SK-N-BE (2)-C and CHP-134 transiently transfected with both N-Myc siRNA-1 or N-Myc siRNA-2 significantly reduce WDR5 mRNA level. Accordingly, western blot assays presented in figure 15 A and B confirm that N-Myc silencing lead to WDR5 repression also at protein level. As negative samples both cell lines were transfected with control siRNA.

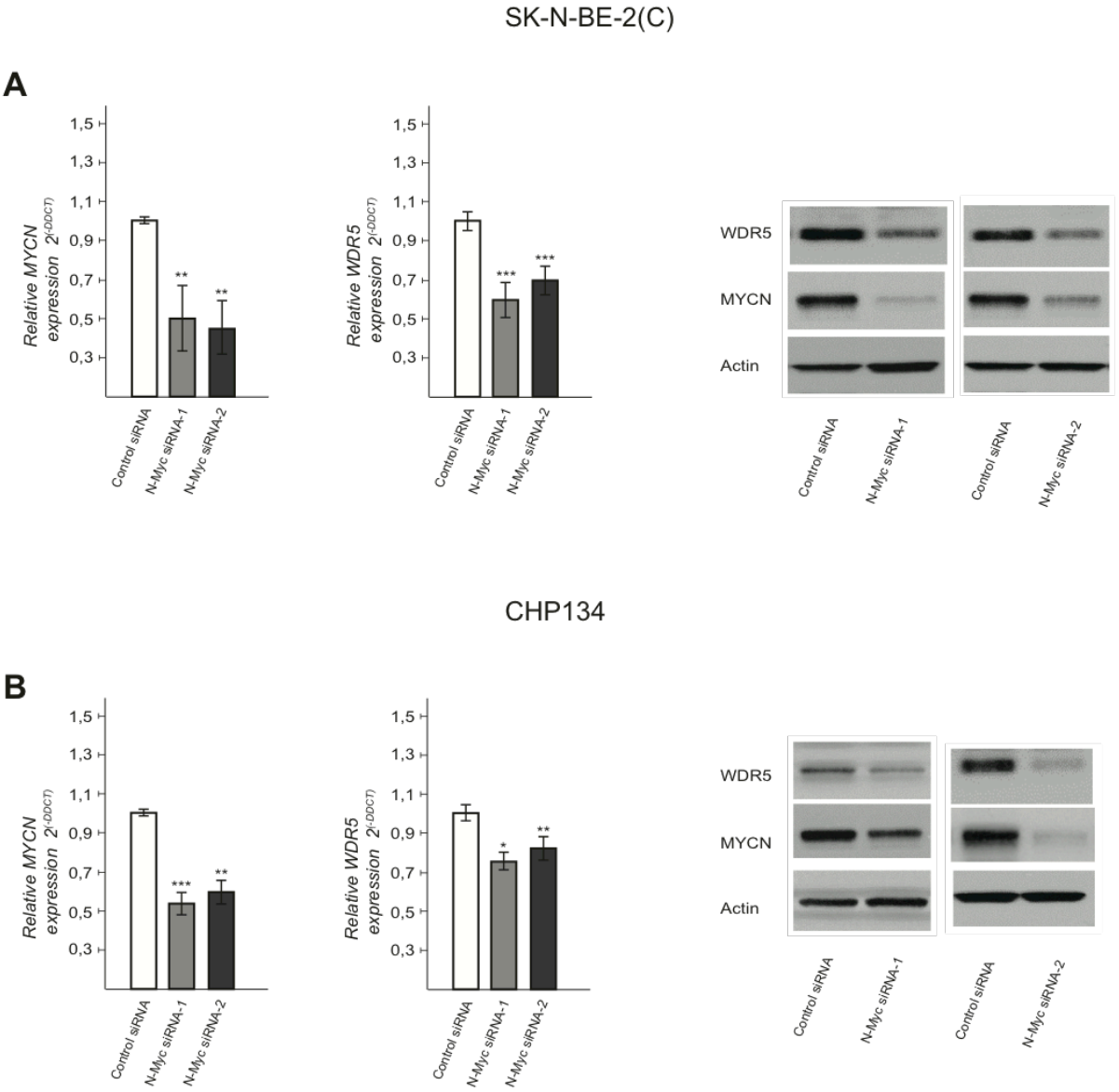

Figure 15: Effect of N-Myc on WDR5 expression. SK-N-BE(2)-C (A)and CHP134(B) cells were transfected with control siRNA, N-Myc siRNA-1 or N-Myc siRNA-2 for 72 hours, followed by RT-PCR (left) and immunoblot (right) analyses of N-Myc and WDR5 expression. White bars indicate control siRNA sample, bright grey and dark grey are respectively N-Myc siRNA-1 and 2. Statistical analysis was performed by using two-way ANOVA. Error bars represented SD. *, ** and *** indicated P < .05, .01 and .001 respectively.

To fully corroborate the hypothesis that N-Myc directly regulates WDR5 expression by binding to E-box elements, Chromatin ImmunoPrecipitation (Ch-IP) assays were performed in SK-N-BE(2)-C cells with a control (normal IgG) or monoclonal anti-N-Myc antibody. All the experiments were carried out in triplicate and the analysis of immunoprecipitated DNA was performed with Real time PCR.

As shown in Figure 16, the anti-N-Myc antibody efficiently immunoprecipitated the WDR5 gene promoter regions containing both canonical and non-canonical E-boxes (Amplicon B).

qRT-PCR, Western-blot and ChIP data strongly indicate that N-Myc up regulates WDR5 gene expression in neuroblastoma cell lines with N-Myc amplification by directly binding to the WDR5 gene promoter.

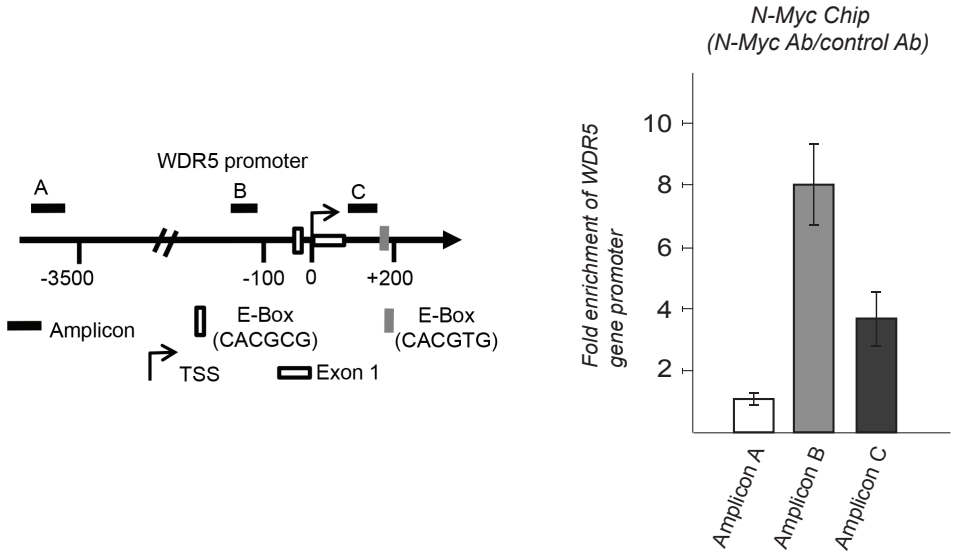

Figure 16: Schematic representation (left) of the WDR5 gene promoter. TSS represented transcription start site. ChIP assays (right) were performed with a control or anti-N-Myc antibody (Ab), followed by Real-time PCR with primers targeting the negative control region (Amplicon A, white bar) or the WDR5 gene promoter containing the E-box (Amplicons B, grey bar and C black bar) in SK-N-BE(2)-C cells. Fold enrichment of the WDR5 gene promoter was calculated as the difference in cycle thresholds obtained with the anti-N-Myc Ab and with the control Ab. Error bars represented SD.

WDR5 POSITIVELY REGULATE MDM2 EXPRESSION

As WDR5 exerts biological function by modulating gene transcription, differential gene expression studies were performed, in collaboration with Prof. Tao Liu, with Affymetrix microarray in SK-N-BE(2)-C cells, 40 hours after transfection with control or WDR5 siRNAs (data not shown). The analyses have showed that well-known N-Myc target genes CyCliN E1 (CCNE1) and MDM2 (33, 178, 179), were among the genes significantly down modulated by WDR5 siRNAs. QRT-PCR and immunoblot have validated the microarray data and confirmed that both WDR5 siRNA 1 and 2 decreased MDM2 mRNA and protein expression in neuroblastoma cell lines (Figure 17, A, B and C).

Specifically, siRNA silencing of WDR5 (20pmol 72h) was performed in both cell lines to seek differences in MDM2 RNA and protein level. All the qRT-PCR experiments were carried out in triplicate and the reference genes used for 2^(-DDCT) normalization are GUSB (GlUcuronidaSeBeta) and B2M (Beta 2 Microglobulin)

As shown in figure 17 panel A and B, both WDR5 siRNA-1 and siRNA-2 significantly reduce gene expression of WDR5, CCNE1 and MDM2 in SK-N-BE (2)-C and CHP-134 neuroblastoma cell lines. Western blot analysis (Figure 17 panel C) also demonstrate reduced MDM2 protein levels after WDR5 knocking down with both siRNA-1 and si-RNA-2. As negative samples both cell lines were transfected with control siRNA.

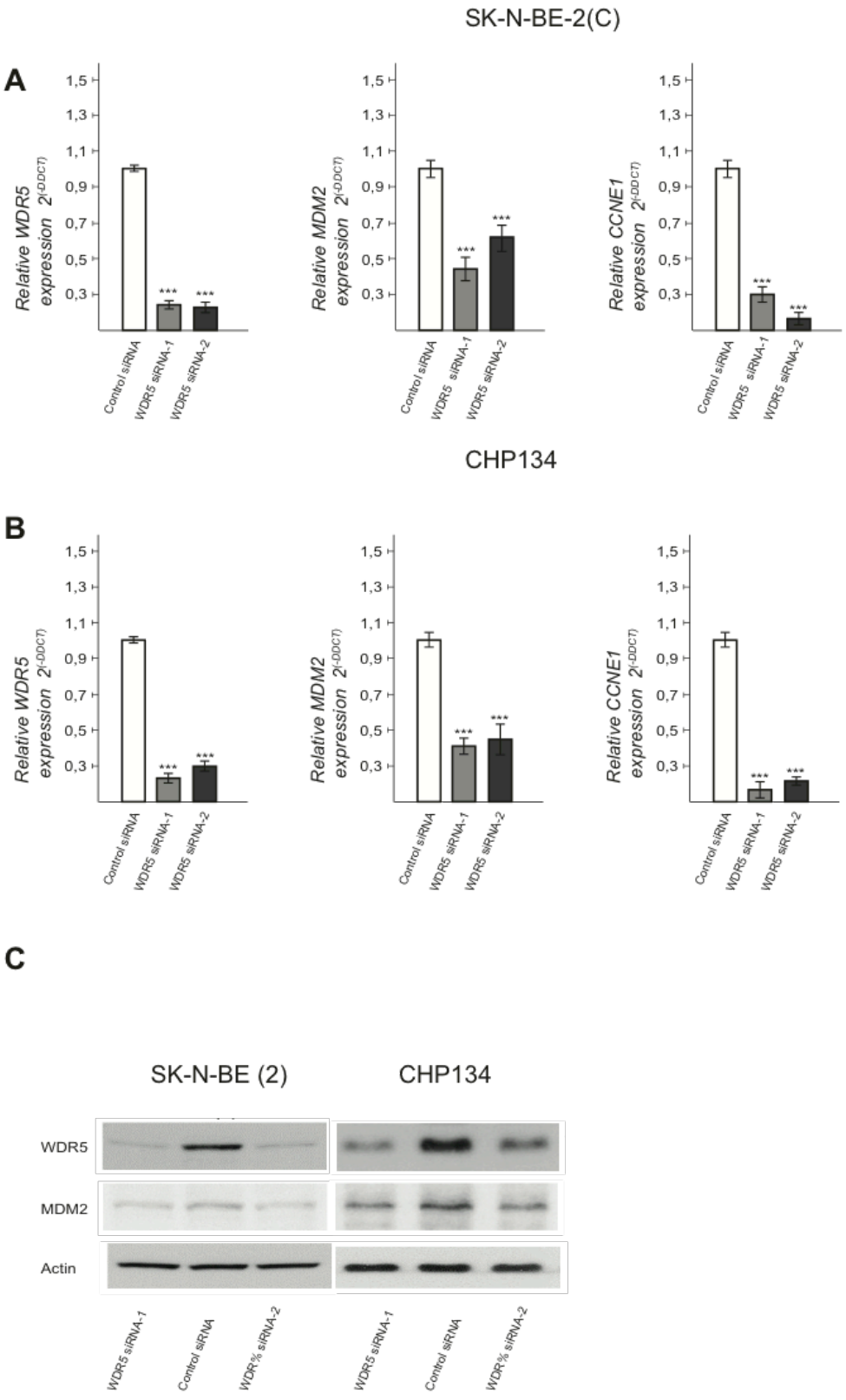

Figure 17: Effect of WDR5 on gene transcription. SK-N-BE(2)-C and CHP134 cells were transfected with control siRNA, WDR5 siRNA-1 or WDR5 siRNA-2. WDR5, CCNE1 and MDM2 mRNA (A and B) and protein expression (C) was analyzed by RT-PCR and immunoblot. White bars indicate control siRNA sample, bright grey and dark grey are respectively WDR5 siRNA-1 and 2. Statistical analysis was performed by using two-way ANOVA. Error bars represented SD. *, ** and *** indicated P < .05, .01 and .001 respectively.

WDR5 IS ESSENTIAL IN N-MYC-WDR5 COMPLEX IN BINDING MDM2 PROMOTER

Because bioinformatics analysis located a canonical E-box at the MDM2 gene promoter (Figure 18, A), we performed dual cross-linking ChIP assays in SK-N-BE(2)-C cells with control, anti-N-Myc and anti-WDR5 antibodies, followed by Real time PCR with specific primers targeting a negative control region or the MDM2 gene promoter. The results showed that the anti-N-Myc and the anti-WDR5 antibodies efficiently immunoprecipitated the MDM2 gene promoter region containing the E-box, compared with the negative control region (mean fold of control antibody ± SD: N-Myc antibody, 7.48 ± 3.91; WDR5 antibody, 31.47 ± 4.28; $P < .01$, two-way ANOVA) (Figure 18, B).

To understand whether WDR5 is essential for both histone H3K4 trimethylation and N-Myc binding to the MDM2 gene promoter, we transfected SK-N-BE(2)-C cells with control or WDR5 siRNAs, followed by ChIP assays with a control, anti-N-Myc or anti-tri-methylated H3K4 (H3K4me3) antibody. QPCR analyses have showed that knocking-down WDR5 expression significantly reduced the N-Myc occupancy (mean fold of N-Myc/control antibody ± SD: control siRNA-1, 5.37 ± 2.17; WDR5 siRNA-1, 2.92 ± 1.04; WDR5 siRNA-2, 3.24 ± 1.09) and trimethylation of histone H3 lysine 4 (mean fold of H3K4me3/control antibody ± SD: control siRNA-1, 1197 ± 971.6; WDR5 siRNA-1, 413.7 ± 236.1; WDR5 siRNA-2, 279.5 ± 387.3) ($P < .001$, two-way ANOVA) at the MDM2 gene promoter in SK-N-BE(2)-C cells (Figure 18, C and D).

Collectively, these data suggest that both WDR5 binding and activity are probably required for N-Myc protein binding and histone H3K4 trimethylation at the MDM2 gene promoter.

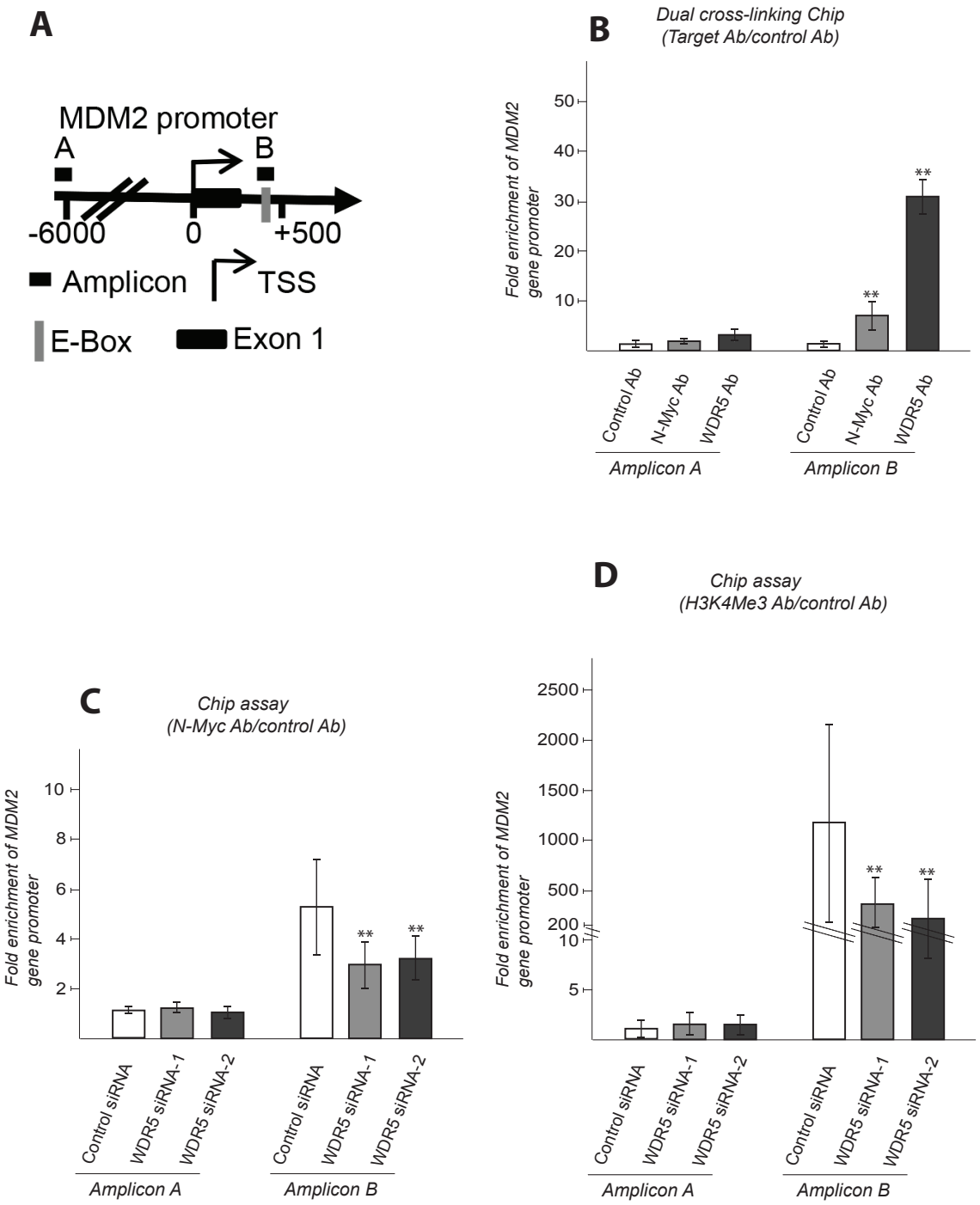

Fig.18: A) Schematic representation of the MDM2 gene promoter containing the N-Myc binding E-box. B) Dual cross-linking ChIP assays were performed in SK-N-BE(2)-C cells with control, anti-N-Myc and anti-WDR5 antibodies (Abs), followed by qPCR with primers targeting the negative control region (Amplicon A) and the N-Myc binding site (Amplicon B) of the MDM2 gene promoter. C-D) SK-N-BE(2)-C cells were transfected with control siRNA, WDR5 siRNA-1 or WDR5 siRNA-2 for 48 hours, followed by ChIP assays with a control IgG, anti-N-Myc (C) or anti-tri-methyl H3K4 (H3K4me3) (D) Ab, and qPCR with primers targeting the negative control region or the E-box of the MDM2 gene promoter. Fold enrichment of the MDM2 promoter region was calculated as the difference in cycle thresholds obtained with the specific Ab and with the control IgG. Error bars represented SD. *, ** and *** indicated P < .05, .01 and .001 respectively.

N-MYC AND WDR5 FORM A PROTEIN COMPLEX

As histone H3K4 trimethylation is essential for Myc binding to target gene promoters and WDR5 induces histone H3K4 trimethylation (70, 180), it has been examined whether N-Myc and WDR5 formed a protein complex. To address this point Co-immunoprecipitation assays were performed on SK-N-BE-(2C) neuroblastoma cell line. Specifically, 1mg of crude nuclear protein extract from SK-N-BE-(2)-C was immunoprecipitated with specific antibodies against N-Myc and WDR5. Normal IgG were used as negative control. Recombinant-Protein A sepharose beads were used for protein complexes isolation. After elution, immunoprecipitated samples were analysed by western blot. As shown in figure 19, anti-N-Myc antibody efficiently co-immunoprecipitated WDR5 protein, and accordingly, anti-WDR5 antibody efficiently co-immunoprecipitated N-Myc protein (Figure 19), demonstrating that the two proteins form a protein complex.

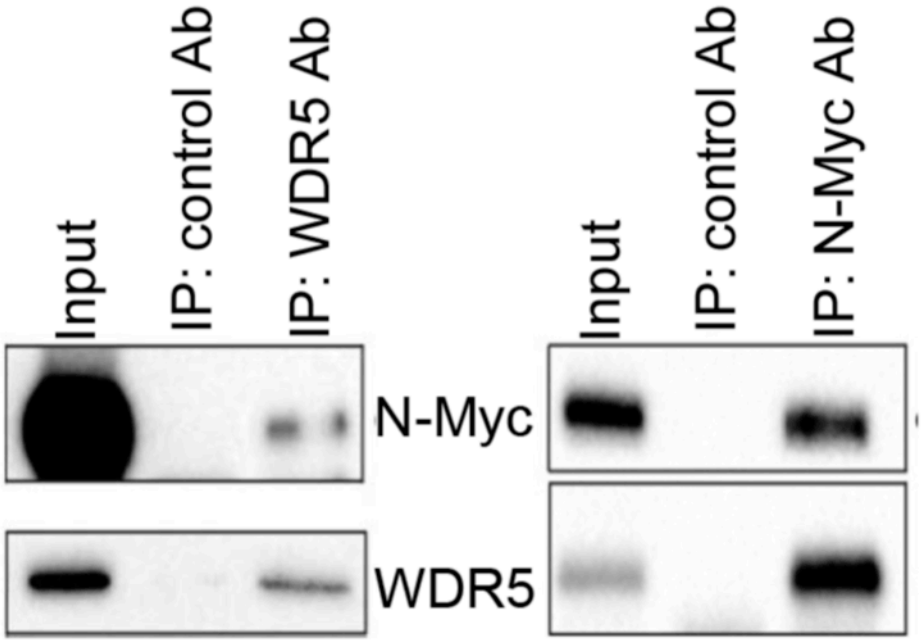

Figure 19: Co-IP assay, 1mg of crude nuclear protein extract from SN-K-BE(2) neuroblastoma cells was immunoprecipitated (IP) overnight with 2 µg of control IgG, anti-N-Myc or anti-WDR5 antibody (Ab). Immunoprecipitated protein was immunoblotted with anti-WDR5 or anti-N-Myc Ab.

WDR5 SILENCING DECREASE N-MYC TRANSACTIVATING POTENTIAL ON MDM2 PROMOTER

Next, Tet-21/N neuroblastoma cells were treated with vehicle control or tetracycline to induce or not to induce exogenous N-Myc expression, respectively (26). The cells were then co-transfected with control or WDR5 siRNAs, together with a pGL3 luciferase report construct expressing wild type or E-box mutant MDM2 gene promoter (178).

Luciferase assays showed that N-Myc induction resulted in a significant increase in luciferase activity in cells transfected with the wild type, but not the E-box mutant, MDM2 promoter construct. In addition, WDR5 siRNAs considerably reduced N-Myc-mediated wild-type MDM2 promoter activity [mean fold of N-Myc (+)/N-Myc (-) ± SD: control siRNA-1, 3.51 ± 0.40; WDR5 siRNA-1, 2.04 ± 0.35; WDR5 siRNA-2, 2.15 ± 0.76; P < .001, two-way ANOVA) (Figure 20). Taken together, the data suggest that WDR5 forms a protein complex with N-Myc at the N-Myc target MDM2 gene promoter, leading to histone H3K4 trimethylation and N-Myc target gene transcription.

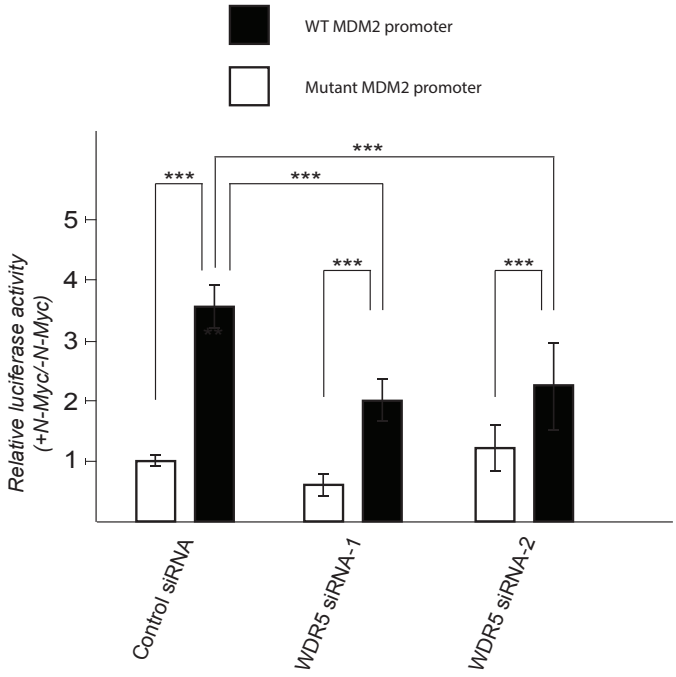

Figure 20: Tet-21/N neuroblastoma cells were cultured with tetracycline to not induce, or without tetracycline to induce, N-Myc expression, respectively. The cells were co-transcfected with a luciferase reporter construct expressing wild type or E-box mutant MDM2 gene promoter, together with control siRNA, WDR5 siRNA-1 or WDR5 siRNA-2. Luciferase assays were performed, and relative luciferase activity of the wild type and the mutant MDM2 promoter constructs under the N-Myc (+) condition was normalized by the luciferase activity of the same reporter construct under the N-Myc (-) condition. Error bars represented SD. *, ** and *** indicated P < .05, .01 and .001 respectively.

N-MYC AND LSD1

Childhood neuroblastoma is the most common solid tumour of infancy, and is highly refractory to therapy. One of the most powerful prognostic indicators for this disease is the N-Myc gene amplification, which occurs in approximately 25% of neuroblastomas (181). The N-Myc oncoprotein is a member of the well-known family of transcription factors MYC, belong to a subset of the larger class of proteins containing Basic-Region/Helix–Loop–Helix/Leucin-Zipper (BR/HLH/LZ) motif. Trough BR/HLH/LZ domain N-Myc interact with MAX (Myc Associated X-factor), and as heterodimers they act as transcription regulator. As mentioned above, N-Myc can be part of different chromatin regulating complexes composed by several components including histone modifiers (45). There is extensively documented the role of N-Myc protein in negative transcription regulation of many cancer related genes involved in several important biological processes like cell cycle control and migration/motility behaviours (37).

In 2013 Corvetta et al. have carried out a deep investigation into mechanism of N-Myc negative regulation against the neuroblastoma oncosuppresor Clusterin (CLU) through direct binding to non-consensus E-box sequences. They also demonstrated the physical and functional interaction between N-Myc and EZH2, methyltransferase part of the Polycomb Repression complex 2 (111). There has also been extensive discussion of the role and actual mechanism of both c-Myc and N-Myc in negative regulation of CKN1A(p21) gene signature.

It was previously reported that LSD1 expression inversely correlates with differentiation status of primary neuroblastic tumors. Consistently, in vitro differentiation assays performed on neuroblastoma cells have clearly indicated a down-regulation of LSD1, and accordingly inhibition or knockdown of LSD1 resulted in differentiation events and reduced cells viability (182). In 2010 Amente et al. have largely discussed the role of c-Myc in LSD1 recruitment on MYC target genes during early transcription events (173).

The present study explored the functional and physical interaction between N-Myc and LSD1 in modify transcription profiles of two neuroblastoma critical genes, CKN1A(p21) and CLU. Specifically, *ex-vivo* and *in-vitro* techniques have suggested that Myc Box III of N-Myc is involved in N-Myc-LSD1 complex. Moreover, qRT-PCR analysis have underlined the critical role of both factors in negative modify CKN1A(p21) and CLU gene signature. Pharmacological treatment was also performed that was intended to inhibit both N-Myc and LSD1 activity to investigate changes in neuroblastoma in cell viability and apoptosis.

LSD1 INTERACTS WITH N-MYC

LSD1 can form different transcription complexes possessing either repression or activation capacities. As already mentioned, c-MYC interacts with LSD1 and because c-MYC and N-Myc proteins are extensively conserved both structurally and functionally, it has been decided to determine whether LSD1 and N-Myc can associate with one another in a neuroblastoma cellular context. In figure 21 panel C are depicted different fragments of N-Myc used for both *ex-vivo* and *in-vitro* pull down assays. Co-immunoprecipitation assays were performed in the human N-Myc amplified SK-N-BE- (2)-C neuroblastoma cell line. Specifically, 500ug of crude nuclear extracts were immunoprecipitated with an monoclonal antibody against N-Myc and normal IgG as negative control. Immuno-complexes were purified using recombinant protein-G, eluted and then separated by SDS-PAGE. Immunoblot analysis have revealed that only N-Myc-IPs extracts can efficiently pull-down endogenous LSD1, demonstrating that high levels of N-Myc can form a complex with LSD1 (Figure 20A).

To better characterize the N-Myc domain involved in N-Myc-LSD1 complex formation pull-down assays were carried out, both *ex-vivo* and *in-vitro,* using mutant recombinant N-Myc proteins.

Specifically, HEK-293T cells were co-transfected with expression vectors encoding human full-length LSD1 together with a series of N-Myc expressing vectors containing different cDNA deletions, d1(1-300aa), d2(1-134aa),and d3(20-90aa). Crude cell extracts were immunoprecipitated with a N-Myc specific antibody, purified and separated by SDS-PAGE. Western blots analyses, as shown in Figure 21 (panel B), have revealed that LSD1 co-immunoprecipitation was not observed with extracts from cells co-transfected with N-Myc mutant **d1**, while **d2** and **d3** deletion constructs retain the ability to bind LSD1. These results suggest that MYC-Box III is involved in interaction between N-Myc and LSD1 (Figure 21, A and B). To confirm *in-vitro* which N-Myc domain can interact with LSD1, a pull down assay was set up using 7 GST-N-Myc overlapping fragments (from N1 to N4B, Figure 21, panel C) and recombinant full length LSD1_3xFlag protein. The seven segments were expressed in E.Coli (BL-21 strain) and then GST recombinant proteins were purified on Gluthatione agarose beads (Sigma-Aldrich). 40µg of crude nuclear protein extracts from HEK-293T cells transiently over expressing exogenous LSD1_3xFlag were incubated with Glutathione agarose beads coated with all the seven GST-N-Myc segments. Protein complexes purified were eluted and the interaction between recombinant GST-N-Myc fragments and exogenous LSD1_3xFlag was determined by western blot analysis using specific antibody against 3xFlag and

GST (Figure 21, panel D). Consistently with Co-immunoprecipitation assay result (Figure 21, panel A), only one distinct region of N-Myc, containing the MB III domain, can interact with LSD1.

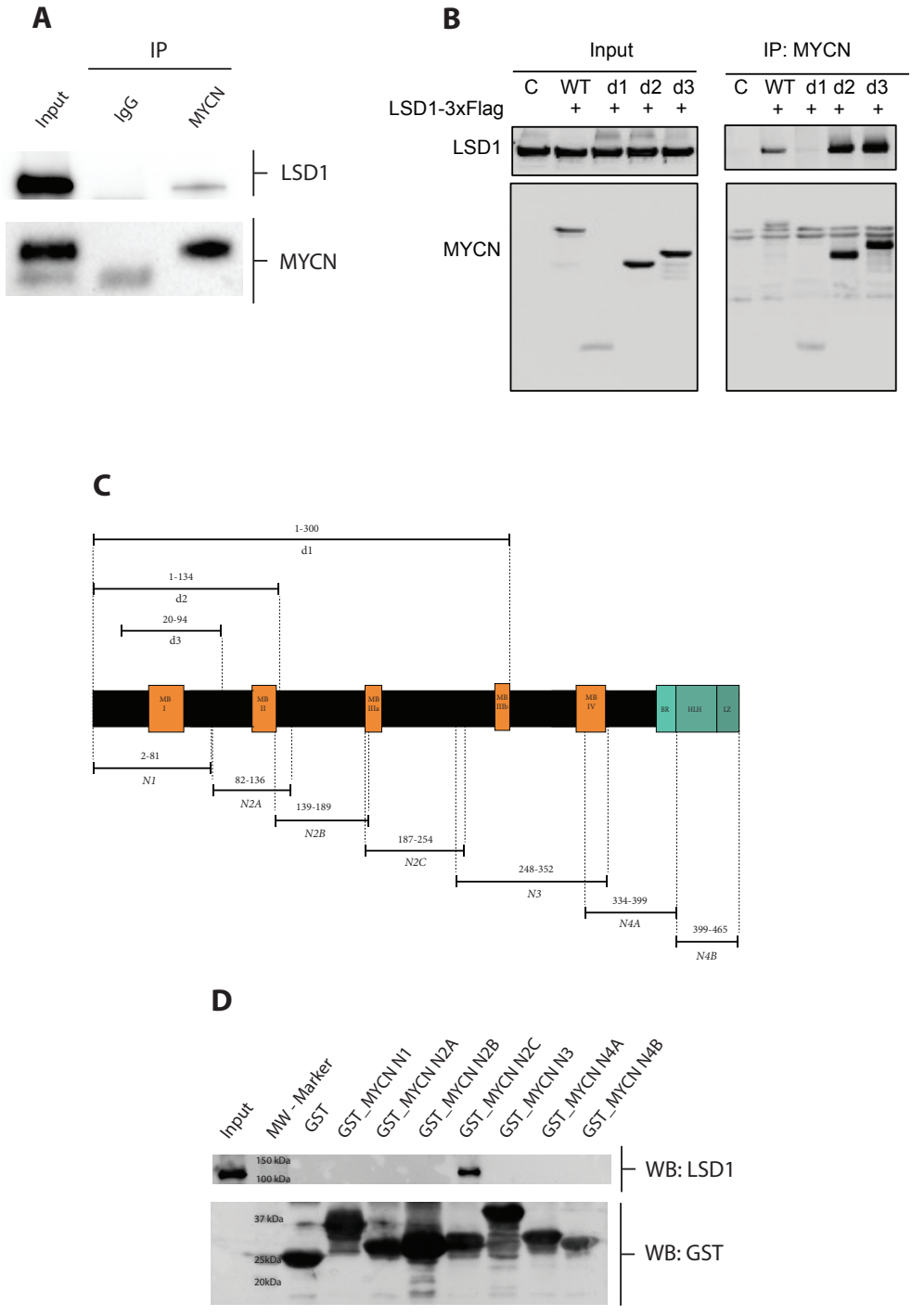

Figure 21: N-Myc physically interacts with LSD1. A, co-immunoprecipitation assay between endogenous LSD1 and N-Myc in SK-N-BE (2C) cells. Nuclear lysates from SK-N-BE (2C) cells were immune-precipitated with a N-Myc antibody and a generic IgG antibody was used as negative control. Western blot analysis was performed on immuno-purified extracts with N-Myc and LSD1 antibodies as indicated. B, N-Myc-LSD1 interaction. 293T were cells co-transfected with an LSD1 expression vector together with different N-Myc deletion expression vectors indicated in panel C. Extract from transfected cells were

Immuno-precipitated with a N-Myc antibody and analyzed by western blotting. C, schematic representation of N-Myc deletion mutants d1, d2 and d3 used in the CoIP assay and of GST-N-Myc constructs used in GST-pull down described in panel D. D, immobilized GST- N-Myc polypeptides were incubated with equal amounts of extract prepared from HEK 293T cells transfected with the recombinant vector LSD1-3xFLAG protein, separated by SDS-PAGE, and probed with an anti-LSD1 antibody.

LSD1 INHIBITION RELEASES N-MYC-MEDIATED REPRESSION OF CDKN1A

To examine the putative LSD1 role in N-Myc mediated transcription it has been decided to investigate the relative levels of CKN1A(p21) gene expression in relation to N-Myc and LSD1 expression in the conditional (TET-OFF system) neuroblastoma N-Myc expressing SHEP Tet-21/N cells in the presence or absence of functional LSD1. The relative RNA expression levels of N-Myc, LSD1 and CDKN1A(p21) were determined by qRT-PCR in tetracycline treated (High N-Myc) and untreated cells (Low N-Myc), in the presence or absence of functional LSD1 obtained through pharmacological functional inhibition by tranylcypromine (TCP). Furthermore, the expression of above cited genes has also been analysed after LSD1 expression ablation using its sequence-specific sh-RNA (sh-LSD1) using Sh-RNA non silencing as control. Western blot analysis of Sh-RNA efficiency to knock-down LSD1 protein levels is presented in figure 22 panel D. The experiments were performed in triplicate and statistical significance was calculated by two-way ANOVA algorithm.

Congruously with previous studies, Tet-21/N cells displayed CKN1A(p21) de-expression in function of N-Myc levels while LSD1 expression is not affected by N-Myc variations(Figure 22, A). Interestingly, we found that 12h of TCP treatment (1mM) as well as specific LSD1 silencing by sh-RNA de-represses CKN1A(p21) expression also in presence of N-Myc over-expression. These findings are consistent with a functional role of LSD1 in N-Myc-mediated repression of CKN1A(p21) (Figure 22,B).

To further corroborate these results it has been used a different approach to modulate N-Myc expression. Tet-21/N cells were treated for 7 days with tetracycline to lowering N-Myc levels (Figure 22,C, black bar), then after washing out of tetracycline, cell samples were collected at 12 hrs in the presence or absence of TCP (Figure 22,C, respectively grey and green bars). As shown in Figure 22 panel C, mRNA N-Myc levels were strongly induced after 12h of tetracycline removal. Conversely, LSD1 expression was largely unaffected. Re-activation of N-Myc (monitored 12 hrs after tetracycline removal) coincided with CKN1A(p21) repression, and this repression was counteracted by TCP treatments (Figure 22 C, green bar). Collectively, these results highlight the crucial role of LSD1 in N-Myc-mediated repression o CKN1A(p21) and demonstrate that LSD1 inhibition is sufficent to de-repress CKN1A(p21) expression in presence of high levels of N-Myc.

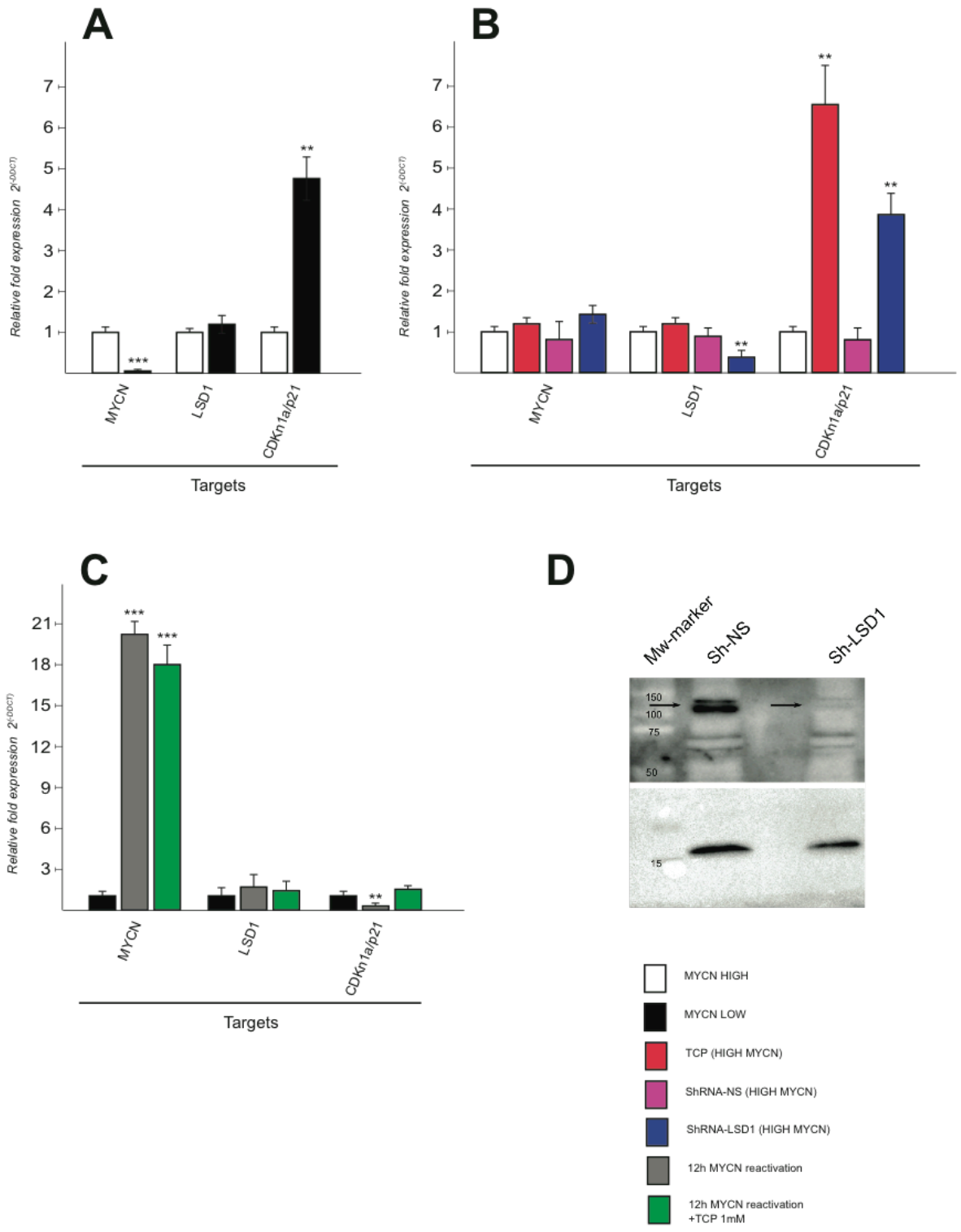

Figure 22: Relative fold expression levels of N-Myc, LSD1 and CKN1A(p21) were determined by qRT-PCR analysis with the indicated targets and samples by using GUSB as reference target and N-Myc HIGH (White bar) as reference sample for panel A and B and N-Myc LOW (Black bar) for panel C. Panel D, western blot analysis of transiently (48h) transduction of TET-21/N with ShRNA non silencing and LSD1. Statistical analysis was performed by using two-way ANOVA Error bars represented SD. *, ** and *** indicated P < .05, .01 and .001 respectively.

N-MYC AND LSD1 CO-LOCALIZE AT CDKN1A(P21) PROMOTER

Expression analysis carried out on TET-21/N cells (Figure 23) clearly revealed the significant role of both N-Myc and LSD1 factors in CDKN1A(p21) negative gene regulation.

To determine whether LSD1 directly binds regulatory elements of CKN1A(p21) gene, we performed ChIP assays on TET-21/N cells to monitor the relative binding of N-Myc and LSD1 in a condition of low N-Myc (1 week of tetracycline treatment), high N-Myc (no tetracycline treatment), in the presence or absence of functional LSD1 (TCP treatment) and by sh-RNA-mediated silencing of LSD1 expression. Immunoprecipitated samples were analysed by qPCR using specific primers for Transcriptional Start Site (TSS) region in the CDKN1A(p21) promoter and the upstream region (-3,3kb) was used as negative control. Data from three independent Chromatin-IP assays were used to make % of input graphs presented in Figure 23. Five different experimental conditions were designed to conditionally alter both N-Myc and LSD1 expression level and/or activity: N-Myc low (white bar), N-Myc high (black bar), Short hairpin non silencing-control (white bar with rhombi), TranylCyPromine TCP (grey bar) and Short hairpin LSD1 (bar with slanting lines). Specifically, N-Myc and LSD1 protein level were reduced by using respectively tetracycline treatment (one week 1μg/ml) and Short hairpin RNA against LSD1(48h), whereas LSD1 activity was reduced using TCP (Monoamine oxidase inhibitor) treatment for 12 hours at 1mM.

As shown in Figure 23 (upper side) both N-Myc and LSD1 binds TSS region of CDKN1A(p21) gene promoter in TET-21/N cells with high level of N-Myc. Both TCP treatment and Short hairpin LSD1 silencing didn't affect N-Myc binding, while a decrease of LSD1 occupancy is registered in case of low N-Myc condition. These data strongly suggest the role of N-Myc in LSD1 recruitment at TSS level of CDKN1A(p21) promoter.

To fully corroborate the hypothesis by which N-Myc-LSD1 complex can negatively affect transcription of CKN1A(p21) gene, were also performed Chromatin-IP assays for four different Histone modification: H3 pan acetylated, H3K4Me2, H3K27Me3 and H3K9Me2.

As shown in Figure 23 (middle part, left side) there is a strong repression of H3 acetylation, positive transcription histone marker, in samples with high level of N-Myc. Coherently with expression data carried out in high N-Myc condition, both LSD1 silencing (Sh-LSD1) and inhibition (TCP) determine a huge increase of H3 Acetylation at TSS level of CKN1A(p21) promoter.

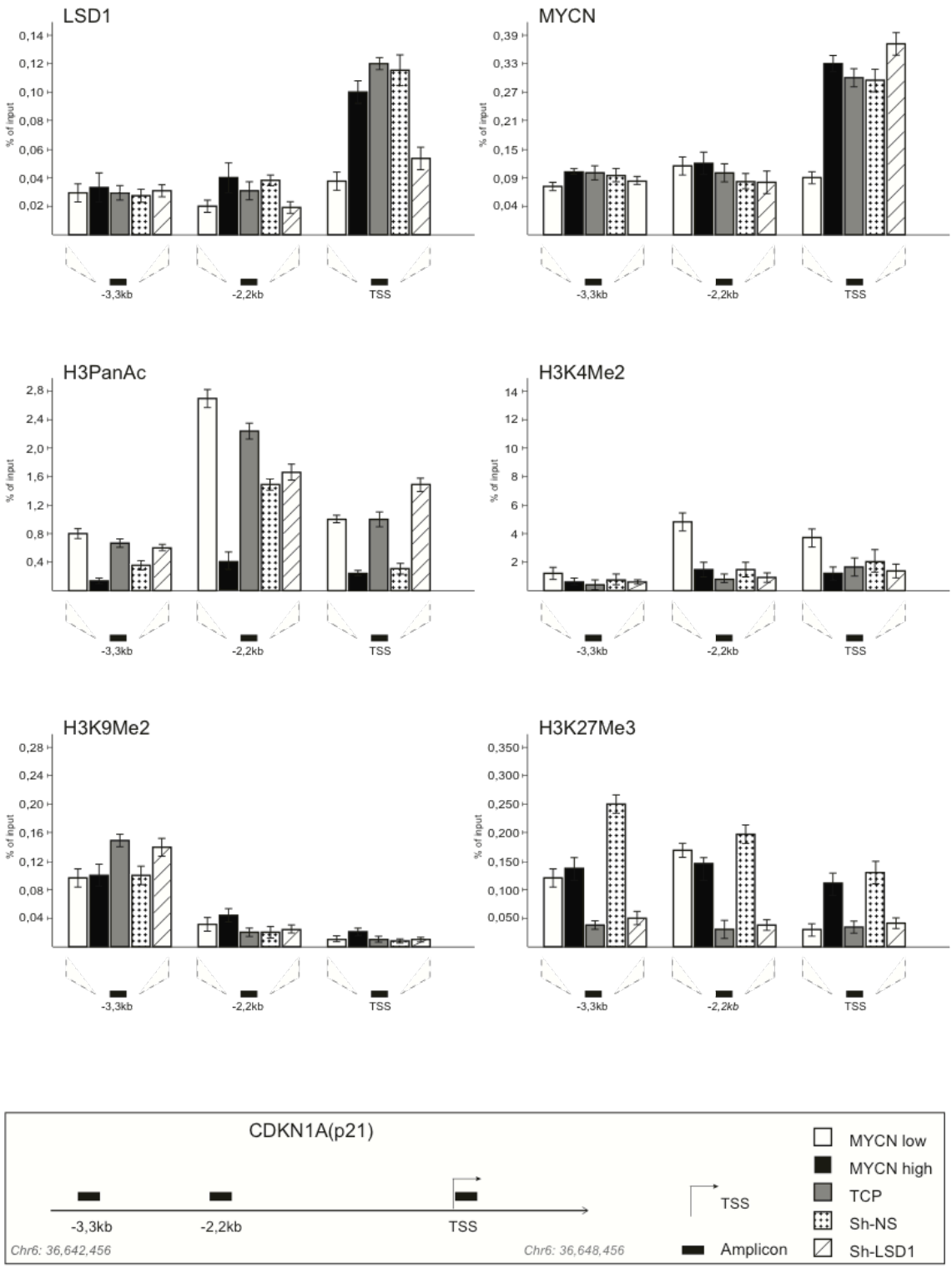

Figure 23: LSD1 and N-Myc bind and repress CKN1A(p21). Chromatin immunoprecipitation assays. N-Myc, LSD1, antibodies were used in IPs. Immunoprecipitated samples were analyzed by qPCR using specific primers for CDKN1A promoter Transcriptional Start Site (TSS) and two upstream regions (-3.3 and - 2,2 Kb). N-Myc-low (white bars), N-Myc-high (black bars), N-Myc-high TCP treated (grey bars), N-Myc-high shNS (dotted bars) N-Myc-high sh-LSD1 (diagonal stripes bars). LSD1 silencing in Tet-21/N cells transduced with shLSD1 and with sh-control was assayed by western blot shown infigure 22. Histone modifications at CKN1A(p21) promoter. H3Ac, H3K27me3, H3K4me2 and H3K9Me2 antibodies were used in IPs. Data from three independent ChIP assays and presented as % of input along with standard deviations, n=3.

As negative transcription histone marker was analysed tri-methylated Lysine 27 of Histone H3.
Data presented in Figure 23 (lower side) show an almost 3 fold increase of H3K27Me3 histone marker level in case of N-Myc repression, whereas both LSD1 silencing and inhibition cause a decrease of this negative histone marker.
Chromatin-IP assays were also performed on di-methylated Lysine 4 and 9 of histone H3 (Figure 23, middle part right side and bottom part left side). H3K4Me2 and H3K9Me2 are also specific substrates of LSD1 de-methylation activity. Consistently with the important repressive role of N-Myc in CKN1A(p21) transcription, high N-Myc level determine an almost 3 fold decrease of H3K4Me2 signal, whereas H3K9Me2 it seems to be not affected. Interestingly and coherently with data already presented by Lim S. et collegues (183), both inhibition and repression of LSD1 did not seems to affect H3K4Me2 signature at TSS level of CDKN1A(p21) promoter. H3K9Me2 modification have also shown no important changes in all the experimental conditions used.
Collectively, our findings suggest that both N-Myc and LSD1 bind to and repress CDKN1A(p21) promoter, and lowering N-Myc levels as well as LSD1-knockdown by shRNA decrease LSD1 recruitment resulting in re-activation of CDKN1A(p21) expression.

LSD1 AND N-MYC COOPERATIVELY REPRESS CLUSTERIN EXPRESSION

It has been recently shown that N-Myc interacts with EZH2, a component of the Polycomb repressor complex PCR2 and that the N-Myc/EZH2 complex represses the tumor suppressor gene Clusterin CLU (111). Because LSD1 can form complexes with both N-Myc and EZH2 we hypothesize that LSD1 could contribute to CLU gene expression.

To prove the function of LSD1 in CLU expression we treated Tet-21/N cells with TCP or knocked down LSD1 expression using its sequence-specific siRNA. Consistent with a repressive function of N-Myc (111), CLU expression is increased in Tet-21/N- cells treated with Tetracycline to lowered N-Myc expression. Thus, CLU expression inversely correlates with N-Myc relative expression levels. Interestingly, TCP treatment and LSD1 silencing by shRNA de-repress CLU expression even in the presence of N-Myc over-expression (Figure 24). These findings are consistent with a functional role of LSD1 in N-Myc-mediated repression of CLU.

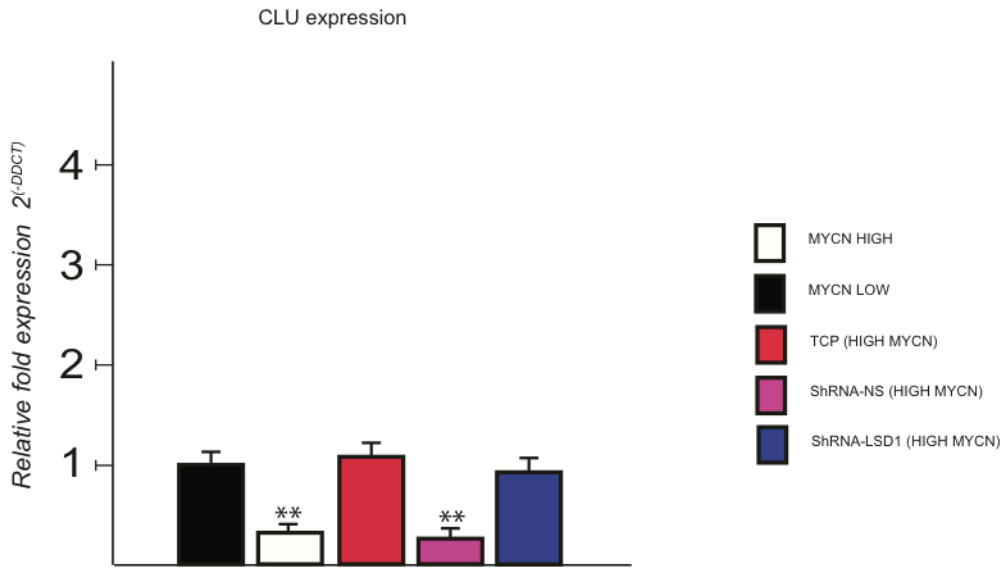

Figure 24: LSD1 and N-Myc cooperatively repress CLU expression. CLU gene expression was analyzed by qRT- PCR, using samples prepared from N-Myc-low cells and N-Myc-high cells untreated and treated with TCP or siLSD1 as indicated. Statistical analysis was performed by using two-way ANOVA Error bars represented SD. *, ** and *** indicated P < .05, .01 and .001 respectively.

To further determine whether LSD1 directly controls CLU expression we conducted ChIP assays in high or low expressing N-Myc Tet-21/N cells. Both N-Myc and LSD1 are recruited at the chromatin regulatory region of CLU, and accordingly with previous study, N-Myc binding to CLU promoter is a function of N-Myc abundance and LSD1 inhibition or protein ablation by shRNA does not reduce binding (Figure 25). It has also been revealed that LSD1 binds to CLU chromatin promoter and this binding increases in function to N-Myc abundance. ShRNA-mediated LSD1-knockdown decreases the amount of LSD1 recruitment at the gene promoter while TCP treatment does not have any effect. Next, ChIP analysis have been carried out to determine modified histones at the CLU promoter. Like in low-expressing N-Myc, shRNA-mediated knockdown of LSD1 enhanced H3-acetylation and it attenuated H3K4me27 (Fig 25), consistent with the induction of CLU expression in these cells. As already determined for N-Myc-LSD1 protein complex activity on CDKN1A(p21) Ch-IPs, H3K4Me2 and H3K9Me2 seems not to be affected by LSD1 negative silencing or repression.

Collectively, these findings suggest that both N-Myc and LSD1 bind to CLU promoter chromatin, and demonstrate that CLU expression is repressed by N-Myc/LSD1 levels and that LSD1 inhibition rescues N-Myc-dependent repression.

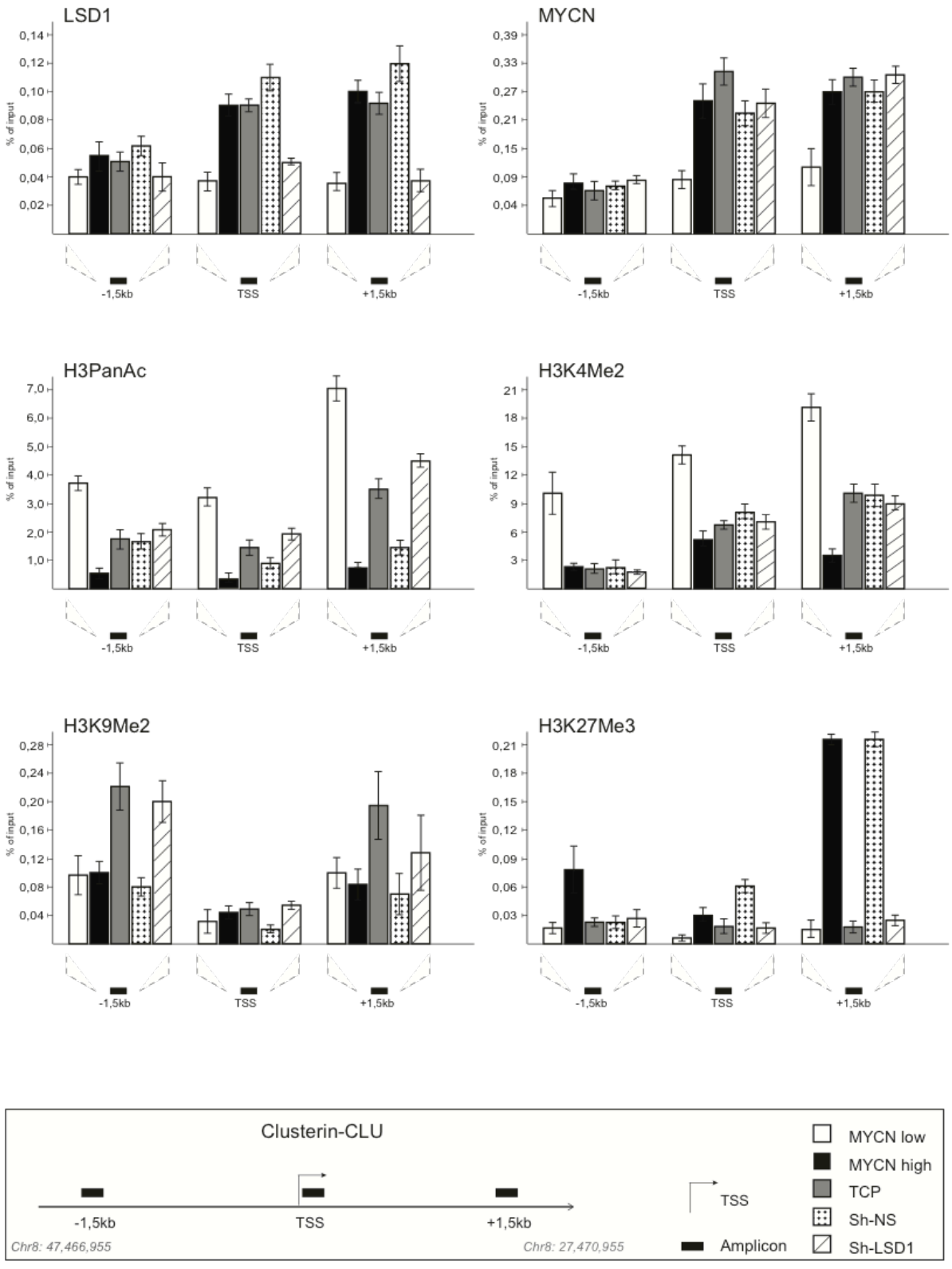

Fig.25: N-Myc and LSD1 binding to CLU chromatin. Cell treatments are indicated at the bottom of the figure and described in the legend of Figure 24. qPCR was performed with primers for CLU TSS, -1kb and +1kb. E, F and G. Histone modifications at CLU gene; ChIPs were carried out using the indicated antibodies and analyzed with primers encompassing the TSS region. Data from three independent ChIP assays and presented as % of input along with standard deviations, n=3.

SYNERGISTIC INHIBITION OF NB CELL GROWTH BY OF LSD1 AND N-MYC INHIBITORS

The findings reported above strongly suggested that both N-Myc and LSD1 cooperatively repress Neuroblastoma suppressor genes such as CDKN1A(p21) and CLU. In the next set of experiments, it has been assessed whether pharmacological inhibition of either N-Myc or LSD1 and combination of both, could have functional relevance in the context of N-Myc-amplified cells. It has been recently reported that the small molecule 10058-F4, extensively utilized as a c-Myc inhibitor, is also effective on N-Myc protein and function by binding to N-Myc preventing N-Myc/MAX dimerization and the functional onset of N-Myc functions (184). It has been first evaluated the effects of these two drugs (10058-F4 and TCP) in cell cycle progression and proliferation by measuring respectively the level of DNA content and Ki67 protein (a marker of proliferative state) in Tet-21/N Neuroblastoma cell line. Flow citometry results shown in Figure 26B demonstrate that TCP has an earlier effect on cell cycle compared to the Myc inhibitor 10058-F4, causing a decrease of S phase with a G1 phase-block after 24h of treatment, while the same effect have been observed in 10058-F4-treated cells only after 48h. In parallel, Ki67 staining reveals an earlier decrease of proliferative state in TCP-treated cells than in 10058-F4 -treated cells. Next, the proliferation rate of N-Myc amplified cell lines Tet-21/N and SKNBE was evaluated after exposing cells to TCP, 10058-F4 alone or in combination. Both drugs affected cell proliferation (Fig26, A); however, co-treatment with combination of both drugs strongly inhibited the proliferation of the Neuroblastoma cells.

A

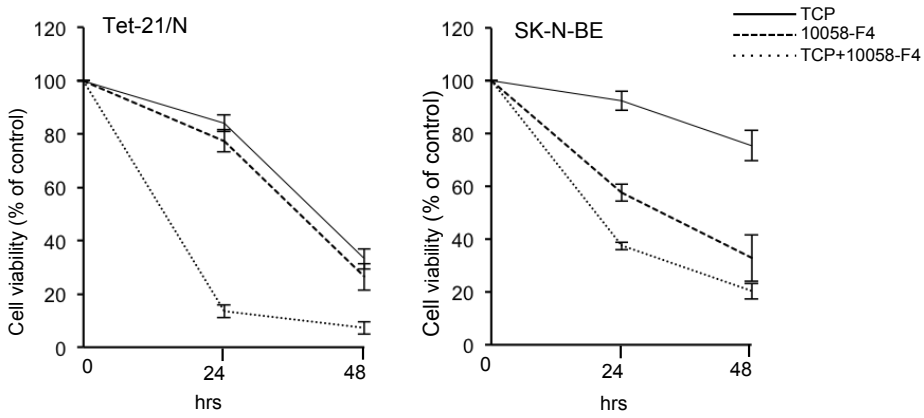

B

Tet-21/N

		G1	S	G2	subG1
24h	Untr.	42	37	20	<1
	TCP	60	25	14	<1
	10058-F4	66	19	14	<1
	TCP+10058-F4	68	15	10	7
48h	Untr.	45	36	18	<1
	TCP	46	44	9	<1
	10058-F4	55	33	11	<1
	TCP+10058-F4	72	7	6	15

SK-N-BE

		G1	S	G2	subG1
24h	Untr.	51	29	15	5
	TCP	47	31	12	10
	10058-F4	49	31	15	5
	TCP+10058-F4	59	18	11	12
48h	Untr.	56	29	12	3
	TCP	50	29	13	8
	10058-F4	49	36	12	3
	TCP+10058-F4	51	14	10	25

D

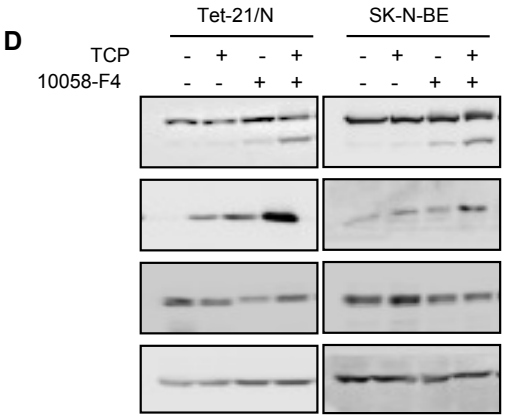

Figure 26: A) MTT assays of Tet-21/N and SK-N-BE cells treated with 1mM TCP, 75 μM 10058-F4, alone and in combination for 24 and 48 hours. Data from two independent experiments were used. B) Percentage of cell-cycle distribution of Tet-21/N and SK-N-BE (2) cells, treated with N-Myc and LSD1 inhibitors as indicated, was measured by Flow cytometry analysis. Cells were treated with TCP and 10058-F4 for 24 and 48 hours and stained with Propidium Iodide for cell cycle profile; the average values from three independent experiments are reported in the tables; all standard deviations are <15%. C) LSD1 and N-Myc inhibitors co-treatment increases apoptosis in NB cells. Western blotting of protein extract from Tet-21/N and SK-N-BE cells, treated with TCP, 10058-F4 or both for 48 hrs, using PARP (detecting both full length protein and cleaved fragment) CKN1A(p21) and N-Myc antibodies. Actin has been probed as loading control.

The strong inhibitory effect observed by drugs co-treatments result in increased apoptosis, indicated by the presence of a large increase of cells with fragmented sub-G1 DNA, and by reduced cell cycle activity, demonstrated by decreased number of cells in the S phase (Figure 6, panel B). Western blot analysis was performed to determine PARP cleavage as marker of the apoptotic events correlated to the reduced viability observed by either TCP and 10058-F4 drugs treatment. PARP cleavage was not observed in TCP treated cells, and barely detectable after 10058F treatment; however, a robust increase of the cleaved PARP was observed in cells treated with combination of the two drugs (Figure 6, panel C). These findings suggest that concurrent inhibition of N-Myc and LSD1, by dedicated inhibitors, effectively suppress Neuroblastoma cell growth and the reduction of cell viability is attributable in part to increased apoptosis.

Discussion and final remarks

Neuroblastoma is one of the most common extracranial solid tumor of the childhood and is responsible for highest number of cancer-related deaths in infants (185). Mis-regulated expression of N-Myc is often found in neuroblastoma and in several other cancers, frequently of embryonic and/or neuroendocrine origin. So far, N-Myc amplification status remains one of the most critical predictor of neuroblastoma prognosis and outcome (75, 185), although other important factors have been identified as important for prognosis prediction.

The current model of N-Myc functions in neuroblastoma implies both transcription activation and repression of selected targets involved in a wide range of biological functions through direct and indirect interactions with other transcription factors and histone modifiers (45).

As extended demonstrated by a huge amount of literature data, N-Myc can regulate transcription events both directly bind to DNA and indirectly through other transcription factors already bound to regulators DNA regions. Transcriptional activation and repression events carried out by MYC factors is determined by recruiting of respectively co-activators and co-repressors complexes involved in chromatin modification and interpretation (45, 186).

In the present work it was underlined the plastic ability of N-Myc to form two different transcriptional regulative complexes with two opposite members of histone methyl modifiers complexes: WDR5 and LSD1.

WDR5 is an essential member of the histone H3K4 methyltransferase complex; it plays a critical role in transcriptional activation via binding to transcription factors and inducing histone H3K4 trimethylation at target gene promoters (156, 180).

In this study it has been suggested that N-Myc-WDR5 protein complex lead to a positive transcription regulation of MDM2 gene signature, whereas N-Myc-LSD1 determine a repression of CKN1A(p21) and CLU gene expression.

MDM2 gene encodes for an E3 ubiquitin ligase involved in the physiological P53 protein degradation. Several cell damage signals can lead to post translational modifications of both factors determining an active P53 status. Then, P53 can lead to block in cell cycle progression and/or apoptosis events, through positive transcriptional activation of many target genes like p21 and BAX (187, 188). Furthermore, MDM2 can directly binds to the MYCN mRNA promoting RNA stabilization (189).

In the present work, both canonical and non-canonical E-boxes were identified at the WDR5 gene core promoter, and confirmed that N-Myc directly binds to the WDR5 promoter and upregulates WDR5 mRNA and protein expression in neuroblastoma cells.

It has been indicated by Guccione et al. that trimethylation of H3K4 at Myc-responsive elements of target gene promoters is a relevant prerequisite for Myc guided transcriptional activation (70). However, the exact mechanism through which H3K4 is tri-methylated during Myc transcriptional activation is still unknown. Genome-wide differential gene expression study with Affymetrix microarray shows that WDR5 siRNAs reduce the expression of several N-Myc target genes, including MDM2 and CCNE1, and GSEA analysis reveals that most of the genes down-regulated by WDR5 silencing show N-Myc/c-Myc responsive element E-box at their promoters.

Co-Immunoprecipitation assay demonstrates that N-Myc and WDR5 form a protein complex. Importantly, ChIP and luciferase assays show that WDR5 and N-Myc bind to the same DNA region of the N-Myc target MDM2 gene promoter. Moreover, the knocking-down of WDR5 expression reduces histone H3K4 trimethylation, reduces N-Myc protein binding to the MDM2 gene promoter, and reduces the activity of the wild type, but not the E-box mutant, MDM2 gene promoter. Taken together, these data indicate that WDR5 and N-Myc form a protein complex at N-Myc target gene promoters, resulting in H3K4 trimethylation and transcriptional activation of N-Myc target genes including MDM2.

Genome-wide analyses have demonstrated that MYC factors repress at least as many targets as they activates. In the repression events, MYC binds to other factors and inhibits transcription of their downstream targets. In this way, cell cycle regulators, pro-apoptotic and cell adhesion genes can be repressed thus promoting rapid growth and an aggressive phenotype (190).

LSD1/KDM1a is a lysine specific demethylase that plays an important role in stem cell biology and tumorigenesis, especially in the maintenance of the silencing of differentiation genes (166). LSD1/KDM1a is involved in maintaining the undifferentiated, malignant phenotype of neuroblastoma cells. Inhibition of LSD1 induces differentiation of tumor cells into post-mitotic neurons and blocks neuroblastoma xenograft growth (166).

In the present study, it has been shown that LSD1 can form a tight complex with N-Myc trough binding to MYC box III domain. This complex determines a negative transcription regulation of two genes involved in neuroblastoma development and progression events, CKN1A(p21) and CLU.

It has been shown that LSD1 and N-Myc functionally cooperates to determine transcription repression of CDKN1A(p21) and CLU N-Myc targets. CDKN1A(p21) is one of the major protein involved in negative regulation of progression through the cell cycle while CLU is a multifunctional protein proposed to function as a tumor suppressor in neuroblastoma (111, 191). Both N-Myc and LSD1 bind to chromatin promoter regions of CDKN1A(p21) and CLU, and the N-Myc binding to these genes is not dependent upon LSD1 recruitment. Conversely, LSD1 binding was drastically

reduced in cells expressing low levels of N-Myc, suggesting that LSD1 recruitment might be dependent upon N-Myc presence and/or abundance. Notably, LSD1 inhibition is sufficient to restore CDKN1A(p21) and CLU expression in presence of high levels of N-Myc. These findings suggest an important role of LSD1 in N-Myc mediated transcriptional repression of these gene targets. Collectively, these data demonstrated that N-Myc and LSD1 cooperate to repress CLU and CKN1A(p21) gene transcription.

Accordingly with the cooperative effects exerted by N-Myc and LSD1 in transcriptional repression events, we found that combined pharmacological inhibition of N-Myc and LSD1, through the use of small molecule inhibitors of N-Myc and LSD1 (TCP and 10058-F4), synergistically reduces neuroblastoma cell viability *ex-vivo* through activation of the apoptotic process. This result is two-fold important. On the one hand the combination of LSD1 and N-Myc inhibitors may have major therapeutic importance in the context of N-Myc-driven neuroblastoma. On the other hand it provides hints on the mechanism by which the N-Myc-LSD1 complex can exert its transcriptional effect. It may appear that N-Myc just serves as a recruiting platform of LSD1. In this case however the displacement of the platform by the N-Myc inhibitor would be sufficient to render LSD1 inoperative with or without TCP. The fact that TCP sinergistically cooperates with the N-Myc inhibitor suggests that N-Myc and LSD1 engagement is of a particular nature; indeed, N-Myc may exert novel functions beyond the simple recruitment. This phenomenon may be related to the idea by which N-Myc and LSD1 operate in the context of different repressive complexes. It was previously showed the role of N-Myc in CKN1A(p21) repression through the interaction with positive transcription factors MIZ-1 and SP1 (86) whereas it represses CLU expression by recruiting the Polycomb member EZH2 (111). Furthermore, a very recent study by Laurent et al. showed that a specific LSD1 isoform can regulate neuronal differentiation (192). Taken together these findings point to the existence of multiple and distinct N-Myc-LSD1 complexes which actuate a transcription repression program through definite mechanisms.

The study carried out on N-Myc-WDR5 complex have strongly suggested the critical role of WDR5 methyltransferase activity in facilitating N-Myc E-box occupancy at MDM2 promoter region. Conversely, chromatin IP experiments focused on N-Myc-LSD1 complex have revealed the clear involvement of N-Myc in LSD1 recruitment at CKN1A(p21) and CLU promoters. It has also been demonstrated the critical role of both factors in modify important histone markers like H3 acetylation and trimethylation of lysine H3K27. Results presented in this work highlight a complex scenario in which the cooperation between methyl histone modifiers and N-Myc is exerted at different and distinct levels.

The possibility to specifically inhibit different N-Myc complexes function is of great importance since it provides the bases to the design and development of novel therapeutic approches to treat MYC-induced cancers.

Materials and methods

CELL CULTURE

Human neuroblastoma SK-N-BE(2)C, TET-21/N, CHP-134 and HEK 293T cells were cultured in DMEM containing 10% heat-inactivated FBS and 2 mM of glutamine and antibiotics (penicillin, 100 U/ml; streptomycin, 100 μ g/ml), in a humidified atmosphere of 5% of CO2 in air at 37 °C.

When indicated, cells were treated with TCP (1mM, Enzo Life Sciences), 10058-F4 (75µM, Sigma) or both (1mM + 75µM) for 12, 24 or 48 hrs. Viability and apoptosis were quantified days after treatments by cell counting with Trypan Blue exclusion. For 3-(4,5-Dimethylthiazol-2-yl)-2,5-diphenyltetrazolium bromide cell proliferation assay cells were seeded at a density of 2,500 per well and cultured in standard medium, replaced daily. The 3-(4,5-dimethylthiazol-2-yl)-2,5-diphenyltetrazolium bromide (MTT) assay was performed according to the manufacture's protocol (Roche). The Tet21/N cells were treated with tetracycline at a final concentration
of 2 μ g/ml for the indicated time

FLOW CYTOMETRY ANALYSIS

Cell treated as described were pelleted by centrifugation and resuspended at 1 x 10^6 cells/mL in Ethanol 70% in PBS at 4°C for one overnight for fixation. Then, 2 x 10^6 cells were permeabilized with 0,1% Triton X-100/PBS for 15', blocked in 5% Bovine Serum Albumin/PBS and and stained with 2,5 µg/mL Propidium Iodide for 1hr. Cells were characterized by using a FACS Calibur (BD) and the data analyzed by Cell Quest Software and Cyflogic softwares.

TOTAL RNA EXTRACTION

The step by step protocol is described for cultured cells grown in two 100- mm dishes, containing 1-1,5 x 107 cells per dish. Remove the medium and add slowly 1ml of PBS1X. Wash and remove. Harvest the cells using trypsin treatment and when the cells detach from the culture dish, add 1 volume of fresh medium and transfer the suspension to a tube. Centrifuge for 5 minutes at 1000 rpm, and then remove the supernatant. Add 1-1,5 ml of TriReagent (Sigma). Pipet gently up and down and incubate for 5 minutes at room temperature. Add 300 µl of chloroform and vortex for 10

seconds. Incubate 5- 10 minutes at room temperature. Centrifuge fo 5 minutes at 12000rpm at 4°C. Transfer aqueous phase in a new tube and add 750 µl of isopropyl alcohol. Mix gently and incubate for 5-10 minutes at room temperature. Centrifuge at 12000rpm for 10 minutes at 4°C. Remove the supernatant and wash the pellet with 1,5 ml EtOH 75% treated with DEPC and centrifuge at 12000 rpm for 5 minutes at 4°C. Remove the supernatant and dry the pellet. Then, resuspend the pellet in 30-50 µl of DEPC-treated water and heat the sample at 55°C for 10 minutes.

DNASE I TREATMENT

After assessing quality of RNA purified and after quantification by spectrophotometric analysis (ratio 260/280 > 1.8, ration 260/230 > 1.7), DNase Treatment is required to digest the contaminant genomic DNA. The reaction is carried out by using DNAse free-kit (Ambion) in which 5ug of RNA are added to DNase I Buffer and 1uL recombinant DNAse I. The reaction is performed at 37°C for 30 minutes and recombinant DNase I is inactivated by DNasi Inactivation Reagent (0.1 volume). Incubate 10 min at room temperature, mixing occasionally. Centrifuge at 10000g for 2 min and transfer RNA to a fresh tube.

REVERSE TRANSCRIPTASE REACTION

The RT-PCR was designed for the sensitive and reproducible detection and analysis of RNA molecules in a two-step process. RT, an avian reverse transcriptase with reduced RNase H activity, was engineered to have higher thermal stability, produces higher yields of cDNA, and produce full-length cDNA. cDNA synthesis was performed using total RNA (up to 1 ug) with iScript Reverse Transcription 5x Supermix (RT (RNase H+), RNAse inhibitors, dNTPs, oligo (dt), random hexamers, buffer, MgCl2 and stabilizers) and Nuclease-free water. Prepare a master reaction mix on ice. Vortex this mix gently. Pipet the amount of master reaction mix into each reaction tube on ice. Transfer the sample to a thermal cycler preheated to the appropriate cDNA synthesis temperature and incubate for 5 min at 25°C (for Priming), for 30 min at 42°C (for Reverse Transcription) and terminate the reaction by incubating at 85°C for 5 min. Add the appropriate volume up to 100 uL and store at -20°C or use for qPCR immediately. Use only 2-5 ml of the cDNA synthesis reaction for qPCR.

SYBR GREEN SUPERMIX FOR REAL TIME QUANTITATIVE-PCR

SsoAdvanced Universal SYBER Green Supermix (BIORAD) for ICycler CFX96 is a ready to use mix containing all components, except primers and template, for real time quantitative PCR (qPCR). It combines a chemically modified "hot-start" version of Sso7d- fusion polymerase. SYBR GreenER qPCR SuperMix was supplied at a 2X concentration and contains the polymerase, MgCl2, dNTPs SYBR Green I dye, enhancers, stabilizers and fluorescein. The protocol used for quantitative real time reaction is: 30 sec at 95°C (for polymerase activation and DNA denaturation, 35-40 cycles of: 95°C for 15 seconds and 60°C for 15-30 seconds. For multiple reactions, prepare a master mix of common components, add the appropriate volume to each tube or plate well, and then the unique reaction components (e.g. template, forward and reverse primers at 200nM final concentration). Cap or seal the reaction tube/PCR plate, and gently mix. Make sure that all components are at the bottom of the tube/plate, centrifuge briefly and place reactions in a pre-heated real-time instrument programmed as described above.
Melting curve analysis is a final step characterized by an increase of temperature (from 65°C to 95°C), with an increment of 0.5°C 2-5 sec/step.

STATISTICAL ANALYSIS

Experiments were performed at least 3 times. Data were analyzed with Graphpad Prism 6 software and expressed as mean ± standard deviation (SD). Differences were analyzed for significance with Analysis of Variance (ANOVA) among groups or two-sided unpaired t test for two groups.
Survival analyses and two genes correlation were performed according to the method of Kaplan and Meier and two-sided log-rank tests (193). Multivariable Cox regression analyses were performed. Probabilities of survival and hazard ratios (HRs) were provided with 95% confidence intervals (CIs). A probability value of 0.05 or less was considered statistically significant. All statistical tests were two-sided.

CH-IP CHROMATIN IMMUNOPRECIPITATION

The step by step protocol is described for cultured cells grown in two 100- mm dishes, containing 1-1,5 x 107 cells per dish. Two 100-mm dishes are used for each immunoprecipitation. In the specific case the protocol is intended for human neuroblastoma cells growing adhesively. Minor adjustments have to be introduced for other cell types especially for those growing in suspension. Based on our experience, one of the most critical steps in performing ChIP regards the conditions of chromatin fragmentation, which need to be empirically set up for each cell types employed.

In each plate add 270 µl of formaldehyde from a 37% stock solution and mix immediately. Incubate samples on a platform shaker for 10 minutes at room temperature. In each plate add 500 ml glycine from a 2,5 M stock solution and mix immediately. Incubate on a platform shaker for 10 minutes at room temperature. Transfer the plates in ice and remove the medium. Harvest the cells with a scraper and then centrifuge at 1500 rpm for 4 minutes in cold centrifuge, then keep samples on ice. Remove the supernatant and wash pellet 3 times with 10 ml ice-cold PBS1X/ 1 mM PMSF. After each washing centrifuge at 1500 rpm for 5 minutes at 4°C. Remove supernatant and resuspend pellet in 500 µl ice-cold Cell Lysis Buffer. Pipet up and down 10- 20 times, then incubate on ice for 10 minutes. Centrifuge at 3000 rpm for 5 minutes at 4°C. Remove supernatant and resuspend pellet in 600 µl ice-cold RIPA buffer. Pipet up and down 10-20 times, then incubate on ice for 10 minutes. Sonication of crosslinked cells is performed in two distinct steps. First, cells are sonicated with a Branson Sonifier 2 times for 15 seconds at 40% setting. Next, cell samples are further sonicated with the Diogene Bioruptor for 20 minutes at high potency in a tank filled with ice/water in order to keep cell samples at low temperature during sonication. Centrifuge samples at 14000 rpm for 15 minutes at 4°C. Transfer supernatant to a new tube and pre-clear lysate by incubating it with 50 µl of Immobilized Protein A for 15 minutes in the cold room at constant rotation. Centrifuge samples at 3000 rpm for 5 minutes at 4°C. Take the supernatant, after having saved 50 µl aliquot for preparation of INPUT DNA, and add 5 µg of specific antibody. Rotate the sample O/N in the cold room. Add 50 µl of Immobilized Protein A and incubate by constant rotation for 30 minutes at room temperature. Centrifuge the sample at 4000 rpm for 5 minutes at room temperature. Remove the supernatant and proceed to wash the beads. For each wash, incubate the sample by constant rotation fro 3 minutes at room temperature and the centrifuge at 4000 rpm for 2 minutes at room temperature. Wash 4 times with 1 ml Ripa Buffer. Wash 4 times with 1 ml Washing Buffer. Wash 2 times with 1 ml TE buffer. Remove the supernatant and add 200 µl TE buffer to the beads. Add 10 µg RNAse A and incubate at 37°C for 30 minutes. Add 50 µl Proteinase

K Buffer 5X and 6 µl Proteinase K (19 mg/ml). Then, incubate at 65°C in a shaker at 950 rpm for 6 hrs. Centrifuge at 14000 rpm for 10 minutes at 4°C, then transfer the supernatant (250 µl) to a new tube. Extract once with phenol/chlorophorm/isoamylalcohol. Recover the aqueous phase (200 µl) and transfer to a new tube. Add 100 µl TE buffer to the remaining phenol/chlorophorm fraction and re-extract DNA. Recover the aqueous phase and add it to the previous one. Extract once with chlorophorm/iso-amyl-alcohol. Recover the aqueous phase (200 µl) and transfer to a new tube. Add 1 µl glycogen (Glycogen is 20 mg/ ml stock solution), 10 µg Salmon Sperm, 1/10 volumes Na-acetate 3M pH 5.2, and 2.5 volumes of cold ethanol100% Vortex and precipitate at -80°C for 40 minutes. Centrifuge at 14000 rpm for 30 minutes at 4°C. Remove the supernatant and wash pellet with 200 µl EtOH 70%. Resuspend IP-DNA and INPUT samples in 50-100 µl 10 mM TrisHCl pH 8. Use 2-4 µl of IP-DNA for Real Time PCR analysis.

Buffers used:

Cell Lysis Buffer	RIPA Buffer	Washing buffer
5 mM PIPES pH 8	150mM NaCl	100mM TrisHCl pH 8
85 mM KCl	1% NP40	500mM LiCl
0,5% NP40	0,5% NaDoc	1% NP40
1 mM PMSF	0,1% SDS	1% NaDoc
Protease inhibitor cocktail	50 mM TrisHCl pH 8	
	1 mM PMSF	
	Protese inhibitor cocktail	

DUAL-STEP CHROMATIN IMMUNOPRECIPITATION

The step by step protocol is described for cultured cells grown in two 100- mm dishes, containing 1-1,5 x 107 cells per dish. Two 100-mm dishes are used for each immunoprecipitation. In the specific case the protocol is intended for human neuroblastoma cells growing adhesively. Minor adjustments have to be introduced for other cell types especially for those growing in suspension. Based on our experience, one of the most critical steps in performing ChIP regards the conditions of chromatin fragmentation, which need to be empirically set up for each cell types employed.

Remove medium and add 2 ml PBS 1X/ 1 mM PMSF to each plate and scrape cells at room temperature. Pool together the cells from two plates and centrifuge at 1500 rpm for 5 minutes at room temperature. Wash cell pellet with 20 ml PBS1X/ 1 mM PMSF at room temperature and centrifuge at 1500 rpm for 5 minutes. Repeat this step 3 times. Resuspend pellet in 20 ml PBS1X/ 1 mM PMSF. Add disuccinimidyl glutarate (DSG) to a final concentration of 2mM and mix immediately. DSG is prepared as a 0.5 M stock solution in DMSO. (Note1) Incubate for 45 minutes at room temperature on a rotating wheel at medium speed (8-10 rpm). At the end of

fixation, centrifuge the sample at 1500 rpm for 10 minutes at room temperature. Wash cell pellet with 20 ml PBS1X/ 1 mM PMSF at room temperature and centrifuge at 1500 rpm for 5 minutes. Repeat this step 3 times. Resuspend pellet in 20 ml PBS1X/ 1 mM PMSF. Add 540 µl formaldehyde from a 37% stock solution and mix immediately. Incubate samples on a rotating wheel for 15 minutes at room temperature. Add 1 ml glycine from a 2,5 M stock solution and mix immediately. Incubate on a rotating wheel for 10 minutes at room temperature. Centrifuge samples at 1500 rpm for 4 minutes in cold centrifuge, then keep samples on ice. Remove the supernatant and wash pellet 3 times with 10 ml ice-cold PBS1X/ 1 mM PMSF. After each washing centrifuge at 1500 rpm for 5 minutes at 4°C. Remove supernatant and resuspend pellet in 500 µl ice-cold Cell Lysis Buffer. Pipet up and down 10-20 times, then incubate on ice for 10 minutes. Centrifuge at 3000 rpm for 5 minutes at 4°C. Remove supernatant and resuspend pellet in 600 µl ice-cold RIPA buffer. Pipet up and down 10-20 times, then incubate on ice for 10 minutes. Sonication of crosslinked cells is performed in two distinct steps. First, cells are sonicated with a Branson Sonifier 2 times for 30 seconds at 40% setting. Next, cell samples are further sonicated with the Diogene Bioruptor for 20 minutes at high potency in a tank filled with ice/water in order to keep cell samples at low temperature during sonication. Centrifuge samples at 14000 rpm for 15 minutes at 4°C. Transfer supernatant to a new tube and preclear lysate by incubating it with 50 µl of Immobilized Protein A for 15 minutes in the cold room at constant rotation. Centrifuge samples at 3000 rpm for 5 minutes at 4°C. Take the supernatant, after having saved 50 µl aliquot for preparation of INPUT DNA, and add 5 µg of specific antibody. Rotate the sample O/N in the cold room. Add 50 µl of Immobilized Protein A and incubate by constant rotation for 30 minutes at room temperature. Centrifuge the sample at 4000 rpm for 5 minutes at room temperature. Remove the supernatant and proceed to wash the beads. For each wash, incubate the sample by constant rotation fro 3 minutes at room temperature and the centrifuge at 4000 rpm for 2 minutes at room temperature. Wash 4 times with 1 ml Ripa Buffer. Wash 4 times with 1 ml Washing Buffer. Wash 2 times with 1 ml TE buffer. Remove the supernatant and add 200 µl TE buffer to the beads. Add 10 µg RNAse A and incubate at 37°C for 30 minutes. Add 50 µl Proteinase K Buffer 5X and 6 µl Proteinase K (19 mg/ml). Then, incubate at 65°C in a shaker at 950 rpm for 6 hrs. Centrifuge at 14000 rpm for 10 minutes at 4°C, then transfer the supernatant (250 µl) to a new tube.

Extract once with phenol/chlorophorm/isoamylalcohol. Recover the aqueous phase (200 µl) and transfer to a new tube. Add 100 µl TE buffer to the remaining phenol/chlorophorm fraction and re-extract DNA. Recover the aqueous phase and add it to the previous one. Extract once with chlorophorm/iso-amyl-alcohol. Recover the aqueous phase (200 µl) and transfer to a new tube. Add

1 µl glycogen (Glycogen is 20 mg/ ml stock solution), 10 µg Salmon Sperm, 1/10 volumes Na-acetate 3M pH 5.2, and 2.5 volumes of cold ethanol100% Vortex and precipitate at -80°C for 40 minutes. Centrifuge at 14000 rpm for 30 minutes at 4°C. Remove the supernatant and wash pellet with 200 µl EtOH 70%. Resuspend IP-DNA and INPUT samples in 50-100 µl 10 mM TrisHCl pH 8 Use 2-4 µl of IP-DNA for Real Time PCR analysis.

Notes

We have tested several crosslinking agents including DSG (disuccinimdyl glutarate), EGS [ethylene glycol bis(succinimidylsuccinate), DMA (dimethyl adipimidate) and DSS (disuccinidimyl suberate). In our conditions, DSG was the one that worked best, although we also obtained good results with EGS.

Sometimes, insoluble aggregates form when DSG is added to cells resuspended in PBS 1X . However, this seems not to preclude the efficiency of the crosslinking reaction.

Through this procedure we could efficiently fragment chromatin in a range between 500 and 200 bp. As stated above, this is a critical step that must be empirically set up for each cell line tested. For example, HL-60 cells that grow in suspension, are sonicated with a Branson Sonifier 4 times for 30 seconds at 40% setting and subsequently with the Biogene Bioruptor at a full power for 30 minutes. This procedure allows fragmentation of HL-60 chromatin to a size range of 1000-500 bp.

DUAL-LUCIFERASE ASSAY

The Dual-Luciferase® Reporter (DLR.) Assay System (Promega) provides an efficient means of performing dual-reporter assays. In the DLR. Assay, the activities of firefly (Photinus pyralis) and Renilla (Renilla reniformis, also known as sea pansy) luciferases are measured sequentially from a single sample. The firefly luciferase reporter is measured first by adding Luciferase Assay Reagent II (LAR II) to generate a stabilized luminescent signal. After quantifying the firefly luminescence, this reaction is quenched, and the Renilla luciferase reaction is simultaneously initiated by adding Stop & Glo® Reagent to the same tube. The Stop & Glo® Reagent also produces a stabilized signal from the Renilla luciferase, which decays slowly over the course of the measurement. In the DLR. Assay System, both reporters yield linear assays with subattomole sensitivities and no endogenous activity of either reporter in the experimental host cells. Furthermore, the integrated format of the DLR. Assay provides rapid quantitation of both reporters either in transfected cells or in cell-free transcription/translation reactions. The assays for firefly luciferase activity and Renilla luciferase

activity are performed sequentially using one reaction tube. The following protocol is designed for use with a manual luminometer or a luminometer fitted with one reagent injector.
Predispense 100µl of LAR II into the appropriate number of luminometer tubes to complete the desired number of DLR. Assays. Program the luminometer to perform a 2-second premeasurement delay, followed by a 10- second measurement period for each reporter assay. Carefully transfer up to 20µl of cell lysate into the luminometer tube containing LAR II; mix by pipetting 2 or 3 times. Do not vortex. Place the tube in the luminometer and initiate reading.

CO-IMMUNOPRECIPITATION AND GST-PULL DOWN ASSAYS

The interaction between different proteins is assessed by immunoprecipitation and Western blotting. Cells are washed two times in PBS 1X+ PMSF (0,1%) and lysed in the following buffer for isolation of nuclei: Hepes 10mM, NaCl 50 mM, EDTA 1mM, DTT 1mM, NaPirophosphate 1 mM, NaOrtovanadate 1 mM, Nafluorophosphate 1 mM, PMSF 1 mM, protease inhibitor (Complete, ROCHE). Nuclei are lysed in Tris-Cl pH 7,5 50 mM, NaCl 150 Mm, EDTA 10 mM, DTT 1 mM, protease inhibitors. Nuclear lysate (1 mg) is immunoprecipitated with specific antibody overnight at 4°C. The day after, specific immunoprecipitated material is incubated with 40µl of slurry-beads protein A, allowing the link between our specific antibody and protein A. The beads with immunocomplexes are washed five times with nuclear lysis buffer + NP40 0,25% and boiled in Laemmli sample buffer for 5 min at 100°C. Eluted proteins are separated by SDS-PAGE and analyzed by Western blot.
The different N-Myc segments were cloned into the pGEX-2T plasmid, in frame with N-terminal GST. Recombinant proteins were expressed in E.Coli (BL21 strain), purified, and immobilized onto glutathione-agarose beads (Sigma-Aldrich).
Lysis buffer: Triton 1%, lysozyme [1µg/µl], EDTA, PMSF, PBS.
GST beads were then incubated with 40µg of HEK-293t nuclear extracts expressing LSD1_3xFlag protein.
Nuclear lysis buffer: Tris-HCl pH 8 50mM, NaCl 150mM, DTT 0,5mM, sodium pyrophosphate 1mM, sodium orthovanadate 1mM, sodium fluoride 1mM, PMSF 1mM and Complete protease inhibitor Roche.
Purified complexes were separated on SDS/PAGE and analyzed by Western Blot analysis, using anti 3xFlag monoclonal antibody (F1804 - Sigma-Aldrich) and anti GST (G7781 - Sigma-Aldrich).

TOTAL PROTEIN EXCRACTS PREPARATION AND WESTERN BLOT

Check the cultured cells under an inverted microscope Detach the cells from the plate using a sterile scraper and pellet at 300-350 rcf for 5-10 min. at R.T. For a 6-well plate:

- Transfer 1 ml of culture medium into a 1.5 ml-volume tube and pellet using a swing- out rotor.
- Scraper the cells in the remaining volume of medium (1 ml)
- Remove the surnatant from the tubes and add the medium where the cells were scrapered in. Pellet again.
- Meanwhile, add 1 ml of non-sterile PBS to the plate and wash the wells
- Remove the surnatant from the tubes and add the PBS. Pellet again.
- Remove the surnatant and wash with 1 ml PBS. Pellet.
- Remove the PBS and resuspend the pellet in lysis buffer (20-30 µl) For a petri dish:
- Scraper the cells into the entire culture volume and transfer to a 15ml-volume falcon tube
- Pellet using a swing-out rotor.
- Meanwhile, wash the dish with 10 ml PBS
- Remove the surnatant from the pelleted cells and add the PBS. Pellet again.
- Remove the surnatant and wash the pellet with 5 ml PBS. Centrifuge again.
- Remove the surnatant and resuspend the pellet into lysis buffer (approx. 100 µl). Resuspend the pellet into ice-cold RIPA buffer (see above for volumes) pipetting 10-15 times. Transfer to 1.5-volume eppendorf tubes, if necessary and incubate on ice for 10' Sonicate for 10' at max. intensity (H) using a Bioruptor immersion sonicator (fill with ice and ddH2O). Centrifuge for 20' at >13000rpm at 4°C using a fixed-angle rotor. Transfer the surnatant to a new tube and keep it on ice for further processing ore store at -80°C.

Ripa buffer:

	Final Conc.	Volume for 1 ml
TrisHCl 1M pH 7.5	50 mM (20X)	50 ml
NaCl 5 M	150 mM (33.3X)	30 ml
Na Deoxycholate 5%	0.5% (10X)	100 ml
NP40 10%	1% (10X)	100 ml
SDS 10%	0.1% (100X)	10 ml
PMSF 100 mM	1 mM (100X)	10 ml
*Complete Protease Inhibitors Cocktail (Roche) 50X **	1 X	20 ml
mqH_2O		680 ml

Prepare a stock adding all but PMSF and Complete 50X, and store it a 4 °C. Add these reagents fresh to a suitable aliquot before each use.

Dissolve 1 capsule into 1 ml mqH2O and vortex until completely dissolved. Store at -20°C.

This protocol refers typical poly-acrylamide concentrations, running and transfer times, and antibodies dilutions; optimize conditions for the protein you seek for.

	10%	12%	15%
40% poly acryl-amide	2.5 ml	3 ml	3.75 ml
TrisHCl 1.5M pH 8.8	2.5 ml	2.5 ml	2.5 ml
10% SDS	100 µl	100 µl	100 µl
10% APS	100 µl	100 µl	100 µl
TEMED	5 µl	5 µl	5 µl
mqH_2O	To 10 ml	To 10 ml	To 10 ml

Both total and nuclear protein extracts were loaded and separated by SDS-PAGE and Western blot was performed with following antibodies: N-Myc (sc-53993, Santa Cruz), LSD1 (ab17721, Abcam), p21 (sc-397, Santa Cruz), p53 (sc-126, Santa Cruz), Clusterin-α (sc-6420, Santa Cruz), PARP-1 (sc-53643, Santa Cruz), Actin (sc-1616, Santa Cruz), α-actinin (sc-17829, Santa Cruz), WDR5(abcam-56919), MDM2(Abcam-3110) And CCNE1(Abcam-5979).

siRNA TREATMENTS SH-RNA PRODUCTION AND SILENCING ASSAYS.

20 or 100nM siRNA targeting LSD1 (GE Dharmacon), N-MYC (Qiagen), WDR5(Qiagen) or scramble were transfected in SHEP Tet-21/N and SK-N-BE (2)-C cells using Lipofectamine 2000 (Invitrogen), in according to the protocol described in manufacturer. In Tet-21/N cells N-Myc was turned off by the addiction of tetracycline 1µg/ml for one week before treatment. In ChIP analysis sh-RNA silencing was performed as described in the next paragraph. Briefly, virus production was carried out on HEK 293T cells transfected (Effectene QIAGEN) with packaging vectors, pMD2.G (#12259 - Addgene) and psPAX2 (#12260 - Addgene), and pLKO.1 TRC ShRNA backbone plasmids. pLKO.1 TRC Lentiviral Non-targeting ShRNA control (#RHS6848) and pLKO.1 TRC Lentiviral ShRNA LSD1 (Clone ID-TRCN0000046068) were purchased at Open Biosystems-GE Dharmacon. Optimization experiment (1–100 multiplicity of infection, MOI) was carried out on Tet-21/N cells using puromycin kill curve (1 µg/ml) and set at MOI 10. For shRNA Chip experiments Tet-21/N cells were transduced for 6 hours with MOI 10 and polybrene concentration

set at 10μg/ml, selected with puromycin for 24 hours and then incubated for 24 hours with complete media without puromycin selection.

PRODUCTION OF TRC VIRAL SUPERNATANT

We routinely use QIAGEN Effectene Transfection Reagent, which works very well for us. Detailed protocols are provided with the kit. The protocol below has been slightly modified from the QIAGEN kit protocol, in that it uses slightly more DNA.

Reagents:

• 293T cells (ATCC)
• 293T is a highly transfectable derivative of the 293 cell line into which the
• temperature sensitive gene for SV40 T-antigen was inserted.
• Cell culture medium
• Effectene reagent (Qiagen)
• EC buffer (comes with the QIAGEN Effectene kit)
• Enhancer (comes with the QIAGEN Effectene kit)
• TRC plasmid DNA (purchased from the RNAi Core Facility)
• psPAX2 (Addgene) _This is the packaging vector
• pMD2.G (Addgene) _This is the envelope vector
• 0.45 μm filter (Millipore)

Method:

Day 1: Plate 1.0x106 to 1.2x106 293T cells in a 6-well plate.
Day 2: a. In a sterile microfuge tube, combine 1 μg of TRC or pGIPZ plasmid
DNA with 1 μg psPAX2 and 0.5 μg pMD2.G (2:2:1 ratio) in 100 μl EC buffer. Add 3.2 μl Enhancer. Mixed by brief vortexing and then spin down to collect the contents of the tube. Incubate at room temperature for 5 minutes. Add 10μl Effectene reagent, mix by brief vortexing and incubate for another 20-30 minutes at room temperature.
b. During the incubation, re-feed the 293T cells (that have been plated out the day before) with 1.6 ml of fresh medium 293T cells peel off easily, use extreme care to re-feed the cells.

c. After the 20-30 minute incubation, add 0.6 ml medium to the DNA-Effectene mixture. Mix well and drop carefully onto the cells.
Day 3: Re-feed the transfected cells with 2.5 ml fresh medium. 293T cells peel off easily, use extreme care to re-feed the cells.
Day 4: 48 hours after infection, filter the supernatant through a 0.45 µ filter, aliquot and store at -80°C until ready for use.

INFECTION USING TRC VIRAL SUPERNATANT

The following protocol works well with most commonly used cancer cell lines. However, be aware that some cells, particularly primary cells, are extremely sensitive to Polybrene. It is therefore a good idea to pre-determine the most suitable concentration of Polybrene to be used in the infection.

Reagents:

Cells of interest to be infected (in this work: TET-21/N)
Cell culture medium, DMEM + 10% FBS
Viral supernatant (sh-RNA LSD1 or sh-RNA non-silencing)
Polybrene, 1 µg/µl (Sigma)
Puromycin (various sources such as Sigma and Clonetech)

The ideal concentration of puromycin should be pre-determined based on the cell line.

Method:
Day 1: Plate 1x105 to 1.25x105 cells per well in a 6-well plate.
Day 2: Aspirate the medium and infect cells with 250 to 500 µl viral supernatant. Add fresh medium to a final volume of 1 ml. Add 10 µl (or predetermined optimized amount) of 1 µg/µl Polybrene.
Day 3: Re-feed the cells with fresh medium.

PLASMID CONSTRUCTION

To generate the pGL3-basic MDM2 WT reporter vector, the MDM2 human promoter region containing the putative N-Myc binding site (E-box) was first amplified by PCR from genomic DNA (the primers used were reported on Primers table). The MDM2 promoter segment was cut with KpnI and XhoI and subcloned into the luciferase pGL3-basic promoter vector (Promega Biosciences, Promega Corp., San Luis Oispo, CA). The pGL3-basic MDM2 MUT reporter vector was obtained by mutation of the E-box sequence located at 444 bp from the transcription start site by whole around PCR mutagenesis. The LSD1 expression vector was obtained by amplifying LSD1 coding sequence (NM_015013.3) by PCR and then cloned into pCMV14-3Xflag using primers reported into Table of Primers. All the PCR products was ligated by using T4 DNA ligase (NEB) and verified by sanger sequencing. The pGL3 MDM2 WT or the pGL3 MDM2 MUT reporter vectors were transiently transfected using Lipofectamine LTX reagent (Invitrogen). Luciferase assays were valueted 48h post transfections. pCMV14-LSD1-3Xflag were were transiently transfected using Lipofectamine LTX reagent (Invitrogen).

TABLE OF PRIMERS USED FOR QRT-PCR, CH-IP AND CLONING

Name	Sequence FW	Sequence RV
N-Myc_qRT-PCR	CACAAGGCCCTCAGTACCT	TGACCACGTCGATTTCTTCCT
WDR5_qRT-PCR	CACGCTGGACAACACTCTGA	GTGGCCAGTGTACGTCTTCA
GUSB_qRT-PCR	GTGGGCATTGTGCTACCTC	ATTTTTGTCCCGGCGAAC
B2M_qRT-PCR	GTATGCCTGCCGTGTGAACC	GCGGCATCTTCAAACCTCCA
MDM2_qRT-PCR	AGGAGATTTGTTTGGCGTGC	TGAGTCCGATGATTCCTGCTG
CCNE1_qRT-PCR	CAGGGAGCGGGATGCG	GGTCACGTTTGCCTTCCTCT
CKN1A(p21) _qRT-PCR	TCACTGTCTTGTACCCTTGTGC	GGCGTTTGGAGTGGTAGAAA
LSD1_qRT-PCR	TGGCTGTGGTCAGCAAACAA	TTTCTCTTTAGGAACCTTGACAGTG
CLU_qRT-PCR	GAGCAGAGCGCTATAAATACGG	CCAATTCTGGAGTCTTTGCAC
WDR5 Amplicon A ChIP	CTAAAACAGGCTGGTGTTCTGC	CTAAAACAGGCTGGTGTTCTGC
WDR5 Amplicon B ChIP	TAGGAAGTGCATTAGAAGGGCC	CAACGCTTTAAAGGGACAGCAC
WDR5 Amplicon C ChIP	CAGAAGCTTCCAAACCGCAC	GGACCGGGTGGAGGGAACTG
MDM2 Amplicon A ChIP	GGCGAAACCCCATCTCTAGTAA	TCTGCCTTAGCCTCCTGAGTAT
MDM2 Amplicon B ChIP	TTCCCAGCCTCTGCCCGTTC	TCCGAAATCCCGCCCTCCTC
Cdkn1A(p21)-3,3kb Ch-IP	CCAGCTGGCTGATGTTAACAAC	TGGTCA TCACACCTGCT A TGTC
Cdkn1A(p21) TSS Ch-IP	TGGCAGA TCACA T ACCCTGTTC	CTCTCTCACCTCCTCTGAGTGCC
Cdkn1A(p21)-2,2kb Ch-IP	GCTGGTGGCTA TTTTGTCCTTG	TGGCAGA TCACA T ACCCTGTTC
CLU -1,0kb Ch-IP	TCCATAGTCCTGATCCTGAACTG	TTTGGAGCCAGGGATGTTTAAG
CLU TSS Ch-IP	TTGAGCAGAGCCACACCAGGAC	TGCGAGCTGTGTCA TCCCTCTC
CLU +1kb Ch-IP	GTGGAGCATTGGGCACAACTG	CCAGAGGCAAAGGTTAGCACTG
LSD1-3xFlag cloning	AAGGTACCATGTTATCTGGGAAGAAGGC	AATCTAGACATGCTTGGGGACTG
pGL3-MDM2 promoter cloning	AAGGTACCTGGGAAAGTAGGTGAGT--CAGAATG	AACTCGAGGACATGTTGGTATTGCACAT--TTGCCTAC

Bibliography

1. Davidoff AM (2012) Neuroblastoma. *Semin Pediatr Surg* 21(1):2-14.
2. Kamijo T & Nakagawara A (2012) Molecular and genetic bases of neuroblastoma. *Int J Clin Oncol* 17(3):190-195.
3. Takahashi Y, Sipp D, & Enomoto H (2013) Tissue interactions in neural crest cell development and disease. *Science* 341(6148):860-863.
4. Maris JM, Hogarty MD, Bagatell R, & Cohn SL (2007) Neuroblastoma. *Lancet* 369(9579):2106-2120.
5. van Noesel MM, Hahlen K, Hakvoort-Cammel FG, & Egeler RM (1997) Neuroblastoma 4S: a heterogeneous disease with variable risk factors and treatment strategies. *Cancer* 80(5):834-843.
6. Brodeur GM (2003) Neuroblastoma: biological insights into a clinical enigma. *Nat Rev Cancer* 3(3):203-216.
7. Ishola TA & Chung DH (2007) Neuroblastoma. *Surg Oncol* 16(3):149-156.
8. Barone G, Anderson J, Pearson AD, Petrie K, & Chesler L (2013) New strategies in neuroblastoma: Therapeutic targeting of MYCN and ALK. *Clin Cancer Res* 19(21):5814-5821.
9. Pugh TJ, *et al.* (2013) The genetic landscape of high-risk neuroblastoma. *Nat Genet* 45(3):279-284.
10. Knudson AG, Jr. & Strong LC (1972) Mutation and cancer: neuroblastoma and pheochromocytoma. *Am J Hum Genet* 24(5):514-532.
11. Kaneko Y, *et al.* (1987) Different karyotypic patterns in early and advanced stage neuroblastomas. *Cancer Res* 47(1):311-318.
12. Van Roy N, *et al.* (1995) Identification of two distinct chromosome 12-derived amplification units in neuroblastoma cell line NGP. *Cancer Genet Cytogenet* 82(2):151-154.
13. Brinkschmidt C, *et al.* (1997) Comparative genomic hybridization (CGH) analysis of neuroblastomas--an important methodological approach in paediatric tumour pathology. *J Pathol* 181(4):394-400.
14. Vandesompele J, *et al.* (1998) Genetic heterogeneity of neuroblastoma studied by comparative genomic hybridization. *Genes Chromosomes Cancer* 23(2):141-152.
15. Brodeur GM, Maris JM, Yamashiro DJ, Hogarty MD, & White PS (1997) Biology and genetics of human neuroblastomas. *J Pediatr Hematol Oncol* 19(2):93-101.
16. Bown N, *et al.* (1999) Gain of chromosome arm 17q and adverse outcome in patients with neuroblastoma. *N Engl J Med* 340(25):1954-1961.

17. Islam A, *et al.* (2000) High expression of Survivin, mapped to 17q25, is significantly associated with poor prognostic factors and promotes cell survival in human neuroblastoma. *Oncogene* 19(5):617-623.
18. Hurlin PJ, *et al.* (1996) Mad3 and Mad4: novel Max-interacting transcriptional repressors that suppress c-myc dependent transformation and are expressed during neural and epidermal differentiation. *EMBO J* 15(8):2030.
19. Pelengaris S, Khan M, & Evan G (2002) c-MYC: more than just a matter of life and death. *Nat Rev Cancer* 2(10):764-776.
20. Hanson KD, Shichiri M, Follansbee MR, & Sedivy JM (1994) Effects of c-myc expression on cell cycle progression. *Mol Cell Biol* 14(9):5748-5755.
21. Wei JS, *et al.* (2008) The MYCN oncogene is a direct target of miR-34a. *Oncogene* 27(39):5204-5213.
22. Munirajan AK, *et al.* (2008) KIF1Bbeta functions as a haploinsufficient tumor suppressor gene mapped to chromosome 1p36.2 by inducing apoptotic cell death. *J Biol Chem* 283(36):24426-24434.
23. Salghetti SE, Kim SY, & Tansey WP (1999) Destruction of Myc by ubiquitin-mediated proteolysis: cancer-associated and transforming mutations stabilize Myc. *EMBO J* 18(3):717-726.
24. Vennstrom B, Sheiness D, Zabielski J, & Bishop JM (1982) Isolation and characterization of c-myc, a cellular homolog of the oncogene (v-myc) of avian myelocytomatosis virus strain 29. *J Virol* 42(3):773-779.
25. Schwab M, *et al.* (1983) Amplified DNA with limited homology to myc cellular oncogene is shared by human neuroblastoma cell lines and a neuroblastoma tumour. *Nature* 305(5931):245-248.
26. Nau MM, *et al.* (1985) L-myc, a new myc-related gene amplified and expressed in human small cell lung cancer. *Nature* 318(6041):69-73.
27. Zimmerman KA, *et al.* (1986) Differential expression of myc family genes during murine development. *Nature* 319(6056):780-783.
28. Hirning U, Schmid P, Schulz WA, Rettenberger G, & Hameister H (1991) A comparative analysis of N-myc and c-myc expression and cellular proliferation in mouse organogenesis. *Mech Dev* 33(2):119-125.
29. Downs KM, Martin GR, & Bishop JM (1989) Contrasting patterns of myc and N-myc expression during gastrulation of the mouse embryo. *Genes Dev* 3(6):860-869.

30. Mugrauer G, Alt FW, & Ekblom P (1988) N-myc proto-oncogene expression during organogenesis in the developing mouse as revealed by in situ hybridization. *J Cell Biol* 107(4):1325-1335.
31. Hatton KS*, et al.* (1996) Expression and activity of L-Myc in normal mouse development. *Mol Cell Biol* 16(4):1794-1804.
32. Conacci-Sorrell M, McFerrin L, & Eisenman RN (2014) An overview of MYC and its interactome. *Cold Spring Harb Perspect Med* 4(1):a014357.
33. Adhikary S & Eilers M (2005) Transcriptional regulation and transformation by Myc proteins. *Nat Rev Mol Cell Biol* 6(8):635-645.
34. Tansey WP (2014) Mammalian MYC Proteins and Cancer. *New Journal of Science* 2014:27.
35. Stone J*, et al.* (1987) Definition of regions in human c-myc that are involved in transformation and nuclear localization. *Mol Cell Biol* 7(5):1697-1709.
36. Herbst A*, et al.* (2005) A conserved element in Myc that negatively regulates its proapoptotic activity. *EMBO Rep* 6(2):177-183.
37. Tu WB*, et al.* (2014) Myc and its interactors take shape. *Biochim Biophys Acta*.
38. Nair SK & Burley SK (2006) Structural aspects of interactions within the Myc/Max/Mad network. *Curr Top Microbiol Immunol* 302:123-143.
39. Baudino TA & Cleveland JL (2001) The Max network gone mad. *Mol Cell Biol* 21(3):691-702.
40. Hurlin PJ, Quéva C, & Eisenman RN (1997) Mnt, a novel Max-interacting protein is coexpressed with Myc in proliferating cells and mediates repression at Myc binding sites. *Genes Dev* 11(1):44-58.
41. Bretones G, Delgado MD, & Leon J (2014) Myc and cell cycle control. *Biochim Biophys Acta*.
42. Grandori C, Cowley SM, James LP, & Eisenman RN (2000) The Myc/Max/Mad network and the transcriptional control of cell behavior. *Annu Rev Cell Dev Biol* 16:653-699.
43. Ciechanover A*, et al.* (1991) Degradation of nuclear oncoproteins by the ubiquitin system in vitro. *Proc Natl Acad Sci U S A* 88(1):139-143.
44. Moens CB, Stanton BR, Parada LF, & Rossant J (1993) Defects in heart and lung development in compound heterozygotes for two different targeted mutations at the N-myc locus. *Development* 119(2):485-499.
45. Meyer N & Penn LZ (2008) Reflecting on 25 years with MYC. *Nat Rev Cancer* 8(12):976-990.

46. Buechner J & Einvik C (2012) N-myc and noncoding RNAs in neuroblastoma. *Mol Cancer Res* 10(10):1243-1253.
47. Kretzner L, Blackwood EM, & Eisenman RN (1992) Myc and Max proteins possess distinct transcriptional activities. *Nature* 359(6394):426-429.
48. Patel JH, Loboda AP, Showe MK, Showe LC, & McMahon SB (2004) Analysis of genomic targets reveals complex functions of MYC. *Nat Rev Cancer* 4(7):562-568.
49. McMahon SB, Van Buskirk HA, Dugan KA, Copeland TD, & Cole MD (1998) The novel ATM-related protein TRRAP is an essential cofactor for the c-Myc and E2F oncoproteins. *Cell* 94(3):363-374.
50. McMahon SB, Wood MA, & Cole MD (2000) The essential cofactor TRRAP recruits the histone acetyltransferase hGCN5 to c-Myc. *Mol Cell Biol* 20(2):556-562.
51. Vervoorts J*, et al.* (2003) Stimulation of c-MYC transcriptional activity and acetylation by recruitment of the cofactor CBP. *EMBO Rep* 4(5):484-490.
52. Cole MD & Cowling VH (2008) Transcription-independent functions of MYC: regulation of translation and DNA replication. *Nat Rev Mol Cell Biol* 9(10):810-815.
53. Lee KK & Workman JL (2007) Histone acetyltransferase complexes: one size doesn't fit all. *Nat Rev Mol Cell Biol* 8(4):284-295.
54. Roth SY, Denu JM, & Allis CD (2001) Histone acetyltransferases. *Annu Rev Biochem* 70:81-120.
55. Dang CV*, et al.* (2006) The c-Myc target gene network. *Semin Cancer Biol* 16(4):253-264.
56. Morrish F, Neretti N, Sedivy JM, & Hockenbery DM (2008) The oncogene c-Myc coordinates regulation of metabolic networks to enable rapid cell cycle entry. *Cell Cycle* 7(8):1054-1066.
57. Kenney AM, Cole MD, & Rowitch DH (2003) Nmyc upregulation by sonic hedgehog signaling promotes proliferation in developing cerebellar granule neuron precursors. *Development* 130(1):15-28.
58. Kohl NE, Gee CE, & Alt FW (1984) Activated expression of the N-myc gene in human neuroblastomas and related tumors. *Science* 226(4680):1335-1337.
59. Nau MM*, et al.* (1986) Human small-cell lung cancers show amplification and expression of the N-myc gene. *Proc Natl Acad Sci U S A* 83(4):1092-1096.
60. Weiss WA, Aldape K, Mohapatra G, Feuerstein BG, & Bishop JM (1997) Targeted expression of MYCN causes neuroblastoma in transgenic mice. *EMBO J* 16(11):2985-2995.

61. Grandori C*, et al.* (2005) c-Myc binds to human ribosomal DNA and stimulates transcription of rRNA genes by RNA polymerase I. *Nat Cell Biol* 7(3):311-318.
62. Gomez-Roman N, Grandori C, Eisenman RN, & White RJ (2003) Direct activation of RNA polymerase III transcription by c-Myc. *Nature* 421(6920):290-294.
63. Poortinga G*, et al.* (2004) MAD1 and c-MYC regulate UBF and rDNA transcription during granulocyte differentiation. *EMBO J* 23(16):3325-3335.
64. Poortinga G, Quinn LM, & Hannan RD (2015) Targeting RNA polymerase I to treat MYC-driven cancer. *Oncogene* 34(4):403-412.
65. Eberhardy SR & Farnham PJ (2002) Myc recruits P-TEFb to mediate the final step in the transcriptional activation of the cad promoter. *J Biol Chem* 277(42):40156-40162.
66. Cowling VH & Cole MD (2007) The Myc transactivation domain promotes global phosphorylation of the RNA polymerase II carboxy-terminal domain independently of direct DNA binding. *Mol Cell Biol* 27(6):2059-2073.
67. Bouchard C, Marquardt J, Bras A, Medema RH, & Eilers M (2004) Myc-induced proliferation and transformation require Akt-mediated phosphorylation of FoxO proteins. *EMBO J* 23(14):2830-2840.
68. Dunn S & Cowling VH (2014) Myc and mRNA capping. *Biochim Biophys Acta*.
69. Cowling VH (2010) Myc up-regulates formation of the mRNA methyl cap. *Biochem Soc Trans* 38(6):1598-1601.
70. Guccione E*, et al.* (2006) Myc-binding-site recognition in the human genome is determined by chromatin context. *Nat Cell Biol* 8(7):764-770.
71. Rohban S & Campaner S (2014) Myc induced replicative stress response: How to cope with it and exploit it. *Biochim Biophys Acta*.
72. Fernandez PC*, et al.* (2003) Genomic targets of the human c-Myc protein. *Genes Dev* 17(9):1115-1129.
73. Li Z*, et al.* (2003) A global transcriptional regulatory role for c-Myc in Burkitt's lymphoma cells. *Proc Natl Acad Sci U S A* 100(14):8164-8169.
74. Patsoukis N, Sari D, & Boussiotis VA (2012) PD-1 inhibits T cell proliferation by upregulating p27 and p15 and suppressing Cdc25A. *Cell Cycle* 11(23):4305-4309.
75. Cotterman R*, et al.* (2008) N-Myc regulates a widespread euchromatic program in the human genome partially independent of its role as a classical transcription factor. *Cancer Res* 68(23):9654-9662.

76. Bordow SB*, et al.* (1994) Expression of the multidrug resistance-associated protein (MRP) gene correlates with amplification and overexpression of the N-myc oncogene in childhood neuroblastoma. *Cancer Res* 54(19):5036-5040.
77. Claassen GF & Hann SR (1999) Myc-mediated transformation: the repression connection. *Oncogene* 18(19):2925-2933.
78. Gherardi S, Valli E, Erriquez D, & Perini G (2013) MYCN-mediated transcriptional repression in neuroblastoma: the other side of the coin. *Front Oncol* 3:42.
79. Cleveland JL*, et al.* (1988) Negative regulation of c-myc transcription involves myc family proteins. *Oncogene Res* 3(4):357-375.
80. Penn LJ, Brooks MW, Laufer EM, & Land H (1990) Negative autoregulation of c-myc transcription. *EMBO J* 9(4):1113-1121.
81. Walz S*, et al.* (2014) Activation and repression by oncogenic MYC shape tumour-specific gene expression profiles. *Nature* 511(7510):483-487.
82. Tanaka H*, et al.* (2002) E2F1 and c-Myc potentiate apoptosis through inhibition of NF-kappaB activity that facilitates MnSOD-mediated ROS elimination. *Mol Cell* 9(5):1017-1029.
83. Crescenzi M, Crouch DH, & Tato F (1994) Transformation by myc prevents fusion but not biochemical differentiation of C2C12 myoblasts: mechanisms of phenotypic correction in mixed culture with normal cells. *J Cell Biol* 125(5):1137-1145.
84. Wanzel M, Herold S, & Eilers M (2003) Transcriptional repression by Myc. *Trends Cell Biol* 13(3):146-150.
85. Herold S*, et al.* (2002) Negative regulation of the mammalian UV response by Myc through association with Miz-1. *Mol Cell* 10(3):509-521.
86. Gartel AL*, et al.* (2001) Myc represses the p21(WAF1/CIP1) promoter and interacts with Sp1/Sp3. *Proc Natl Acad Sci U S A* 98(8):4510-4515.
87. Ellenrieder V (2008) TGFbeta regulated gene expression by Smads and Sp1/KLF-like transcription factors in cancer. *Anticancer Res* 28(3A):1531-1539.
88. Seoane J, Le HV, & Massague J (2002) Myc suppression of the p21(Cip1) Cdk inhibitor influences the outcome of the p53 response to DNA damage. *Nature* 419(6908):729-734.
89. Chandramohan V*, et al.* (2008) c-Myc represses FOXO3a-mediated transcription of the gene encoding the p27(Kip1) cyclin dependent kinase inhibitor. *J Cell Biochem* 104(6):2091-2106.

90. Yang W*, et al.* (2001) Repression of transcription of the p27(Kip1) cyclin-dependent kinase inhibitor gene by c-Myc. *Oncogene* 20(14):1688-1702.

91. Staller P*, et al.* (2001) Repression of p15INK4b expression by Myc through association with Miz-1. *Nat Cell Biol* 3(4):392-399.

92. Warner BJ, Blain SW, Seoane J, & Massague J (1999) Myc downregulation by transforming growth factor beta required for activation of the p15(Ink4b) G(1) arrest pathway. *Mol Cell Biol* 19(9):5913-5922.

93. Knoepfler PS, Cheng PF, & Eisenman RN (2002) N-myc is essential during neurogenesis for the rapid expansion of progenitor cell populations and the inhibition of neuronal differentiation. *Genes Dev* 16(20):2699-2712.

94. Dauphinot L*, et al.* (2001) Analysis of the expression of cell cycle regulators in Ewing cell lines: EWS-FLI-1 modulates p57KIP2and c-Myc expression. *Oncogene* 20(25):3258-3265.

95. Yang BS, Gilbert JD, & Freytag SO (1993) Overexpression of Myc suppresses CCAAT transcription factor/nuclear factor 1-dependent promoters in vivo. *Mol Cell Biol* 13(5):3093-3102.

96. Lee TC, Li L, Philipson L, & Ziff EB (1997) Myc represses transcription of the growth arrest gene gas1. *Proc Natl Acad Sci U S A* 94(24):12886-12891.

97. Amundson SA, Zhan Q, Penn LZ, & Fornace AJ, Jr. (1998) Myc suppresses induction of the growth arrest genes gadd34, gadd45, and gadd153 by DNA-damaging agents. *Oncogene* 17(17):2149-2154.

98. Barsyte-Lovejoy D, Mao DY, & Penn LZ (2004) c-Myc represses the proximal promoters of GADD45a and GADD153 by a post-RNA polymerase II recruitment mechanism. *Oncogene* 23(19):3481-3486.

99. Kime L & Wright SC (2003) Mad4 is regulated by a transcriptional repressor complex that contains Miz-1 and c-Myc. *Biochem J* 370(Pt 1):291-298.

100. Inghirami G*, et al.* (1990) Down-regulation of LFA-1 adhesion receptors by C-myc oncogene in human B lymphoblastoid cells. *Science* 250(4981):682-686.

101. Coller HA*, et al.* (2000) Expression analysis with oligonucleotide microarrays reveals that MYC regulates genes involved in growth, cell cycle, signaling, and adhesion. *Proc Natl Acad Sci U S A* 97(7):3260-3265.

102. Tikhonenko AT, Black DJ, & Linial ML (1996) Viral Myc oncoproteins in infected fibroblasts down-modulate thrombospondin-1, a possible tumor suppressor gene. *J Biol Chem* 271(48):30741-30747.

103. Wu KJ, Polack A, & Dalla-Favera R (1999) Coordinated regulation of iron-controlling genes, H-ferritin and IRP2, by c-MYC. *Science* 283(5402):676-679.
104. Henderson MJ*, et al.* (2011) ABCC multidrug transporters in childhood neuroblastoma: clinical and biological effects independent of cytotoxic drug efflux. *J Natl Cancer Inst* 103(16):1236-1251.
105. Gartel AL & Shchors K (2003) Mechanisms of c-myc-mediated transcriptional repression of growth arrest genes. *Exp Cell Res* 283(1):17-21.
106. Brenner C*, et al.* (2005) Myc represses transcription through recruitment of DNA methyltransferase corepressor. *EMBO J* 24(2):336-346.
107. Fuks F, Burgers WA, Godin N, Kasai M, & Kouzarides T (2001) Dnmt3a binds deacetylases and is recruited by a sequence-specific repressor to silence transcription. *EMBO J* 20(10):2536-2544.
108. Peukert K*, et al.* (1997) An alternative pathway for gene regulation by Myc. *EMBO J* 16(18):5672-5686.
109. Facchini LM & Penn LZ (1998) The molecular role of Myc in growth and transformation: recent discoveries lead to new insights. *FASEB J* 12(9):633-651.
110. Claassen GF & Hann SR (2000) A role for transcriptional repression of p21CIP1 by c-Myc in overcoming transforming growth factor beta -induced cell-cycle arrest. *Proc Natl Acad Sci U S A* 97(17):9498-9503.
111. Corvetta D*, et al.* (2013) Physical interaction between MYCN oncogene and polycomb repressive complex 2 (PRC2) in neuroblastoma: functional and therapeutic implications. *J Biol Chem* 288(12):8332-8341.
112. Mao DY*, et al.* (2003) Analysis of Myc bound loci identified by CpG island arrays shows that Max is essential for Myc-dependent repression. *Curr Biol* 13(10):882-886.
113. Waddington CH (2012) The epigenotype. 1942. *Int J Epidemiol* 41(1):10-13.
114. Dawson MA & Kouzarides T (2012) Cancer epigenetics: from mechanism to therapy. *Cell* 150(1):12-27.
115. Berger SL, Kouzarides T, Shiekhattar R, & Shilatifard A (2009) An operational definition of epigenetics. *Genes Dev* 23(7):781-783.
116. Kouzarides T (2007) Chromatin modifications and their function. *Cell* 128(4):693-705.
117. Plongthongkum N, Diep DH, & Zhang K (2014) Advances in the profiling of DNA modifications: cytosine methylation and beyond. *Nat Rev Genet* 15(10):647-661.

118. Cedar H & Bergman Y (2009) Linking DNA methylation and histone modification: patterns and paradigms. *Nat Rev Genet* 10(5):295-304.
119. Davis CD & Uthus EO (2004) DNA methylation, cancer susceptibility, and nutrient interactions. *Exp Biol Med (Maywood)* 229(10):988-995.
120. Robertson KD (2005) DNA methylation and human disease. *Nat Rev Genet* 6(8):597-610.
121. Robertson KD & Wolffe AP (2000) DNA methylation in health and disease. *Nat Rev Genet* 1(1):11-19.
122. Day JJ & Sweatt JD (2010) DNA methylation and memory formation. *Nat Neurosci* 13(11):1319-1323.
123. Ehrlich M (2002) DNA methylation in cancer: too much, but also too little. *Oncogene* 21(35):5400-5413.
124. Bannister AJ & Kouzarides T (2011) Regulation of chromatin by histone modifications. *Cell Res* 21(3):381-395.
125. Virani S, Colacino JA, Kim JH, & Rozek LS (2012) Cancer epigenetics: a brief review. *ILAR J* 53(3-4):359-369.
126. Rando OJ (2012) Combinatorial complexity in chromatin structure and function: revisiting the histone code. *Curr Opin Genet Dev* 22(2):148-155.
127. Huang J*, et al.* (2007) p53 is regulated by the lysine demethylase LSD1. *Nature* 449(7158):105-108.
128. Marks P*, et al.* (2001) Histone deacetylases and cancer: causes and therapies. *Nat Rev Cancer* 1(3):194-202.
129. Falkenberg KJ & Johnstone RW (2014) Histone deacetylases and their inhibitors in cancer, neurological diseases and immune disorders. *Nat Rev Drug Discov* 13(9):673-691.
130. You JS & Jones PA (2012) Cancer genetics and epigenetics: two sides of the same coin? *Cancer Cell* 22(1):9-20.
131. Li B, Carey M, & Workman JL (2007) The role of chromatin during transcription. *Cell* 128(4):707-719.
132. Mehnert JM & Kelly WK (2007) Histone deacetylase inhibitors: biology and mechanism of action. *Cancer J* 13(1):23-29.
133. Zhou VW, Goren A, & Bernstein BE (2011) Charting histone modifications and the functional organization of mammalian genomes. *Nat Rev Genet* 12(1):7-18.

134. Santer FR*, et al.* (2011) Inhibition of the acetyltransferases p300 and CBP reveals a targetable function for p300 in the survival and invasion pathways of prostate cancer cell lines. *Mol Cancer Ther* 10(9):1644-1655.

135. Chen L*, et al.* (2013) Lysine acetyltransferase GCN5 potentiates the growth of non-small cell lung cancer via promotion of E2F1, cyclin D1, and cyclin E1 expression. *J Biol Chem* 288(20):14510-14521.

136. Wang F, Marshall CB, & Ikura M (2013) Transcriptional/epigenetic regulator CBP/p300 in tumorigenesis: structural and functional versatility in target recognition. *Cell Mol Life Sci* 70(21):3989-4008.

137. Gayther SA*, et al.* (2000) Mutations truncating the EP300 acetylase in human cancers. *Nat Genet* 24(3):300-303.

138. Cheung P, Allis CD, & Sassone-Corsi P (2000) Signaling to chromatin through histone modifications. *Cell* 103(2):263-271.

139. Cohen I, Poreba E, Kamieniarz K, & Schneider R (2011) Histone modifiers in cancer: friends or foes? *Genes Cancer* 2(6):631-647.

140. Rossetto D, Avvakumov N, & Cote J (2012) Histone phosphorylation: a chromatin modification involved in diverse nuclear events. *Epigenetics* 7(10):1098-1108.

141. Thomson S, Mahadevan LC, & Clayton AL (1999) MAP kinase-mediated signalling to nucleosomes and immediate-early gene induction. *Semin Cell Dev Biol* 10(2):205-214.

142. Nowak SJ & Corces VG (2004) Phosphorylation of histone H3: a balancing act between chromosome condensation and transcriptional activation. *Trends Genet* 20(4):214-220.

143. Young NL, Dimaggio PA, & Garcia BA (2010) The significance, development and progress of high-throughput combinatorial histone code analysis. *Cell Mol Life Sci* 67(23):3983-4000.

144. Greer EL & Shi Y (2012) Histone methylation: a dynamic mark in health, disease and inheritance. *Nat Rev Genet* 13(5):343-357.

145. Zhang N*, et al.* (2014) MYC interacts with the human STAGA coactivator complex via multivalent contacts with the GCN5 and TRRAP subunits. *Biochim Biophys Acta* 1839(5):395-405.

146. Brough DE, Hofmann TJ, Ellwood KB, Townley RA, & Cole MD (1995) An essential domain of the c-myc protein interacts with a nuclear factor that is also required for E1A-mediated transformation. *Mol Cell Biol* 15(3):1536-1544.

147. Liu T, *et al.* (2007) Activation of tissue transglutaminase transcription by histone deacetylase inhibition as a therapeutic approach for Myc oncogenesis. *Proc Natl Acad Sci U S A* 104(47):18682-18687.
148. Marshall GM, *et al.* (2010) Transcriptional upregulation of histone deacetylase 2 promotes Myc-induced oncogenic effects. *Oncogene* 29(44):5957-5968.
149. Marshall GM, *et al.* (2011) SIRT1 promotes N-Myc oncogenesis through a positive feedback loop involving the effects of MKP3 and ERK on N-Myc protein stability. *PLoS Genet* 7(6):e1002135.
150. Valli E, *et al.* (2012) CDKL5, a novel MYCN-repressed gene, blocks cell cycle and promotes differentiation of neuronal cells. *Biochim Biophys Acta* 1819(11-12):1173-1185.
151. Iraci N, *et al.* (2011) A SP1/MIZ1/MYCN repression complex recruits HDAC1 at the TRKA and p75NTR promoters and affects neuroblastoma malignancy by inhibiting the cell response to NGF. *Cancer Res* 71(2):404-412.
152. Zhang X, *et al.* (2012) Myc represses miR-15a/miR-16-1 expression through recruitment of HDAC3 in mantle cell and other non-Hodgkin B-cell lymphomas. *Oncogene* 31(24):3002-3008.
153. Trievel RC & Shilatifard A (2009) WDR5, a complexed protein. *Nat Struct Mol Biol* 16(7):678-680.
154. Kim JY, *et al.* (2014) A role for WDR5 in integrating threonine 11 phosphorylation to lysine 4 methylation on histone H3 during androgen signaling and in prostate cancer. *Mol Cell* 54(4):613-625.
155. Dharmarajan V, Lee JH, Patel A, Skalnik DG, & Cosgrove MS (2012) Structural basis for WDR5 interaction (Win) motif recognition in human SET1 family histone methyltransferases. *J Biol Chem* 287(33):27275-27289.
156. Wysocka J, *et al.* (2005) WDR5 associates with histone H3 methylated at K4 and is essential for H3 K4 methylation and vertebrate development. *Cell* 121(6):859-872.
157. Shilatifard A (2012) The COMPASS family of histone H3K4 methylases: mechanisms of regulation in development and disease pathogenesis. *Annu Rev Biochem* 81:65-95.
158. Ruthenburg AJ, *et al.* (2006) Histone H3 recognition and presentation by the WDR5 module of the MLL1 complex. *Nat Struct Mol Biol* 13(8):704-712.
159. Garapaty S, *et al.* (2009) Identification and characterization of a novel nuclear protein complex involved in nuclear hormone receptor-mediated gene regulation. *J Biol Chem* 284(12):7542-7552.

160. Chow CM, *et al.* (2005) Variant histone H3.3 marks promoters of transcriptionally active genes during mammalian cell division. *EMBO Rep* 6(4):354-360.
161. Cuthbert GL, *et al.* (2004) Histone deimination antagonizes arginine methylation. *Cell* 118(5):545-553.
162. Wang Y, *et al.* (2004) Human PAD4 regulates histone arginine methylation levels via demethylimination. *Science* 306(5694):279-283.
163. Shi Y, *et al.* (2004) Histone demethylation mediated by the nuclear amine oxidase homolog LSD1. *Cell* 119(7):941-953.
164. Bannister AJ, *et al.* (2001) Selective recognition of methylated lysine 9 on histone H3 by the HP1 chromo domain. *Nature* 410(6824):120-124.
165. Klose RJ & Zhang Y (2007) Regulation of histone methylation by demethylimination and demethylation. *Nat Rev Mol Cell Biol* 8(4):307-318.
166. Amente S, Lania L, & Majello B (2013) The histone LSD1 demethylase in stemness and cancer transcription programs. *Biochim Biophys Acta* 1829(10):981-986.
167. Humphrey GW, *et al.* (2001) Stable histone deacetylase complexes distinguished by the presence of SANT domain proteins CoREST/kiaa0071 and Mta-L1. *J Biol Chem* 276(9):6817-6824.
168. Shi YJ, *et al.* (2005) Regulation of LSD1 histone demethylase activity by its associated factors. *Mol Cell* 19(6):857-864.
169. Ballas N, *et al.* (2001) Regulation of neuronal traits by a novel transcriptional complex. *Neuron* 31(3):353-365.
170. Forneris F, *et al.* (2006) A highly specific mechanism of histone H3-K4 recognition by histone demethylase LSD1. *J Biol Chem* 281(46):35289-35295.
171. Lee MG, *et al.* (2006) Functional interplay between histone demethylase and deacetylase enzymes. *Mol Cell Biol* 26(17):6395-6402.
172. Metzger E, *et al.* (2005) LSD1 demethylates repressive histone marks to promote androgen-receptor-dependent transcription. *Nature* 437(7057):436-439.
173. Amente S, *et al.* (2010) LSD1-mediated demethylation of histone H3 lysine 4 triggers Myc-induced transcription. *Oncogene* 29(25):3691-3702.
174. Calo E & Wysocka J (2013) Modification of enhancer chromatin: what, how, and why? *Mol Cell* 49(5):825-837.
175. Eissenberg JC & Shilatifard A (2010) Histone H3 lysine 4 (H3K4) methylation in development and differentiation. *Dev Biol* 339(2):240-249.

176. van Nuland R, *et al.* (2013) Nucleosomal DNA binding drives the recognition of H3K36-methylated nucleosomes by the PSIP1-PWWP domain. *Epigenetics Chromatin* 6(1):12.

177. Molenaar JJ, *et al.* (2012) Sequencing of neuroblastoma identifies chromothripsis and defects in neuritogenesis genes. *Nature* 483(7391):589-593.

178. Slack A, *et al.* (2005) The p53 regulatory gene MDM2 is a direct transcriptional target of MYCN in neuroblastoma. *Proc Natl Acad Sci U S A* 102(3):731-736.

179. Strieder V & Lutz W (2003) E2F proteins regulate MYCN expression in neuroblastomas. *J Biol Chem* 278(5):2983-2989.

180. Ang YS, *et al.* (2011) Wdr5 mediates self-renewal and reprogramming via the embryonic stem cell core transcriptional network. *Cell* 145(2):183-197.

181. Schwab M (2002) Amplified MYCN in human neuroblastoma: paradigm for the translation of molecular genetics to clinical oncology. *Ann N Y Acad Sci* 963:63-73.

182. Schulte JH, *et al.* (2009) Lysine-specific demethylase 1 is strongly expressed in poorly differentiated neuroblastoma: implications for therapy. *Cancer Res* 69(5):2065-2071.

183. Kim J, Park UH, Moon M, Um SJ, & Kim EJ (2013) Negative regulation of ERalpha by a novel protein CAC1 through association with histone demethylase LSD1. *FEBS Lett* 587(1):17-22.

184. Zirath H, *et al.* (2013) MYC inhibition induces metabolic changes leading to accumulation of lipid droplets in tumor cells. *Proc Natl Acad Sci U S A* 110(25):10258-10263.

185. Zimmerman KA, *et al.* (1986) Differential expression of myc family genes during murine development. *Nature* 319(6056):780-783.

186. Rosenfeld MG, Lunyak VV, & Glass CK (2006) Sensors and signals: a coactivator/corepressor/epigenetic code for integrating signal-dependent programs of transcriptional response. *Genes Dev* 20(11):1405-1428.

187. Manfredi JJ (2010) The Mdm2-p53 relationship evolves: Mdm2 swings both ways as an oncogene and a tumor suppressor. *Genes Dev* 24(15):1580-1589.

188. Jelinkova I, *et al.* (2014) Platinum(IV) complex LA-12 exerts higher ability than cisplatin to enhance TRAIL-induced cancer cell apoptosis via stimulation of mitochondrial pathway. *Biochem Pharmacol* 92(3):415-424.

189. Gu L, *et al.* (2012) MDM2 regulates MYCN mRNA stabilization and translation in human neuroblastoma cells. *Oncogene* 31(11):1342-1353.

190. Herkert B & Eilers M (2010) Transcriptional repression: the dark side of myc. *Genes Cancer* 1(6):580-586.

191. Maeda T, Nishimura N, Nakamura H, & Sano K (1997) p21 (WAF1/Cip1/Sdi1/Pic1) mRNA is expressed in neuroblastoma cell lines but not in Ewing's sarcoma and primitive neuroectodermal tumor cell lines. *Acta Paediatr Jpn* 39(5):590-594.
192. Laurent B*, et al.* (2015) A Specific LSD1/KDM1A Isoform Regulates Neuronal Differentiation through H3K9 Demethylation. *Mol Cell*.
193. Kaplan EL & Meier P (1958) Nonparametric Estimation from Incomplete Observations. *Journal of the American Statistical Association* 53(282):457-481.